SYVAC3-CC4 Verification and Validation Summary

NWMO TR-2013-14 **December 2013**

Frank Garisto and Mark Gobien

Nuclear Waste Management Organization

nwmo

NUCLEAR WASTE MANAGEMENT ORGANIZATION

SOCIÉTÉ DE GESTION DES DÉCHETS NUCLÉAIRES

Nuclear Waste Management Organization
22 St. Clair Avenue East, 6th Floor
Toronto, Ontario
M4T 2S3
Canada

Tel: 416-934-9814
Web: www.nwmo.ca

SYVAC3-CC4 Verification and Validation Summary

NWMO TR-2013-14

December 2013

Frank Garisto and Mark Gobien

Nuclear Waste Management Organization

Document History

Title:	SYVAC3-CC4 Verification and Validation Summary		
Report Number:	NWMO TR-2013-14		
Revision:	R000	Date:	December 2013
Nuclear Waste Management Organization			
Authored by:	Frank Garisto and Mark Gobien		
Reviewed by:	Neale Hunt, Paul Gierszewski		
Approved by:	Paul Gierszewski		

ABSTRACT

Title: **SYVAC3-CC4 Verification and Validation Summary**
Report No.: **NWMO TR-2013-14**
Author(s): Frank Garisto and Mark Gobien
Company: Nuclear Waste Management Organization
Date: December 2013

Abstract
The SYVAC3-CC4 code is the reference Canadian system model for assessing the safety of a deep geological repository for used CANDU fuel. It consists of the SYVAC3 executive code and the CC4 system model. The CC4 system model describes a particular repository concept – used CANDU fuel in long-lived containers surrounded by bentonite clay in a stable host rock environment.

The purpose of this report is to summarize the verification and validation studies that have been carried out on SYVAC3-CC4. Many of these studies are documented in various detailed reports; this document serves as a reference summary report. Since the SYVAC3-CC4 code was developed over many years, portions of the current code were tested in earlier studies. These tests are included in this report where relevant.

Full validation of models for long-term assessment of a deep geological repository is not possible, notably because of the long time periods involved. Most of the validation tests involve comparison either with short-term field and laboratory data, or with other similar but independently developed codes or models. A specific focus of the work has been to provide testing of all the functional elements within the system model. The approach adopted is to view validation as an ongoing activity that progressively improves confidence in the code results.

Overall, the results summarized in this report indicate that at least partial validation tests have been done for a large number of the models in SYVAC3-CC4. The model results are sufficiently reliable for use in safety assessment of a deep geological repository, where the calculated safety margins are significant. Further tests will extend the range of confidence in the results.

TABLE OF CONTENTS

LIST OF TABLES

Page

LIST OF FIGURES

Page

1. INTRODUCTION

The SYVAC3-CC4 computer code is the reference Canadian system model for providing a quantitative assessment of the potential long-term impacts from a deep geological repository for used CANDU fuel.

It consists of the SYVAC3 executive code and the CC4 system model. The CC4 system model consists of 3 main submodels: a repository submodel, a geosphere submodel (GEONET) and a biosphere submodel (BIOTRAC). The repository model includes processes occurring in the repository near-field, e.g., fuel dissolution, radionuclide release from the fuel and radionuclide transport from the container to the geosphere. The geosphere model handles the transport of nuclides through the geosphere using a three-dimensional network of groundwater or transport pathways. The biosphere model covers the transport of nuclides through the biosphere, and calculates contaminant (radionuclide or chemical element) concentrations in various media as well as radiological doses for both human and biota.

The SYVAC3-CC4 system model has been under development since the 1980's. Earlier versions were tested in various international code comparisons, and were applied in all the Canadian used fuel repository safety assessment case studies: CC3 was used in the Environmental Impact Statement (EIS) (Goodwin et al. 1994); PR4 was used in the Second Case Study (SCS) (Wikjord et al. 1996); and CC4 was used in the Third Case Study (TCS) (Gierszewski et al. 2004; Garisto et al. 2004; Garisto et al. 2005a,b; Garisto et al. 2010) and the Fourth Case Study (NWMO 2012a). The most recent versions are SYVAC3.12 and CC4.09.

A detailed description of the CC4 code is provided in NWMO (2012b). Andres (1999) describes the use and structure of SYVAC3.

The purpose of this report is to summarize the verification and validation tests that have been carried out on the SYVAC3-CC4 computer program or its submodels. Many tests were carried out in the late 1980s and early 1990s during the preparation of the EIS and SCS safety assessments for a deep geological repository for used fuel. Most of the described tests have been previously published, so the present report serves primarily as a single reference summary document. Since SYVAC3 and the CC4 codes have been continuously developed and updated over many years, portions of the current codes were tested in earlier studies. These prior tests are included in this report where the code feature is still relevant.

2. OVERVIEW OF SYVAC3-CC4 VERIFICATION AND VALIDATION

2.1 SOFTWARE QUALITY ASSURANCE

The Nuclear Waste Management Organization (NWMO) supports the management principles of CSA N286.7 standard (CSA 1999), and has defined a managed system that meets this commitment through a hierarchy of governing documents and procedures. These procedures include quality assurance requirements.

Software for use in postclosure safety assessments of a deep geological repository is being developed and maintained by the NWMO consistent with these governing documents and procedures. For SYVAC3-CC4, these procedures identify CSA N286.7-99 (CSA 1999) as the relevant software standard. Its associated guideline is CSA N286.7.1-09 (CSA 2012).

The CSA N286.7-99 software standard identifies requirements for:

- configuration management and change control,
- documentation, and
- verification.

The configuration management approach selected for the NWMO postclosure safety assessment software is based on controlled access, defined releases, and a formal change request system. Figure 2-1 summarizes the procedure followed for making changes to code and data.

Documentation requirements include a problem definition, a software plan, requirements specification, design description, verification report, programmers manual, program abstract, theory manual, user manual, validation report and a version tracking record.

The CSA N286.7-99 standard distinguishes between verification and validation testing. Verification is the process of ensuring that each phase of the software development is consistent with the previous phase. For example, it ensures that the source code is consistent with the code design, or that the installed version on a new system is consistent with the archived version. Validation is the process of demonstrating that a model adequately represents the physical system that it is meant to describe. A model is validated when it provides a sufficiently good representation of the actual processes occurring in a real system, consistent with the intended use of the model.

Verification and validation are discussed further in the Section 2.2.

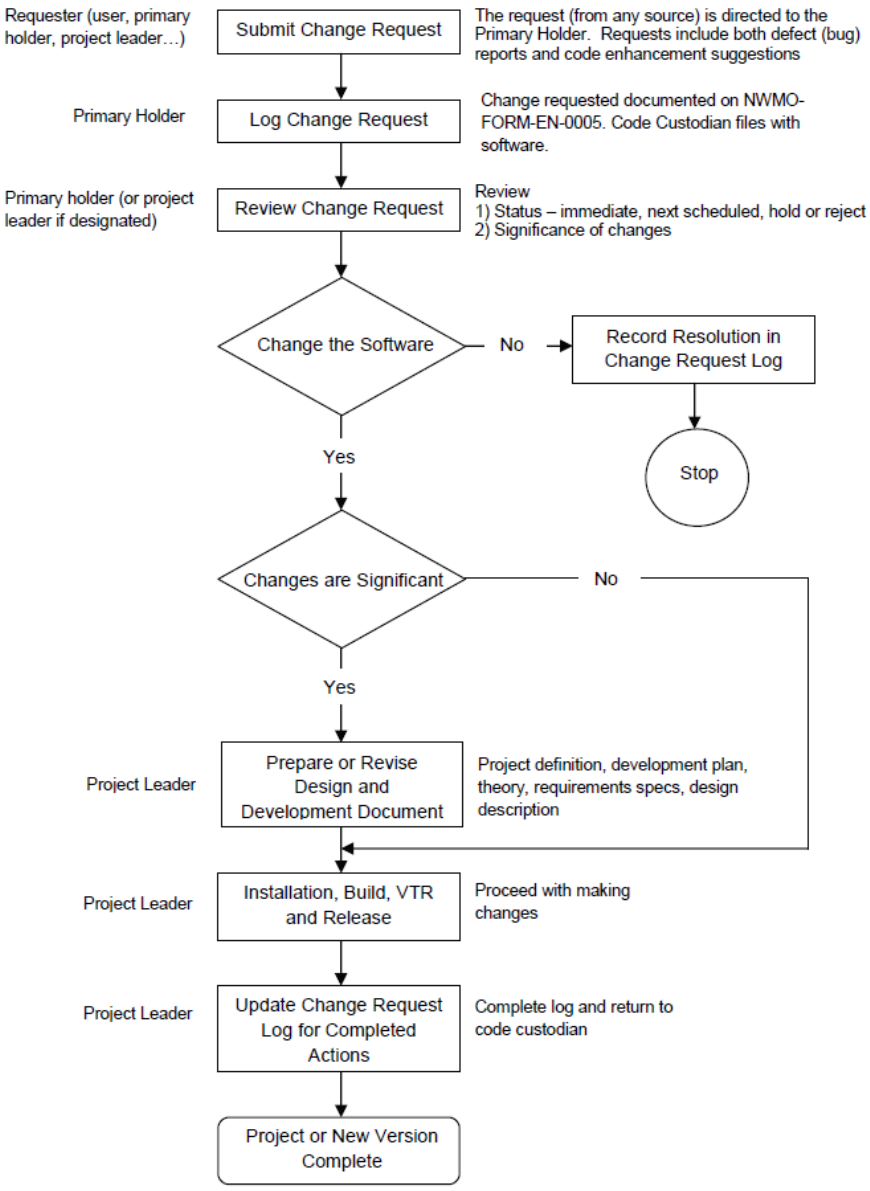

Figure 2-1: Software change control process followed for the NWMO postclosure safety assessment software and data

2.2 VERIFICATION AND VALIDATION

2.2.1 Verification

Verification is the process of demonstrating that a computer program adequately implements a given model.

Verification of each SYVAC3-CC3 version was originally carried out by AECL as part of their development of the code. Since 1996, OPG and subsequently NWMO have been responsible for code development.

Verification of SYVAC3-CC4 is aided by the software development procedures discussed in Section 2.1. The software development process includes:

- A software plan that identifies the changes, and the process for making the code changes.
- Use of specific software tools that ensure, among other things, consistent use of variables, clear definition of variables and their units, balancing of units for variables on both sides of any assignment statements, and consistent formatting of modules.
- Documentation of the code design basis, including Requirements Specifications, User Manual (Kitson et al. 2012), and Theory Manual (NWMO 2012b).
- Reviewing and testing all changes to the code to ensure that the results of the changes are consistent with expectations.

Historical verification tests include:

- An independent unit test of CC3 by the U.S. Department of Energy (Oliver et al. 1995, Kersch and Oliver 1994).
- Earlier generations of the SYVAC executive code were used by other countries, and therefore subjected to further independent tests.
- SYVAC3 was incorporated into the AECL low-level waste safety assessment model SYVAC3-NSURE (Rowat et al. 1996), and was used in the safety assessment of the Intrusion Resistant Underground Structure (IRUS) disposal concept (Dolinar et al. 1996). A modified version of INROC, together with BIOTRAC, GEONET and SYVAC3 were also used for studies of low level and intermediate level waste disposal in the Michigan basin (Sheppard et al. 1997).
- Various comparisons of specific functional calculations with analytic or independent calculations at AECL during the original code development.

More recent and / or more relevant verification tests are described in Sections 3 to 6.

2.2.2 Validation

Validation, in contrast to verification, is the process of demonstrating that a model adequately represents the system that it is meant to describe. A model is validated when it provides a sufficiently good representation of the actual processes occurring in a real system, consistent

with the intended use of the model. Validation should provide a measure of the uncertainty in the model predictions.

Validation is best achieved by comparing model predictions with field or experimental observations. Such a test is not possible for SYVAC3-CC4 since actual used-fuel repository long-term performance data are not available for making comparisons with model predictions.

Consequently, for such codes, validation must rely on other approaches to improve confidence in the model predictions as much as practical. The types of approaches include:

- comparison with partial field or experimental data (e.g., short term experiments or experiments involving only a specific process);
- comparison with natural analogs;
- comparison with independently developed codes and models;
- demonstration that the model has realistic sensitivity to input data variations;
- peer review and acceptance;
- ensuring the model conforms to physical limits such as mass balance; and
- use of conservative models where it is sufficient for the predicted consequences to be above or below some threshold.

There is no firm criterion for determining what constitutes an acceptable level of validation or confidence in the results (Flavelle 1987). In part, this is a matter for the public, government and regulator to assess during each major stage of the licensing process, such as site selection, operating license, and closure. The full safety case will in general include other arguments besides the results of the postclosure model (e.g., age of groundwaters at the site depth).

However, a reasonable expectation is that:

- models for processes believed to be most important to the safety assessment conclusions should be tested against real data under similar conditions at least for short times;
- overall results should be tested against independent codes for comparable complex cases and for long times, preferably codes that use different modelling approaches; and
- the models and tests should be reviewed, through presentation in peer-reviewed forums or through widespread use.

There will be an ongoing testing effort to continuously improve our confidence in the long-term SYVAC3-CC4 systems model. This will in due course also include calibration and validation of the model using site-specific data collected during the operational and monitoring phase of a repository - a period of 100 years or more.

2.3 ORGANIZATION OF VERIFICATION AND VALIDATION TESTS

Subsequent sections of this report describe the studies relevant to “verifying”, "validating" or "building confidence in" SYVAC3-CC4 predictions for a deep geological repository for used fuel. Published tests are emphasized, since this establishes a reasonable level of peer review of the results. It is recognized that some tests are "stronger" than others.

Most of these comparisons are relevant to specific functions of the code, and so are described in the following order: repository, geosphere and biosphere.

Although the specific model for each of these submodels was generated within a specific computer program package, all these packages interacted extensively with the SYVAC3 executive code for input, output and some numerical functions (e.g., time series manipulation). Therefore, many of the repository, geosphere and biosphere validation tests also test the SYVAC3 executive code. The exception is many of the original biosphere validation tests, especially the BIOMOVSII tests, which were run outside of the SYVAC environment.

It should be noted that the accuracy of the model results depend in part on the input data. This report does not, in general, deal with the accuracy of the input data. However, the data that are used in a safety assessment are maintained as a reference dataset, and controlled and verified to the same standard as the SYVAC3-CC4 code itself.

In the following descriptions, the version of CC4 that was tested is explicitly identified. However, these results are still applicable to the current version of the code if the particular section of the code that was tested has not been changed. Tests on particular models or sections of the code that have subsequently been changed significantly are not reported here.

Appendix A presents a simple categorization of the processes included in the SYVAC3-CC4 model, and the types of verification and validation tests undertaken, as discussed in this report.

3. REPOSITORY MODEL

The repository model describes the processes occurring in the near-field around the used fuel containers. These include container failure, radionuclide release from the fuel and cladding, and transport of radionuclides out of the container, through the buffer, backfill, and excavation damage zone (EDZ) layers and into the geosphere. The tests for the different repository modules are summarized in this section.

3.1 RADIONUCLIDE INVENTORY

The radionuclide inventory in the repository is initially defined through user-input parameters. The repository model accounts for subsequent changes in the radionuclide inventories with time due to ingrowth and decay. These processes are well known over relevant timescales. Within CC4, they are analytically solved using the well-known Bateman equations for radioactive decay chains (Bateman 1910).

CC4 can handle only linear decay chains and assumes 100% decay to a given daughter. Therefore, branching chains must be arranged by use of parallel linear decay chains, which can be accomplished as described in Goodwin et al. (2001) and by conservatively neglecting some side branches to stable nuclides.

The decay inventories calculated by CC4 (Version SCC402) were compared with nuclide inventories calculated with the ORIGEN-S code for a fuel bundle with a burnup of 280 MWh/kgU (Goodwin et al. 2002). ORIGEN-S is a CANDU-industry standard code, and the accuracy of the ORIGEN-S numerical algorithm is estimated as 0.1% (Hermann and Westfall 2000). A maximum absolute difference of up to 0.15% between the SCC402 and ORIGEN-S inventories was deemed acceptable, based on the precision of the values outputted by the two codes. In comparison, the accuracy of the ORIGEN-S results relative to experimental measurements on CANDU used fuel is estimated as within 5% for most nuclides (Tait et al. 1995).

The radionuclides and decay chains considered in the inventory tests are shown in Table 3-1. Although Table 3-1 indicates that some nuclear decays have branching ratios less than one, all branching ratios in CC4 were implicitly set equal to one. This can result in higher inventories for some nuclides. For instance, the branching ratio for chain a1 is only 0.917, so that an implicit value of unity would overestimate inventories for Pu-244 and its progeny. In the test, this limitation was overcome by appropriately assigning the initial radionuclide inventories. Thus, for example, the initial inventory (at t = 10 years) for Np-236 was apportioned so that 91.1% is associated with the c branch and the remaining 8.9% with the d branch. Similarly, the initial inventories of Cf-252 and Cm-248 (at t = 10 years) were apportioned so that 91.7% go to the a1 branch and 8.3% to the a2 branch.

Table 3-2 compares the radionuclide inventories predicted by SCC402 and ORIGIN-S. The radionuclide inventories at t = 10 years from ORIGEN-S were used as initial inventories for the CC4 runs.

Table 3-1: Decay Sequences Considered in the Inventory Tests*

Nuclides	Branch Label	Linear Decay Chains (and branching ratios)
Nuclides from light element impurities	--	Mo-93 → Nb-93m Zr-93 → Nb-93m
Nuclides from fission products	--	I-129 Sn-126 $\xrightarrow{0.14}$ Sb-126
Nuclides from the 4n actinide decay series	a1	Cf-252 → Cm-248 $\xrightarrow{0.917}$ Pu-244 → Pu-240 → U-236 → Th-232 → Ra-228 → Th-228 → Ra-224
	a2	Cf-252 → Cm-248 $\xrightarrow{0.083}$ (unspecified spontaneous fission products)
	b	Cm-244 → Pu-240 → U-236 → Th-232 → Ra-228 → Th-228 → Ra-224
	c	Np-236 $\xrightarrow{0.911}$ U-236 → Th-232 → Ra-228 → Th-228 → Ra-224
	d	Np-236 $\xrightarrow{0.089}$ Pu-236 → U-232 → Th-228 → Ra-224

*The final stable nuclides in each chain are not shown. .

The differences between CC4 and ORIGIN-S are within the acceptable test criteria (0.15%) except for Nb-93m and Pu-240. The differences are particularly large for Nb-93m, reaching a maximum of about 22%.

A detailed examination of the results indicates that the large differences in the Nb-93m inventories calculated by CC4 and ORIGIN-S are due to differences in the decay schemes employed by the two codes. CC4 assumes that the branching ratio is unity for the decay of Mo-93 to Nb-93m, consistent with information in Eckerman and Leggett (1996) and ICRP (1983). However, examination of the ORIGEN-S data library (Hermann and Wesfall 2000) indicates that a branching ratio of 0.820 is used in the ORIGEN-S code for the same decay process. To confirm that the different branching ratio could explain the difference, the original results produced by CC4 were adjusted using the following equation:

$$I_{cor}(t) = 0.82 \times [\, I_{SCC}(t) - I_{SCC}(0)\exp(-\lambda t)\,] + I_{SCC}(0)\exp(-\lambda t) \qquad (3.1)$$

where $I_{SCC}(t)$ is the Nb-93m inventory calculated by CC4 at time t, $I_{SCC}(0)$ is the inventory at t = 0 years (i.e., the 'initial' inventory supplied to SCC402) and λ is the decay constant of Nb-93m. The results from application of Equation (3.1) are shown in Table 3-2 under the heading 'Nb-93m adjusted' and show good agreement with the computed ORIGIN-S inventories.

Table 3-2: Comparison of Results from ORIGEN-S and CC4

Nuclide	Percentage Difference* at Time =					
	100 yr.	1000 yr.	10^4 yr.	10^5 yr.	10^6 yr.	10^7 yr.
Cf-252	-0.005	--	--	--	--	--
Cm-244	-0.025	0.026	--	--	--	--
Cm-248	0.029	0.018	-0.006	-0.006	0.009	0.017
I-129	0.001	0.014	0.011	-0.003	0.000	0.019
Mo-93	-0.011	-0.009	-0.003	0.000	--	--
Nb-93m	**2.000**	**21.965**	**21.939**	-0.011	-0.026	0.029
Nb-93m (adjusted)	-0.011	0.014	0.004	-0.011	-0.026	0.029
Np-236	-0.001	0.010	0.006	0.011	-0.022	--
Pu-236	0.017	0.011	0.009	0.001	0.000	--
Pu-240	0.001	-0.001	-0.013	0.019	**-0.225**	0.104
Pu-244	-0.025	-0.031	-0.024	-0.036	-0.035	-0.047
Ra-228	-0.019	-0.013	-0.011	-0.045	-0.042	-0.026
Sn-126	0.008	-0.004	0.006	0.009	-0.002	--
Th-228	0.020	-0.019	-0.014	-0.038	-0.037	-0.024
Th-232	0.003	0.008	-0.005	-0.024	-0.034	-0.013
U-232	0.008	0.007	0.071	0.094	0.070	--
U-236	-0.018	-0.012	-0.002	-0.049	-0.036	-0.007
U-238	-0.001	-0.001	-0.001	-0.001	-0.015	-0.009
Zr-93	-0.004	0.021	-0.001	0.029	0.017	0.008
Ra-224	0.000	-0.005	-0.025	-0.055	-0.022	-0.013
Sb-126	-0.001	0.004	0.017	0.011	-0.011	--

***** Percentage difference is positive if the SCC402 inventory exceeds the ORIGEN-S inventory. Differences exceeding the acceptance criterion are highlighted. The row with the nuclide label “Nb-93m adjusted’ is discussed in the text.

The differences for Pu-240 in the predicted CC4 and ORIGEN-S inventories are within the expected margin of error (0.15%) except at t = 10^6 years. No evidence has been found to show that this difference is due to the approximations made to model the 4n actinide decay series in CC4. For example, there is no systematic deviation, but rather the differences vary from positive to negative, suggesting a numerical cause rather than a missing physical process. Furthermore, an analytical expression for the Pu-240 inventory can be derived from the Bateman equations, and subsequent comparison of inventories from the analytical solution and CC4 show a maximum absolute difference of less than 0.01%. It is considered likely, therefore, that the 0.2% difference in Table 3-2 for Pu-240 at 10^6 years is caused by an accumulation of round-off errors in ORIGEN-S.

3.2 CONTAINER FAILURE

CC4 generally assumes that the used fuel containers are durable; but, a few containers fail (i.e., have small penetrations, allowing water to enter the container) due to manufacturing or installation defects (Maak et al. 2001). However, CC4 does not model the processes or mechanisms by which a used fuel container is breached.

The container failure rate is random within a given repository sector, with user defined failure frequency, failure time and defect size. The failure time is defined as the time at which a continuous groundwater pathway exists between the inside and the outside of the container, allowing contaminants to diffuse out of the container. The failure time could be input as early, for example assuming a manufacturing defect and fast repository resaturation. Or it could be set for a longer time, respecting realistic resaturation processes as well as gas generation processes that might inhibit water entry into a failed container (SKB 1999).

The size of the defect does not change with time in the CC4 model, although there may be mechanisms by which the defect size could increase, depending on the design of the used fuel container (NWMO 2012a). This could be addressed in the CC4 model by choosing a large initial defect size.

Evidence for the durability of the NWMO reference copper-shell container for used fuel (see Figure 3.1) is summarized in Kwong (2011) and King et al. (2010), as well as the extensive testing program on copper in general, and of copper containers in particular, by NWMO and other waste management programs (SKB 2010a). The particular container failure mode depends upon repository-specific conditions, but the assumption of some initial through-container defects, early buffer and container saturation, and neglect of the Zircaloy cladding or steel insert barriers is considered to be conservative.

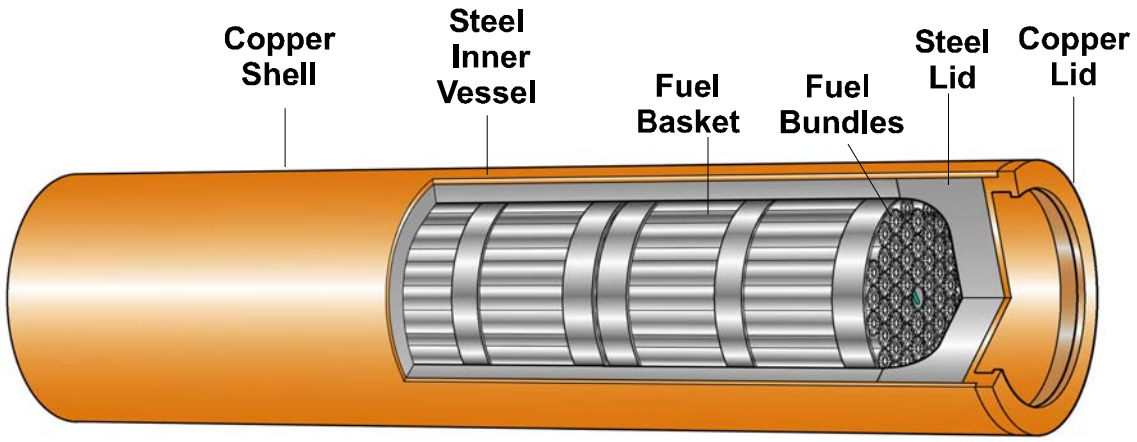

Figure 3-1: Cut-away view of the NWMO reference copper-shell container for used fuel, showing the inner and outer vessels

Processes and mechanisms by which used fuel containers could fail more extensively than expected in the normal evolution scenario have been proposed (NWMO 2012a, Chapter 6). For such disruptive events, the defect size would be very large. The validity of the CC4 repository model for such situations is discussed below.

3.3 CONTAMINANT RELEASES FROM USED FUEL

Contaminants (i.e., radionuclides or potentially chemical toxic elements) in used fuel bundles are found in the fuel-cladding gap, the grain boundaries of the fuel and within the UO_2 grains, with more than 95% within the UO_2 grains (Gobien et al. 2013, and references therein). The UO_2 ceramic fuel matrix is durable and resistant to radiation damage.

CC4 models two mechanisms by which contaminants are released from the fuel. Specifically, radionuclides in the fuel-cladding gap and grain boundaries are released instantly when the groundwater contacts the fuel, whereas the radionuclides in the fuel grains are released congruently as the fuel grains dissolve.

3.3.1 Instant Release Model

The radionuclide instant-release model has been shown to be appropriate for used-fuel bundles irradiated under a wide range of conditions (Garisto et al. 1990), and is also accepted in used fuel models used by other international organizations (SKB 2011, Johnson et al. 2004).

The amount of the radionuclide inventory that can be instantly released in the CC4 model is a user-input parameter. It is a measured or estimated value, and is the fraction of the inventory that is present in both the fuel-cladding gap and at the grain boundaries of the fuel. Gap inventories for CANDU fuel have been well characterized for a number of nuclides (Stroes-Gascoyne 1996, Stroes-Gascoyne et al. 1993) whereas data on the quantities and availability of fission products at grain boundaries are more limited (Gray and Strachan 1991, Stroes-Gascoyne 1996, Stroes-Gascoyne et al. 1993). Although release rates from the grain boundaries is typically slower than release rates from the gap, the time scale is still much shorter compared to that from fuel dissolution; and, for conservatism, they are both included in the instant release fraction. The instant releases are found to correlate with fission gas release behaviour, which is well-studied (Gobien et al. 2013, and references therein).

3.3.2 Congruent Release Model

The bulk of the radionuclides in used fuel are held within the grains of the UO_2 fuel, near where they are created by fission. These radionuclides are assumed to be released congruently as the fuel dissolves. A congruent release model is supported by long-term leaching experiments that show that the fractional releases of different nuclides are comparable in spite of the widely varying chemical properties of the leached elements (Johnson et al. 1982, Neal et al. 1988, Tait and Luht 1997).

The natural mineral uraninite has many similarities with used UO_2 fuel. These materials are uranium oxides with the same crystallographic structure, they form solid solutions with oxides of actinides and rare earths and they are resistant to radiation damage. Thus, the existence of old

uranium ore (uraninite) deposits, such as those at Cigar Lake, suggests that used UO_2 fuel would be stable for millions of years under the reducing conditions expected in a repository.

At Cigar Lake, natural fission in the high-grade mineralization has produced very small quantities of fission and activation products. The relative abundances of Pu-239, I-129 and Tc-99 in Cigar Lake ore samples were measured (Cramer and Smellie 1994, Section 3.8.2). The measured Pu-239/U, I-129/U and Tc-99/U atom ratios were found to be in good agreement with predicted ratios, suggesting both good retention of the isotopes in the natural-UO_2 matrix and congruent dissolution of the matrix.

3.3.3 UO_2 Dissolution Model

The UO_2 ceramic fuel matrix is durable, and dissolves slowly in water. The most important factor determining the dissolution rate of UO_2 in water is the redox conditions in the surrounding groundwater. Under the reducing conditions expected in the repository, the UO_2 fuel would dissolve very slowly.

However, after the fuel is contacted by groundwater, the conditions at the used fuel surface are likely to be oxidizing for a long time due to the production of oxidants in the water from radiolysis (Grambow et al. 2010, Poinssot et al. 2005) that is caused by the α-, β-, and γ-radiations emitted by the used fuel. In the current CC4 model, the rate of used fuel is modelled as linearly proportional to the local α-, β- and γ-radiation field intensity, as indicated in the equations below

$$R_\alpha = A_{cont}\, G_\alpha\, D_\alpha(t) \tag{3.2}$$

$$R_\beta = A_{cont}\, G_\beta\, D_\beta(t) \tag{3.3}$$

$$R_\gamma = A_{cont}\, G_\gamma\, D_\gamma(t) \tag{3.4}$$

where

- R_α, R_β, and R_γ are the fuel dissolution rates ($mol \cdot a^{-1}$) due to α-, β- and γ-radiation, respectively;
- $D_\alpha(t)$, $D_\beta(t)$ and $D_\gamma(t)$ are the time-dependent dose rates ($Gy \cdot a^{-1}$);
- t is the age of the fuel (years);
- G_α, G_β and G_γ are empirical rate constants for fuel dissolution in the presence of alpha, beta and gamma radiation fields, respectively ($mol \cdot m^{-2} \cdot Gy^{-1}$); and
- A_{cont} is the effective (geometric) surface area of the dissolving fuel, per container (m^2); and

Note that the CC4 model has the capability of treating dissolution models in which, for example, the fuel dissolution rate due to alpha-radiolysis is proportional to any power of the alpha dose rate. However, the linear rate law adequately represents the measured data.

In CANDU fuel, the beta/gamma contribution is expected to be dominant for the first 500 years, as shown in Figure 3-2. After this time, alpha radiolysis will control the fuel dissolution rate. After the alpha radiation field decays sufficiently, i.e., after millions of years, the fuel dissolution rate is controlled by the chemical fuel dissolution rate. Therefore, the total matrix dissolution rate, R_{TOT} ($mol \cdot a^{-1}$) is given by

$$R_{TOT} = R_{\alpha} + R_{\beta} + R_{\gamma} + R_{ch} * A_{cont} \quad (3.5)$$

where R_{ch} ($mol \cdot m^{-2} a^{-1}$) is the chemical fuel dissolution rate, i.e., the dissolution rate of the fuel in the absence of radiolysis.

The value of G_{α} and its uncertainty is based on the experimental corrosion rate data compiled by Poinssot et al. (2005) (Shoesmith 2007), as described in Gobien et al. (2013). These corrosion rates are for α-doped UO_2, non-doped UO_2 (0.01 MBq/g) and used fuel. Although the dissolution data show a clear trend of increasing corrosion rate with increasing alpha activity, it also seems to show that there is a threshold activity below which no effect of alpha activity is observed (at approximately 1 MBq/g(UO_2)). Below the threshold activity, the corrosion rate of unirradiated UO_2 should be well described by the chemical dissolution rate R_{ch}.

In the current CC4 model, it is assumed that $G_{\beta} = G_{\gamma}$ because beta and gamma radiation are both low linear energy radiation, which produces more radicals (e.g., H, $OH^{\bullet}$) than high linear energy radiation. The value G_{γ} and its uncertainty is obtained using the data in Johnson et al. (1996) which shows that the dissolution rate of unirradiated UO_2 is linearly dependent on the intensity of the externally imposed gamma field.

The value of the chemical dissolution rate, R_{ch}, and its uncertainty was derived from data compiled from the literature (Gobien et al. 2013). In many cases, these data actually represent the minimum observed fuel corrosion rate, which was taken to be representative of the chemical dissolution rate. (The data may include radiolysis effects or be at measurement accuracy limits, and thus overestimate the true chemical dissolution rate.)

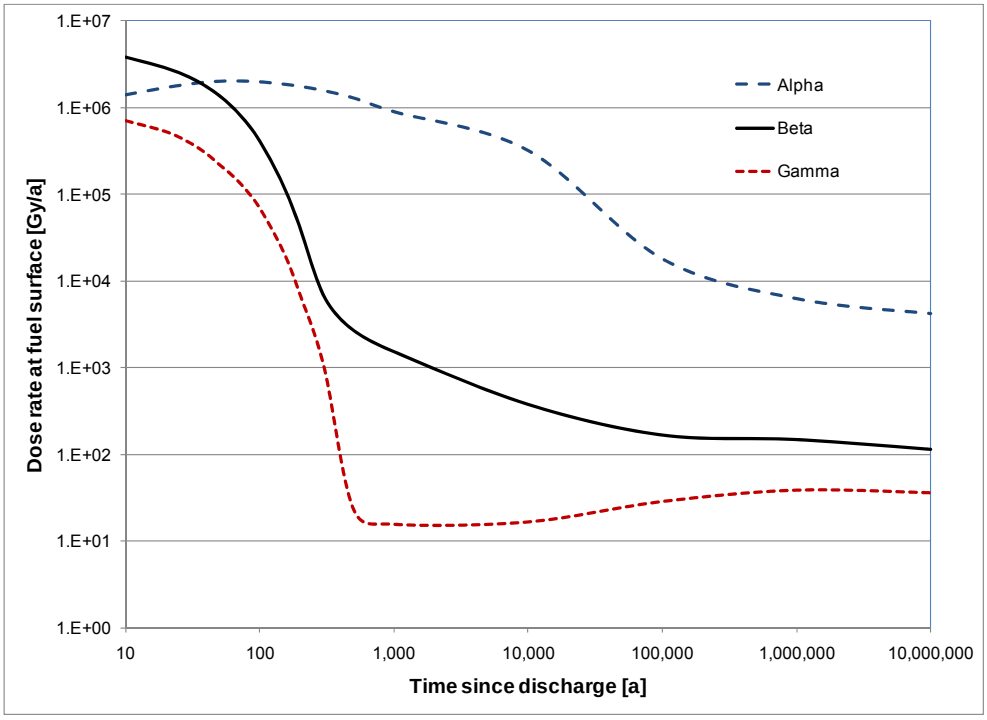

Figure 3-2: Radiation dose rates in water at the fuel surface (220 MWh/kgU burnup) showing that alpha radiolysis dominates after a few hundred years

The selected values of G_α, G_β, G_γ, and R_{ch} are shown in Table 3-3. Using the median values of these parameters, all the fuel in a defective container would dissolve in about 13 million years. In comparison, SKB (2011) selects a (best-estimate) fractional fuel dissolution rate of 1.0×10^{-7}/year, based on the work of Werme et al. (2004); in which case all the fuel dissolves in 10 million years.

Table 3-3: Used Fuel Dissolution Rate Parameters

Parameter	Best-estimate value	Probability Distribution Function (PDF)[1]
Fuel surface area per container[2]	1570 m^2	Lognormal PDF with GM=1570 m^2, GSD = 3, bounds of 340 and 7860 m^2
G_α	1.4×10^{-10} $mol \cdot m^{-2} \cdot Gy^{-1}$	Lognormal PDF with GM= 1.4×10^{-10} $mol \cdot m^{-2} \cdot Gy^{-1}$, GSD = 6.0, bounds of $3.5 \cdot 10^{-12}$ and $2.1 \cdot 10^{-9}$ $mol \cdot m^{-2} \cdot Gy^{-1}$
G_β and G_γ	1.1×10^{-9} $mol \cdot m^{-2} \cdot Gy^{-1}$	Loguniform PDF with bounds of 3.7×10^{-11} and 3.3×10^{-8} $mol \cdot m^{-2} \cdot Gy^{-1}$
Chemical dissolution rate	4.0×10^{-7} $mol \cdot m^{-2} \cdot a^{-1}$	Loguniform PDF with bounds of 4.0×10^{-8} and 4.0×10^{-6} $mol \cdot m^{-2} \cdot a^{-1}$

[1] GM = Geometric mean, GSD = Geometric standard deviation.
[2] Fuel surface area for a container with 360 fuel bundles.

Since the empirical rate constants G_α, G_β and G_γ and their uncertainties were derived from experimental data as described in detail in Gobien et al. (2013), it is expected that the fuel dissolution rates calculated by the CC4 model would correctly reflect the dissolution data from which these empirical rate constants were derived. Independent data, not used in the derivation of these rate constants, are needed to validate the selected rate constants. These additional data are discussed below.

- Muzeau et al. (2009) carried out dissolution experiments using Pu-238/Pu-239 doped UO_2 pellets. Their data fall within the selected range of G_α values.

- Clarens et al. (2003, 2005) performed leaching experiments on UO_2 powder in a continuous flow reactor over a pH range of 3.6 to 9.7 in the presence of β radiation. The beta source generated a dose rate of 4.6×10^4 Gy/a and the experiments lasted between 480 hours and 744 hours. The fuel dissolution rate and hydrogen peroxide concentration increased as the pH decreased, similar to trends observed in earlier experiments (Shoesmith 2000). Except for one measurement, the UO_2 dissolution rates for pH > 6 fall within the 95% confidence bounds of dissolution rates calculated using the selected value of G_β. Although this suggests that the selected value of G_β may underestimate the fuel dissolution rate at pH values of 6 or so, additional data are needed to confirm this supposition. However, it is not expected that this underestimation would affect CC4 results, given that the beta and gamma contributions to the total fuel dissolution rate become unimportant for times greater than about 500 years.

At very long times, after the radiation fields have decayed to very low levels, the CC4 model uses the chemical dissolution rate. The selected long-term dissolution rate can be compared

with data from natural analogue studies. Natural uraninite, for example, can be considered as an analogue to UO_2 fuel (Cramer 1994). Geological evidence indicates that natural uraninite, located in reducing environments (e.g., Cigar Lake and Oklo) shows very long-term stability, i.e., billions of years. This indicates that the chemical dissolution rate used in the CC4 model, which predicts that all the fuel in the repository would dissolve in about 50 million years, conservatively overestimates the extent of fuel dissolution at long-times.

Finally, in a breached used fuel container, hydrogen gas would be generated by corrosion of the inner steel vessel. Experimental evidence indicates that small concentrations of hydrogen gas would greatly reduce the dissolution rate of used fuel, as discussed in detail by Shoesmith (2008). However, this effect is conservatively neglected in the CC4 fuel dissolution model.

3.3.4 Alpha, Beta and Gamma Dose Rates

The alpha dose rates in water in contact with used CANDU fuel with a burnup of 220 MWh/kgU were calculated by Garisto et al. (2009) and are shown in Figure 3-2. These dose rates were calculated from the alpha dose rates in fuel and the relative stopping power of alpha particles in water relative to uranium dioxide. A similar approach was used to calculate the beta dose rates in water.

The main uncertainties in these calculations arise from the uncertainties in the radionuclide inventories and the variability (with particle energy) of the relative mass stopping power of alpha and beta particles. At times > 1000 years, the largest uncertainty in the calculated alpha dose rates, about 15%, is due the variability of the relative mass stopping of alpha particles (Garisto et al. 2009). Similarly, independent of the decay time, the largest uncertainty in the calculated beta dose rates, about 20%, is due to the variability of the relative mass stopping power of beta particles (Garisto et al. 2009).

Garisto et al. (2009) also calculated the gamma dose rates in various locations within a water filled used fuel container. In this case, the main uncertainty in the calculated gamma dose rates arises from the uncertainties in the gamma photon spectra, which are related to the uncertainties in the radionuclide inventories. Garisto et al. (2009) estimate that the uncertainties in the gamma dose rates vary from about 20% at decay times less than about 300 years, when gamma dose rates are high, to about 10% at long decay times.

3.4 RADIONUCLIDE RELEASE FROM THE ZIRCALOY CLADDING

The Zircaloy cladding is a small contributor to the total radioactivity in used fuel, as indicated in Figure 3-3, which was calculated using data from Tait et al. (2000). Thus, radionuclides from the Zircaloy cladding are generally not important contributors to the calculated total radiological dose rates to a critical group (NWMO 2012a; Garisto et al. 2004, 2005a).

CC4 models the release of contaminants from the Zircaloy as having a fast component (instant release) and a slow congruent release component. However, in the current CC4 dataset, only the radionuclide C-14 has a non-zero instant release fraction.

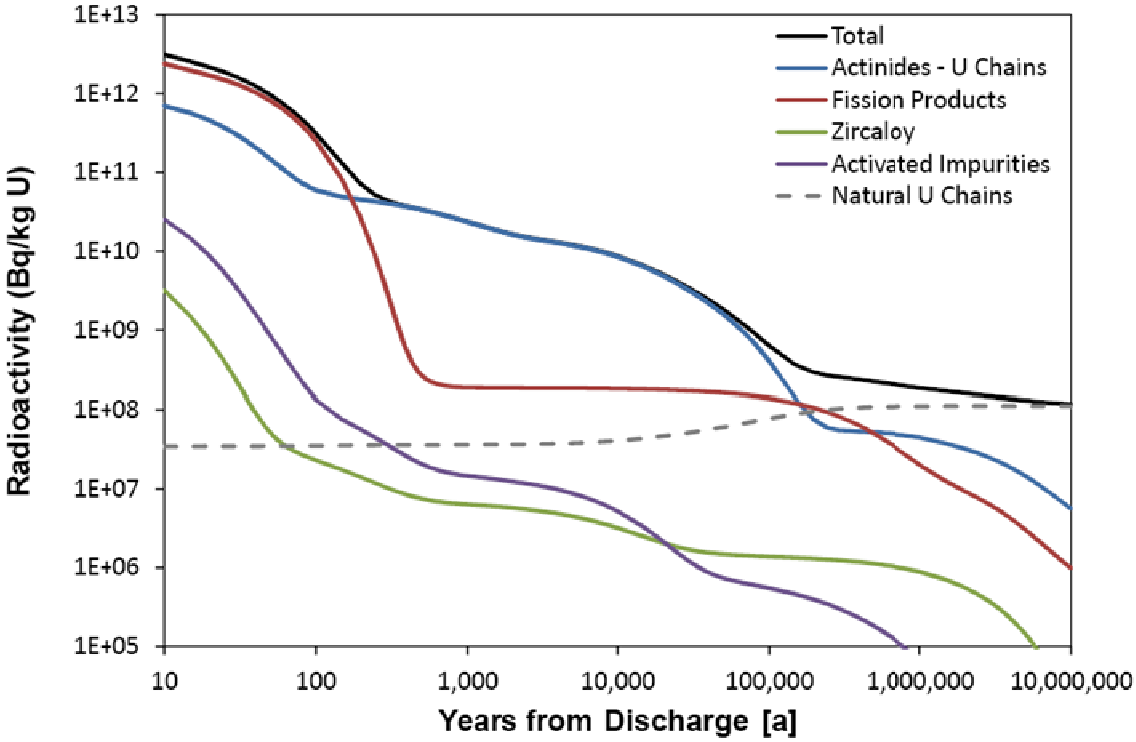

Note: After about 1 million years, the remaining activity is largely that due to the natural uranium content of the fuel.

Figure 3-3: Radioactivity of used fuel (220 MWh/kgU burnup) as a function of time after discharge from reactor showing that fission products dominate at short times, but have decayed to low levels after 1000 years

Radionuclides are generated in the Zircaloy cladding by neutron activation while the fuel is in reactor. These products should be uniformly distributed within the Zircaloy due to the thinness of the Zircaloy. Similarly, chemical element impurities within the Zircaloy, which are potential contaminants, should also be uniformly distributed within the Zircaloy. Consequently, as the Zircaloy in a breached used fuel container corrodes, the contaminants (radionuclides or chemical elements) should be congruently incorporated into the growing zirconium oxide corrosion layer, given the strong adherence of the corrosion product to the Zircaloy (Shoesmith and Zagidulin 2010). As a result, contaminants would only be released from the Zircaloy as the oxide film dissolves. This oxide film is expected to dissolve slowly because of its low solubility under repository conditions, i.e., 1.8×10^{-5} mol/m^3 (Duro et al. 2010).

In CC4, the rate of dissolution of the zirconium oxide film is calculated using a solubility-limited dissolution model (Johnson et al. 1994). In this model, the concentration of zirconium in the failed container is set equal to the solubility of the oxide and the oxide dissolves at the rate required to maintain this zirconium concentration. Thus, the rate of Zircaloy dissolution is equal to the rate at which zirconium is transported out of the container. This transport rate is based on the steady-state diffusion gradients through the defect in the container wall and into the surrounding buffer and uses well-founded mass transport principles. Validation of the container release model is described in Section 3.6.

There have been no tests of the solubility-limited dissolution model used to calculate contaminant release rates from the Zircaloy cladding.

3.5 SOLUBILITY

Radionuclides in the container are precipitated if their concentration exceeds the solubility limit of the element. The solubilities of the elements can be calculated using chemical equilibrium codes such as PHREEQC (Parkhurst and Appelo 1999), based on the expected groundwater composition in the container, as was done for the Fourth Case Study (Duro et al. 2010). PHREEQC is widely used internationally for doing chemical equilibrium calculations. The reliability of the calculated solubilities depends mainly on the reliability of the selected thermodynamic data used in the calculations.

CC4 has the capability to calculate solubilities for uranium, thorium, plutonium, neptunium and technetium (NWMO 2012b), if the solids controlling the element solubility are known *a priori*. Although this capability was not used in the recent Fourth Case Study, the solubilities calculated by the two codes should be the same, if the thermodynamic data and groundwater composition used by the two codes are identical.

There may be more than one isotope of a chemical element released inside the container. All such isotopes contribute to the element solubility limit. If precipitation occurs, all isotopes precipitate together. Since significant isotopic separation is not expected in the release processes, the element solubility is distributed among the isotopes according to their time-dependent inventory in either the UO_2 fuel or Zircaloy. Conservatively, the solubility limits are applied separately to the contaminants from the UO_2 fuel and Zircaloy wasteforms, i.e., contaminants released from one wasteform are assumed not to influence precipitation of isotopes from the other wasteforms.

3.6 CONTAINER RELEASE MODEL

Radionuclides (or chemical contaminants) released from the fuel are assumed to dissolve in the water within the container and, in CC4, their concentrations in the container are calculated assuming they are well-mixed on timescales of interest. Radionuclide releases from the container occur by diffusion through the defect in the container, with the diffusion rate controlled either by the defect size or by the surrounding clay-based buffer material. CC4 assumes that the defect size, container dimensions and the material properties are constant. Nuclide transport through the defect is modelled using the standard 1-D diffusion equation.

The general nature of a defect as a result of an undetected fabrication fault is illustrated by the full-scale copper container fabrication tests conducted by SKB and Posiva. These tests indicate that an undetected fabrication defect is most likely to occur within the copper lid weld, and not exceed 20 mm depth. In part as a result of this evidence, SKB does not consider an initial container defect as part of its normal evolution scenario (SKB 2011), while Posiva assumes one such defective container (Posiva 2013, Smith et al. 2007).

3.6.1 Small Defects

CC4 implicitly assumes that the defects in the container are small. In CC4, the release rate of a contaminant from the container is bounded by two cases (NWMO 2012b):

1. Release is limited by mass transport in the buffer layer surrounded the container, referred to as "buffer-limited" release; or

2. Release is limited by mass transport through the defect, referred to a "defect-limited" release.

The case with the lower release rate provides the principal mass transport resistance and is taken as the release rate from the container. For long-lived contaminants, after attainment of steady state conditions, the two release rates are given by the equations:

$$F_{buff} = 4R_{def}D_{e,buf}\,C_0\ , \text{ for buffer-limited release} \quad (3.6)$$

$$F_{def} = A_{def}\,D_{def}/L_{def}\,C_0, \text{ for defect-limited release.} \quad (3.7)$$

where R_{def} is the circular radius of the defect, A_{def} is the area of the defect, L_{def} is the length of the defect, D_{def} is the diffusion coefficient of the contaminant in the defect, $D_{e,buf}$ is the intrinsic diffusivity of the contaminant in the buffer and C_0 is the nuclide concentration in the container interior. Steady state conditions are generally approached rapidly relative to the time scale of interest (NWMO 2012b, LeNeveu 1996).

Use of the minimum of Equation 3.6 or 3.7 is conservative, since the mass transport resistances of the defect and the buffer both affect the release rate of contaminants out of the container. An approximation to the release rate out of the container, taking into account both mass transport resistances, is given by

$$F_{tot} = 1/(1/F_{buff} + 1/F_{def}) \quad (3.8)$$

For I-129 releases from a container, Table 3-4 compares the three release rates in Equations 3.6 to 3.8.

3.6.1.1 Comparison of CC4 Analytical Equations with COMSOL

A COMSOL model was developed by Beauregard et al. (2010) to calculate the rate of release of contaminants out of a breached container with a small defect. Their results are shown in Table 3-4. Comparison of the analytical and COMSOL results indicates that Equation 3.7 is conservative since it assumes that the contaminant is well mixed in the container, whereas the concentration near the entrance to the defect becomes slightly lower than that in the middle of the container (Beauregard et al. 2010). Also, the COMSOL results show that releases from the container are affected by both the mass transport resistance of the defect and the buffer. The COMSOL results for F_{tot} is not identical to the analytical result because Equation (3.8) is an approximation and because Equation (3.6) is valid for a semi-infinite geometry whereas, in COMSOL, a zero concentration boundary condition was used at outer boundary of the (finite) model domain (Beauregard et al. 2010).

Table 3-4: Various Release Rates of I-129 from a Container (Beauregard et al. 2010)

Defect Properties	I-129 Properties
R_{def} = 8.25x10^{-4} m L_{def} = 0.025 m	$D_{e,buf}$ = 8.73x10^{-4} m^2/a D_{def} = 0.172 m^2/a C_0 = 7.69x10^{-2} mol/m^3
Analytical Results	COMSOL Results
F_{def} = 1.13x10^{-6} mol/a	F_{def} = 1.05x10^{-6} mol/a
F_{buff} = 2.22x10^{-7} mol/a	F_{buff} = not determined
F_{tot} = 1.85x10^{-7} mol/a	F_{tot} = 1.95x10^{-7} mol/a

3.6.1.2 Comparison of CC4 and COMSOL

Releases out of the container calculated by CC4 (Version SCC4.09.1) for several radionuclides (Ca-41, I-129 and Cs-135) and a radionuclide decay chain (Pu-242 → U-238 → U-234) were also compared to the corresponding results from COMSOL. For this test case, the two models used data from the Fourth Case Study (Garisto et al. 2012), with the exception that the radionuclides were assigned high solubilities, i.e., there was no radionuclide precipitation in the container. For this case, the defect radius was 0.001 m.

The radionuclide releases from the fuel were identical in the two models. COMSOL models the container internal volume as a porous medium, with a pore volume equal to the void volume of the container in the CC4 model. In COMSOL, radionuclide releases from the fuel are applied equally throughout the interior of the container and diffusion of radionuclides within the interior of the container is explicitly modelled, using the radionuclide free water diffusion coefficients. However, in CC4, radionuclides are assumed to be well mixed within the container.

Another key difference between the two models is how releases from the container are calculated. As previously noted, in CC4, releases from the container are calculated using the smaller of Equation 3.6 or 3.7. In COMSOL, radionuclide transport through the defect and into the buffer is explicitly modelled, and the radionuclide release rate out of the container is affected by the mass transport resistances of both the defect and the buffer. Accumulation of a radionuclide in the buffer due to ingrowth from a parent nuclide would be expected to affect the release rate of the progeny from the container. This effect is apparent in the COMSOL results for U-234 (see below) but is conservatively neglected in CC4.

The COMSOL and CC4 radionuclide mass flows out of the container are compared in Figure 3-4 and Table 3-5. The mass flows out of the container calculated by the two models are similar, although the CC4 mass flows are consistently marginally higher. As sorption in the buffer increases, the difference in the calculated peak mass flows increases (see Table 3-5). Thus, for the non-sorbing I-129, the peak mass flow out of the container is 9% larger in CC4; whereas, for the strongly sorbing Pu-242, the peak mass flow is 28% larger in CC4.

At long times, the calculated mass flows calculated by the CC4 and COMSOL models agree very well except for U-234, with the CC4 mass flow for U-234 more than 2-fold higher at 10^6 years. At these long times, the U-234 mass flow out of the container calculated by COMSOL is much lower because it is affected by the ingrowth of U-234 from the U-238 that has accumulated in the buffer outside the defect. That is, the additional U-234 generated by decay of U-238 reduces the U-234 concentration gradient between the inside of the container and buffer porewater and, hence, the U-234 mass flow out of the container. This effect is more apparent at longer times because U-238 has a long half-life. As previously noted, this effect is conservatively neglected in the CC4 model.

Overall, the results in Figure 3-4 and Table 3-5 indicate that there is good agreement between the CC4 and COMSOL models, although the peak mass flows calculated by CC4 are higher.

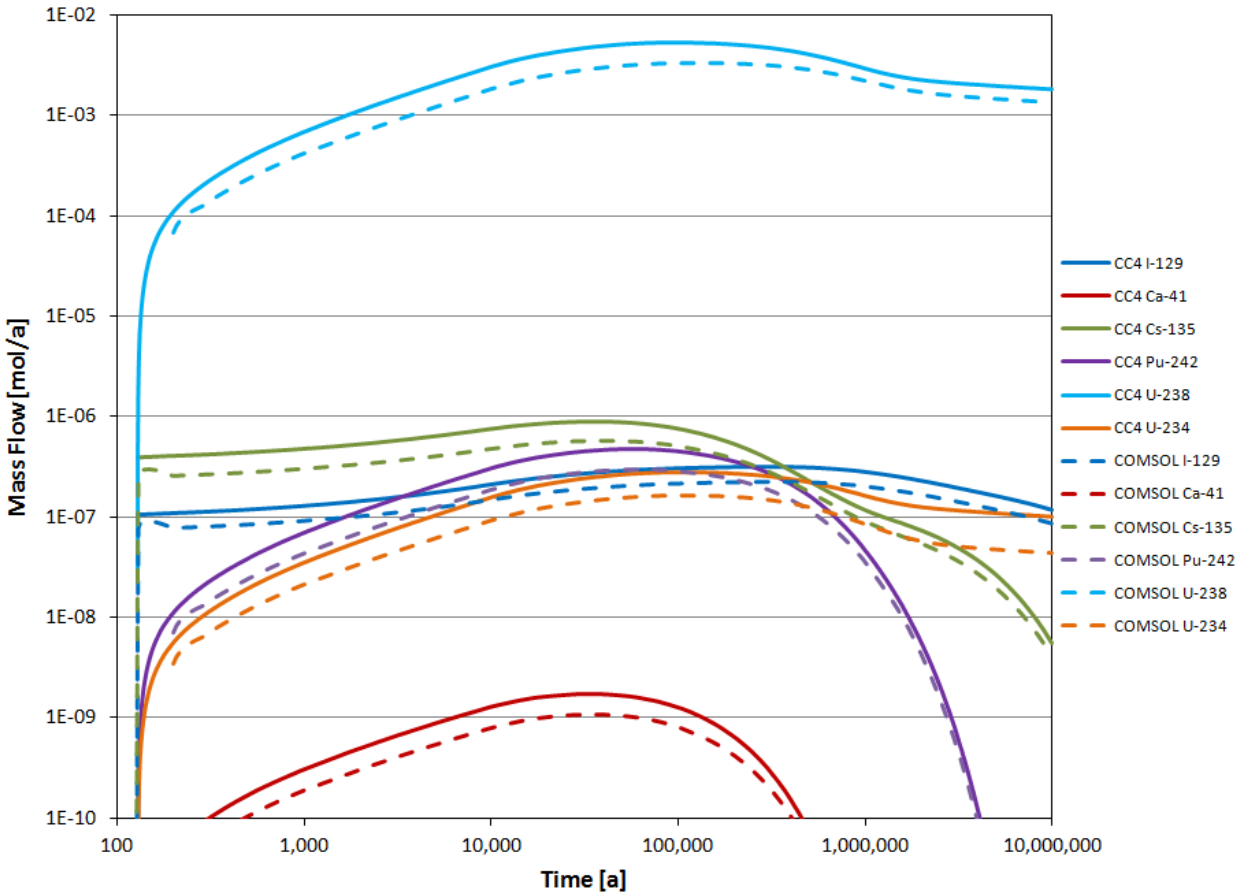

Note: In this calculation, the radionuclide solubilities are assumed to be large so there is no radionuclide precipitation in the container.

Figure 3-4: CC4 and COMSOL mass flows out of a container with a small defect

Table 3-5: CC4 and COMSOL Mass Flows out of a Container with a Small Defect[1]

Nuclide	CC4 Time of Peak [a]	CC4 Peak Mass Flow [mol/a]	COMSOL Time of Peak [a]	COMSOL Peak Mass Flow [mol/a]	Ratio of CC4 to COMSOL Time of Peak	Ratio of CC4 to COMSOL Peak Mass Flow
I-129	2.87×10^{5}	3.12×10^{7}	3.00×10^{5}	2.86×10^{7}	0.96	1.09
Ca-41	3.20×10^{4}	1.71×10^{9}	3.00×10^{4}	1.36×10^{9}	1.07	1.26
Cs-135	3.70×10^{4}	9.01×10^{7}	4.00×10^{4}	7.45×10^{7}	0.92	1.21
Pu-242	5.60×10^{4}	4.80×10^{7}	6.00×10^{4}	3.76×10^{7}	0.93	1.28
U-238	2.74×10^{4}	4.51×10^{3}	1.00×10^{5}	4.23×10^{3}	0.27	1.07
U-234	4.90×10^{4}	2.59×10^{7}	1.00×10^{5}	2.08×10^{7}	0.49	1.25

[1]Defect radius = 0.001 m.

3.6.1.3 Comparison of CC4 and ANSYS

Goodwin et al. (2002) compared the I-129 release rates from a container with a small defect calculated by SYVAC3-CC4 (Version SCC02) with those calculated using the finite element code ANSYS. The steady-state results are shown in Table 3-6. As expected, the release rates calculated by CC4 are larger than those calculated with ANSYS because CC4 uses either the mass transport resistance of the buffer or the defect, whichever is larger, in calculating the release rates from the container whereas in the ANSYS model both mass transport resistances affect the release rates from the container.

Table 3-6: Steady-State Release Rates of I-129 from a Container (Goodwin et al. 2002)

Test	Defect Radius (m)	CC4 (mol/a)	ANSYS (mol/a)	Ratio (CC4 to ANSYS)
Test 1 Buffer limited	1.5×10^{-3}	7.07×10^{-5}	4.06×10^{-5}	1.74
Test 2 Defect limited	1.5×10^{-4}	2.25×10^{-6}	1.55×10^{-6}	1.45
Test 3 Buffer and defect limited	4.7×10^{-4}	2.21×10^{-5}	9.14×10^{-6}	2.41

Note: D_{def} = 0.094 m^2/a, $D_{e,buf}$ = $1.4\times10^{-3} m^2/a$, K_d = 0 m^3/kg and C_0 = 8.49 mol/m^3

Goodwin et al. (2002) also examined the influence of the buffer capacity factor on radionuclide releases from the container at shorter times, i.e., before attainment of steady-state conditions. Their results are shown in Figure 3-5. In Tests 4, 5 and 6 the buffer capacity factor was set to 10^4, 0.05 and 10^4, respectively. Also, the defect radius was 1.5×10^{-3} m for these three tests and the values of D_{def}, $D_{e,buf}$, and C_0 are the same as shown in Table 3-6

At short times (t < 20 years), release rates from the container are underestimated by CC4 by about a factor of three for cases in which the buffer capacity factor is large and releases from the container are mainly controlled by the mass transport resistance in the buffer (i.e., Tests 4

and 6). However, at longer times the CC4 release rates are conservative by about a factor of two. Thus, over the time scales of interest (t >> 20 years), the total radionuclide releases from the container calculated by CC4 are larger than that those calculated with the more exact numerical model.

ANSYS was also used to investigate whether the shape or aspect ratio of the defect (i.e., the ratio of the width to height of the defect) affects radionuclide releases from a container. The ANSYS results indicate that releases are mostly dependent on the cross-sectional area of the idealized defect, with only a small dependence on the shape of the defect even when the aspect ratio is changed from 1:1 to 10:1 (Goodwin et al. 2002). This is in accord with analytical results that indicate that for an elliptical defect with semi-axes ratios > 0.1, the steady-state releases out of the elliptical defect are less than 1.4 times larger than for a circular defect with the same area as the elliptical defect (Chambre et al. 1986).

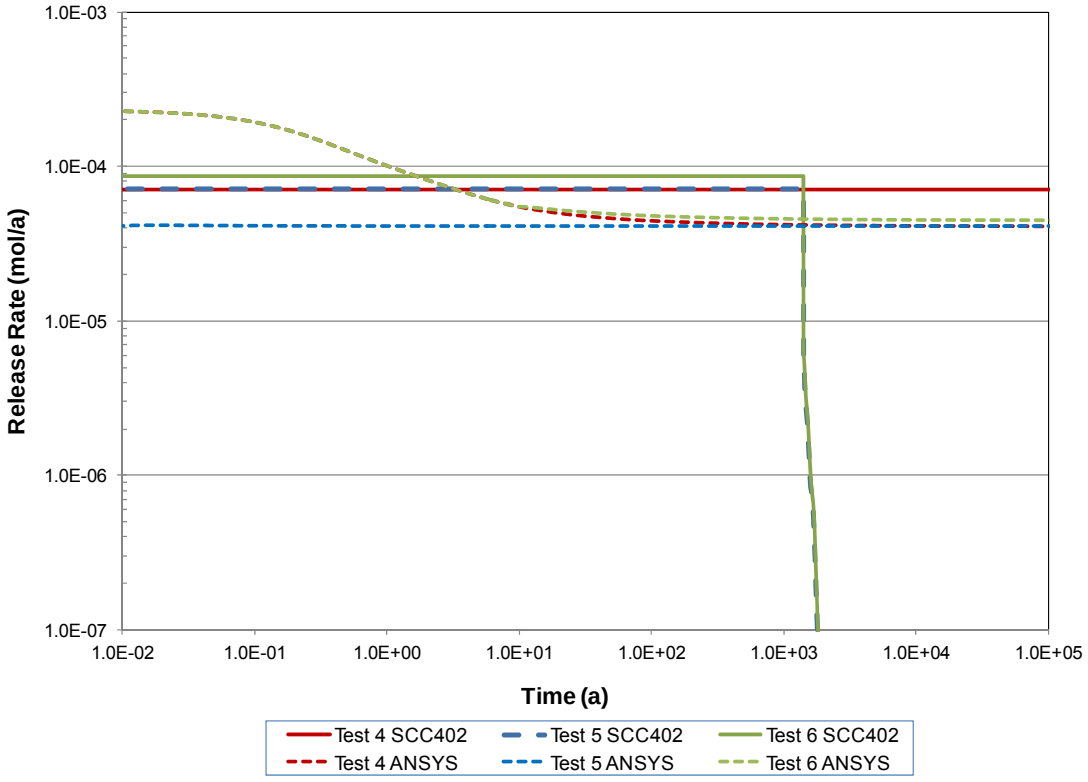

Note: For Tests 5 and 6, the radionuclide decay constant, λ, was set to 0.01/a in CC4 but not in ANSYS. This makes the releases rates calculated by CC4 go to zero at about 1500 years. For all tests, defect radius = 1.5×10^{-3} m, D_{def} = 0.094 m^2/a, $D_{e,buf}$ = $1.4 \times 10^{-3} m^2/a$ and C_0 = 8.49 mol/m^3.

Figure 3-5: Comparison of CC4 and ANSYS models for mass flow out of defect (Goodwin et al. 2002)

3.6.2 Large Defects

In this section, the calculated release rates of I-129 and U-238 from a breached container calculated by CC4 are compared to the corresponding results from COMSOL for a variety of defect sizes.

For this test case, the two models used data from the Fourth Case Study (Garisto et al. 2012). Thus, I-129 is not sorbed in the buffer whereas U-238 is strongly sorbed. Also, U-238 was assigned a solubility of 3.5×10^{-5} mol/m^3 in the CC4 calculations, based on the data in Garisto et al. (2012); whereas, in COMSOL, the U-238 concentration in the container was set to 3.5×10^{-5} mol/m^3 throughout the simulations. This difference should not affect the model comparisons since U-238 reaches its solubility limit in the CC4 simulations fairly rapidly. I-129 is assigned a high solubility limit in both models and so does not precipitate in the container.

I-129 releases from the fuel were identical in the two models. COMSOL models the container internal volume as a porous medium, with a pore volume equal to the void volume of the container in the CC4 model. Further, in COMSOL, radionuclide releases from the fuel are applied equally throughout the interior of the container and diffusion of radionuclides within the interior of the container is explicitly modelled, using the radionuclide free water diffusion coefficients. However, in CC4, radionuclides are assumed to be well mixed within the container.

The results of the CC4 and COMSOL calculations are compared in Figure 3-6 through Figure 3-8 and in Table 3-7. Generally, the I-129 mass flows out of the container calculated by the two models agree fairly well regardless of the defect size. This is due to the fact that, for large defects, the I-129 release rate out of the container is controlled by the fuel dissolution rate and not by the defect size or buffer transport properties. However, for very large defect sizes, the I-129 mass flows out of the container calculated by COMSOL are significantly larger at shorter times; consequently, the peak I-129 mass flows calculated by COMSOL are significantly larger than those from CC4 for very large defect sizes (see Table 3-7).

Table 3-7: Peak Mass Flows from Container as a Function of Defect Size

Defect Size [m]	SYVAC3-CC4		COMSOL		I-129	U-238
	Peak I-129 Mass Flow [mol/a]	Peak U-238 Mass Flow [mol/a]	Peak I-129 Mass Flow [mol/a]	Peak U-238 Mass Flow [mol/a]	Ratio of CC4 to COMSOL Peak Mass Flow [-]	Ratio of CC4 to COMSOL Peak Mass Flow [-]
0.001	3.12×10^{-7}	1.40×10^{-10}	2.68×10^{-7}	1.17×10^{-10}	1.16	1.20
0.01	2.19×10^{-6}	6.15×10^{-9}	2.14×10^{-6}	1.25×10^{-8}	1.02	0.49
0.05	7.41×10^{-6}	3.08×10^{-8}	7.70×10^{-6}	1.32×10^{-7}	0.96	0.23
0.1	1.24×10^{-5}	6.17×10^{-8}	2.32×10^{-5}	4.36×10^{-7}	0.53	0.14
0.3	3.20×10^{-5}	1.86×10^{-7}	1.63×10^{-4}	1.98×10^{-6}	0.20	0.09
0.5	5.24×10^{-5}	3.12×10^{-7}	4.16×10^{-4}	4.52×10^{-6}	0.13	0.07

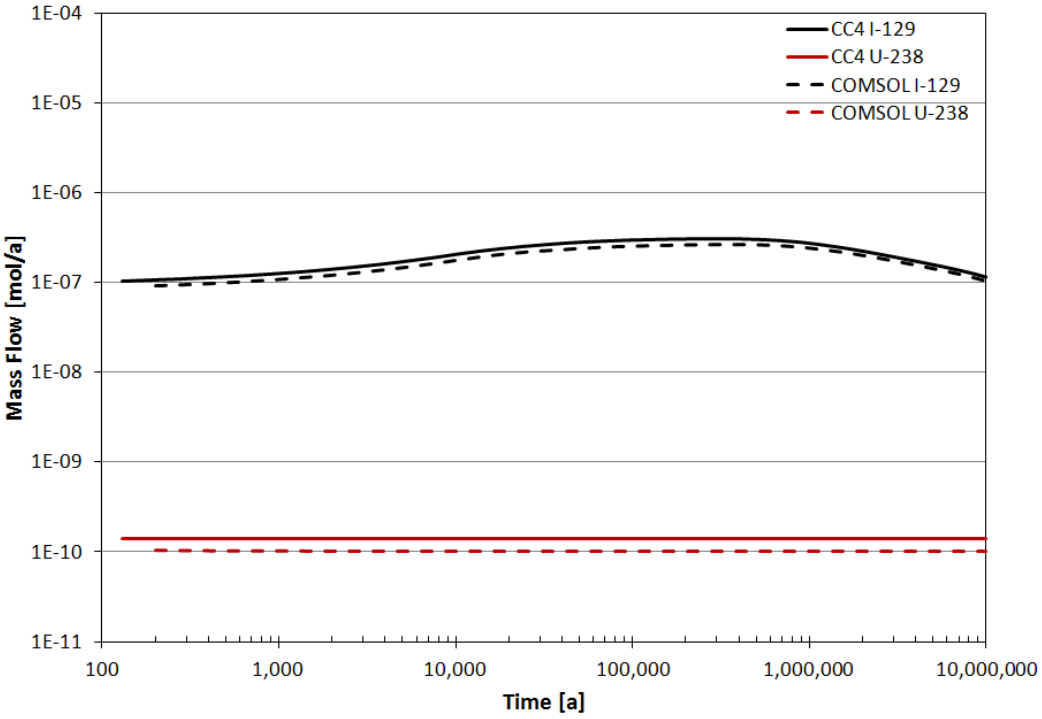

Figure 3-6: CC4 versus COMSOL for a defect radius of 1 mm

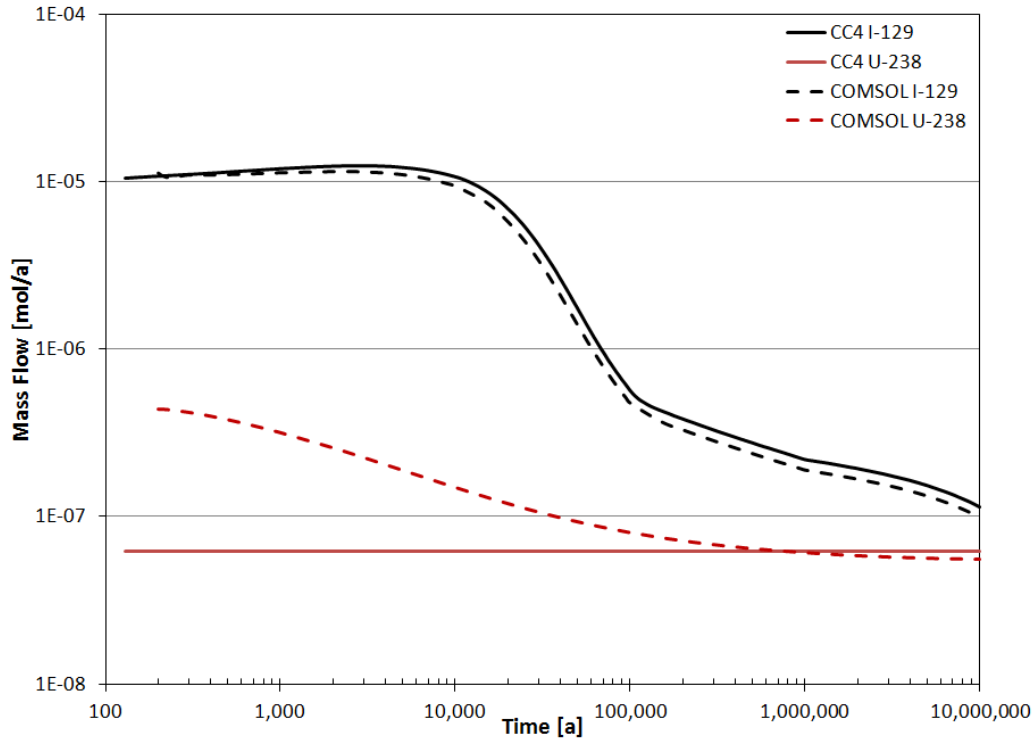

Figure 3-7: CC4 versus COMSOL for a defect radius of 10 cm

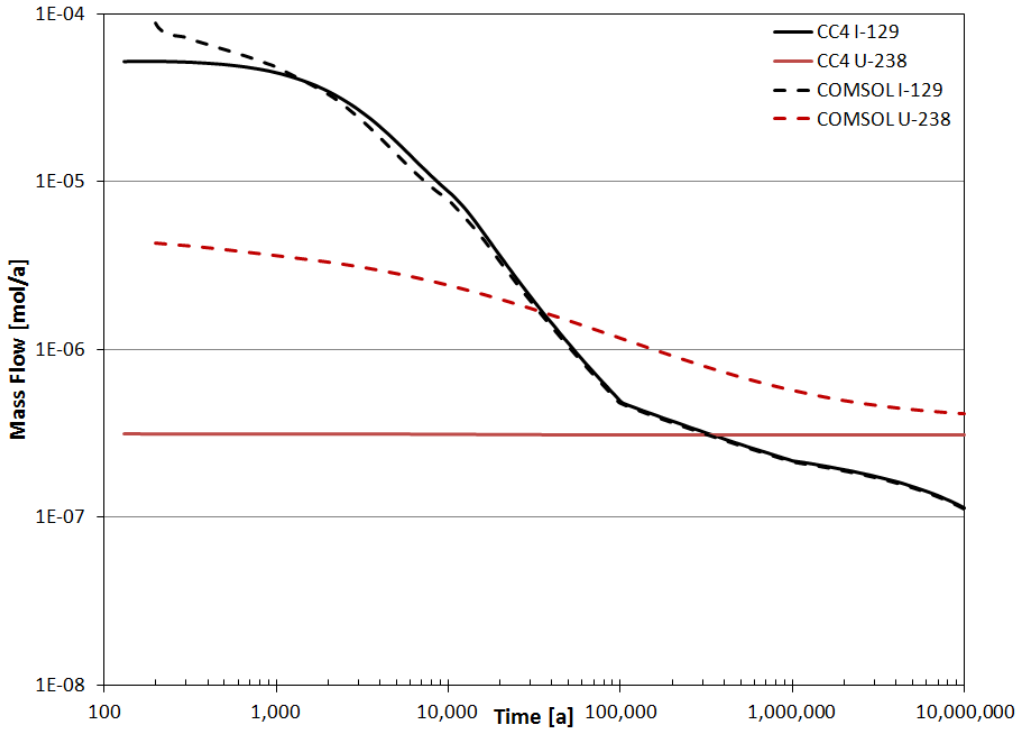

Figure 3-8: CC4 versus COMSOL for a defect radius of 50 cm

For U-238, the mass flows out of the container predicted by CC4 and COMSOL progressively diverge as the defect size increases. For small defect sizes (see Figure 3-6), the agreement between the SYVAC3-CC4 and COMSOL models is quite good for U-238. However, for the largest defect sizes, the peak U-238 mass flow out of the container calculated by COMSOL is more than 10-fold larger than the corresponding CC4 value (see Table 3-7). Note that, in comparison to the I-129 case, the U-238 concentration in the container is essentially constant and so the U-238 mass flow out of the container is independent of the U-238 releases from the fuel even for large defect sizes.

The large differences between the two models for U-238 for large defects are due to the fact that the CC4 model uses the steady state mass flow rate out of the container (as determined by the minimum of Equation 3.6 or 3.7). That is, the transient portion of the container release curve is neglected in CC4 and, consequently, CC4 underestimates the mass flow rate out of the container at shorter times for large defects. For U-238, the transient portion of the container release curve is long (and increases with defect size) because U-238 sorbs strongly to the bentonite buffer. For non-sorbing radionuclides, the transient portion of the container release curve would be much shorter and so steady state would be attained much sooner.

In conclusion, for sufficiently long times, the radionuclide mass flows out of a defective container calculated by CC4 agree fairly well with COMSOL for defects with a radius smaller than a couple of centimetres. (The CC4 model is conservative in these cases since, as discussed above, it uses the minimum of the buffer-limited or defect-limited mass transport resistances.) For defects with a radius greater than a couple of centimetres, CC4 remains valid for

radionuclides that do not precipitate in the container since, in this case, the radionuclide release rate out of the container is limited by the radionuclide release rate from the fuel. However, CC4 can significantly underestimate the container release rates at earlier times (i.e., before attainment of steady state) for radionuclides that precipitate in the container, particularly for radionuclides that are sorbed strongly by the buffer. This limitation of CC4 needs to be considered when carrying out safety assessment calculations.

3.7 NUCLIDE TRANSPORT IN THE REPOSITORY

In CC4, transport from the container, through the repository and into the geosphere is modelled with the INROC repository transport model. INROC was developed to model radionuclide transport through a repository using in-room container placement or horizontal borehole container placement, as illustrated in Figure 3-9.

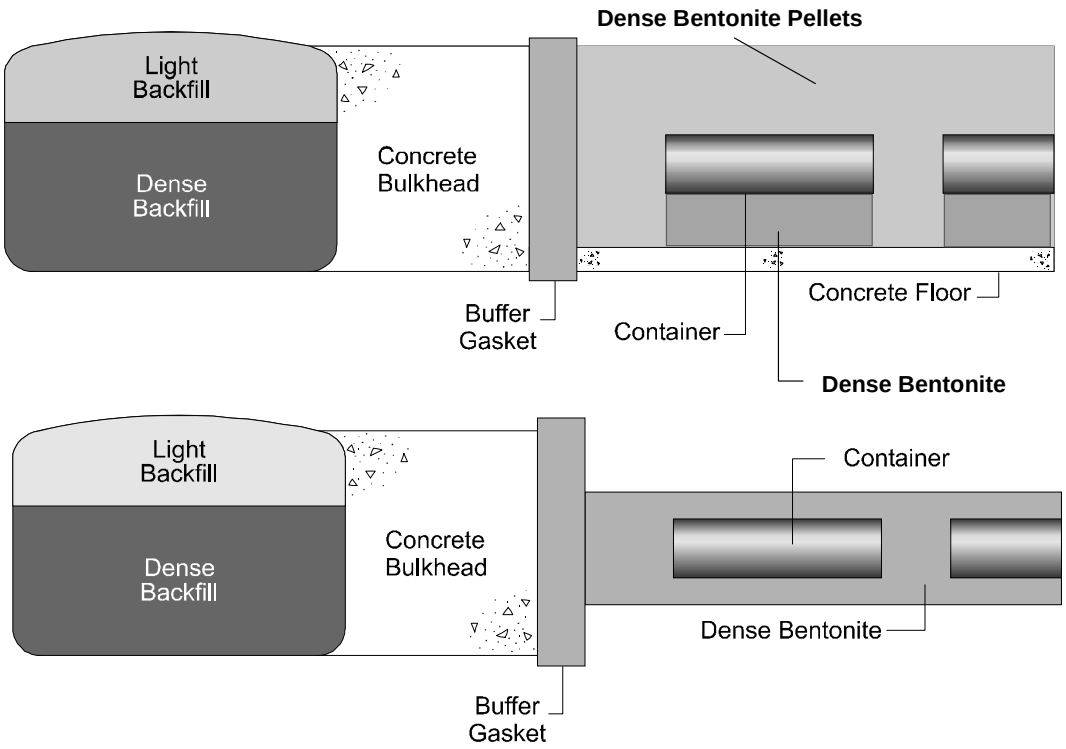

Figure 3-9: Schematic representations of container placement options (not to scale): in-room (top) and horizontal borehole (bottom)

In INROC, each placement room is modelled as a set of three concentric cylinders representing the buffer, backfill and EDZ, as shown in Figure 3-10. The radionuclide source (i.e., the container defect) is located on the axis of the cylinders; the container itself is not modelled explicitly. The advection-dispersion equation for this repository geometry is solved approximately using a semi-analytical algorithm to obtain, given the release rate of a radionuclide out of the container, the radionuclide transport rate out of the buffer, out of the backfill, and out of the excavation damage zone (EDZ) and into the geosphere. The approximations made include the following: the space occupied by the containers in the room is excluded from the model; the radius of the buffer and backfill zones are chosen to conserve the volumes of these materials; and continuity of flux and concentration, integrated over the interface between the different materials, are used as the interfacial boundary conditions. One consequence of using integrated continuity conditions is that the model results become insensitive to the position of the source within the room (LeNeveu and Kolar 1996).

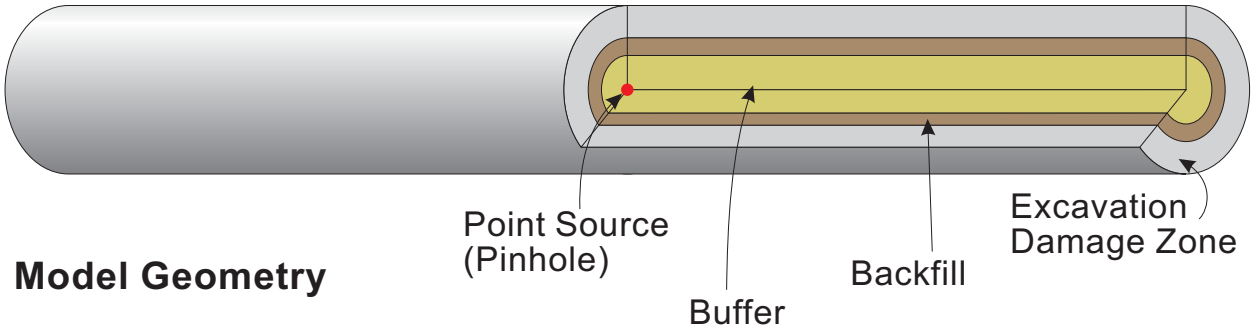

Figure 3-10: Placement geometry used in the SYVAC3-CC4 repository model (not to scale)

The CC4 model assumes that the bentonite based sealing materials (buffer and backfill layers) are durable and do not change with time. This assumption is supported by an examination of the properties of bentonite as it occurs in the field. Oscarson et al. (1990) studied the properties of intact, unprocessed clay from the Avonlea deposit, which is about 80 million years old. The clay still maintains a significant swelling capacity and low hydraulic conductivity and exhibits a remarkable ability to self seal. Similar observations have been made by others (Pusch et al. 1987, Pusch and Karnland 1990). A summary of buffer and backfill properties and stability is provided in Pusch (2001). These results provide confidence that the sealing materials will remain an effective barrier for millions of years.

Factors that would affect the clay durability are high temperatures (greater than 100°C) for an extended period, high alkalinity (e.g., if there is large amounts of nearby cement), high water flow rates (leading to erosion), high levels of certain species in groundwater (notably K), and very low salinity groundwater (which allows the clay to gel and become susceptible to dispersion). These factors are considered in the design of the repository (e.g., spacing of placement rooms and containers to control temperature) and repository siting (e.g., groundwater composition).

The applicability of the advection-dispersion equation is supported by laboratory and field evidence. Laboratory diffusion experiments, for example, have shown that the movement of radionuclides in clay-based buffer and backfill materials can be predicted by use of diffusion models. In fact, the apparent diffusion coefficients of radionuclides through the clay-based buffer and backfill are derived by fitting nuclide breakthrough curves to analytical solutions of the diffusion equation (Hume 1995, Oscarson et al. 1995).

CC4 uses standard mathematical techniques (the boundary integral method, Laplace transforms) to solve the 3-D advection-dispersion equation, assuming certain symmetries, linear sorption coefficients, constant material properties, and simplifying boundary conditions (LeNeveu 1994). The numerical techniques (e.g., numerical inversion of Laplace transform using Talbot algorithm) have been extensively verified. Both mass balance and behavioural checks (e.g., verifying that release is delayed with larger sorption values) have been applied.

Although idealized, the suitability of the CC4 placement room model solution has been tested by comparison with the results from other models as described in the sections below. The comparisons are generally shown in chronological order.

3.7.1 MOTIF Comparison

INROC, the repository transport model, which was previously referred to as the BIM model, was used in the Second Case Study as part of the SYVAC3-PR4 code (Wikjord et al. 1996). It was verified by comparison to MOTIF, a finite element groundwater flow and contaminant transport code (Chan et al. 2000) as described by Johnson et al. (1996) and LeNeveu and Kolar (1996). In this comparison, MOTIF modelled a placement room as three nested regions of square cross-section with volumes equal to those in the INROC model. The container was not present in either model. INROC makes simplifying assumptions regarding the groundwater flow in the buffer, backfill and EDZ, whereas MOTIF uses self-consistent flow rates in each region.

In the comparison, the INROC and MOTIF codes were used to calculate the mass flow of I-129 out of the buffer, backfill and EDZ regions (Johnson et al. 1996, LeNeveu and Kolar 1996). The I-129 source was a unit mass located along the horizontal axis of the buffer region. Two source locations were used, one at the centre of the axis and the other 10.5 metres from the right side of the room (with the horizontal groundwater flow going from left to right). The boundary conditions used in MOTIF were selected to mimic as closely as possible those used by INROC, but an exact match was not possible (LeNeveu and Kolar 1996). Several tests were carried out in order to verify INROC for different groundwater velocities in the buffer, backfill and EDZ regions. In these two studies, only the cumulative total mass flows of I-129 out of the three regions were compared (i.e., the integral over time of the total mass flow exiting a region).

The MOTIF and INROC results agreed well in the absence of groundwater flow or when the groundwater flow was in the vertical direction, i.e., perpendicular to the horizontal axis of the placement room. In these cases, the MOTIF results were independent of the source location. This good agreement between the INROC and MOTIF suggests that the exact shape of the placement room (circular in INROC and rectangular in MOTIF) is not very important as long as the total volumes of each material (buffer, backfill and EDZ) are the same in both models. This justifies approximating the placement room, which was elliptical in the Second and Third Case Studies, by a cylindrical room in INROC.

The differences between the two models increased as the horizontal groundwater velocities increased (see Figure 3-11, Figure 3-12 and Figure 3-13). Also, when the horizontal velocity was non-zero, the MOTIF results depended on the source location, and the largest differences between MOTIF and INROC occurred when the horizontal groundwater velocity was largest and the source was located near the right end of the placement room (with the groundwater flow from left to right).

For the case of a large horizontal velocity in the EDZ (see Figure 3-13), the integrated releases calculated by MOTIF preceded the INROC releases when the source is close to the end of the room; however, INROC is conservative with respect to MOTIF when the source is at the centre of the room. The larger differences seen in this case are partially due to the fact that, in INROC, the mass flows out of the different regions are not dependent on the source location due to the use of integrated continuity conditions, as previously discussed; and, partially due to the fact that the boundary conditions at the ends of the room are different in the two models.

From this information, for large axial flow velocities and for randomly occurring source positions, it can be inferred that the INROC model, on average, gives conservative values for the integrated releases from a placement room compared with MOTIF results.

The agreement between the two models is also best when comparing the cumulative nuclide flows out of the buffer. The differences observed between the cumulative nuclide flows out of the backfill (and EDZ), which are largest during the period when the cumulative nuclide flows increase rapidly, suggest that the predicted nuclide flows out of the backfill would differ significantly in the two models over this time period. However, for all cases investigated, the cumulative nuclide flows predicted by INROC are larger than those predicted by MOTIF as long as the source is in the centre of the placement room.

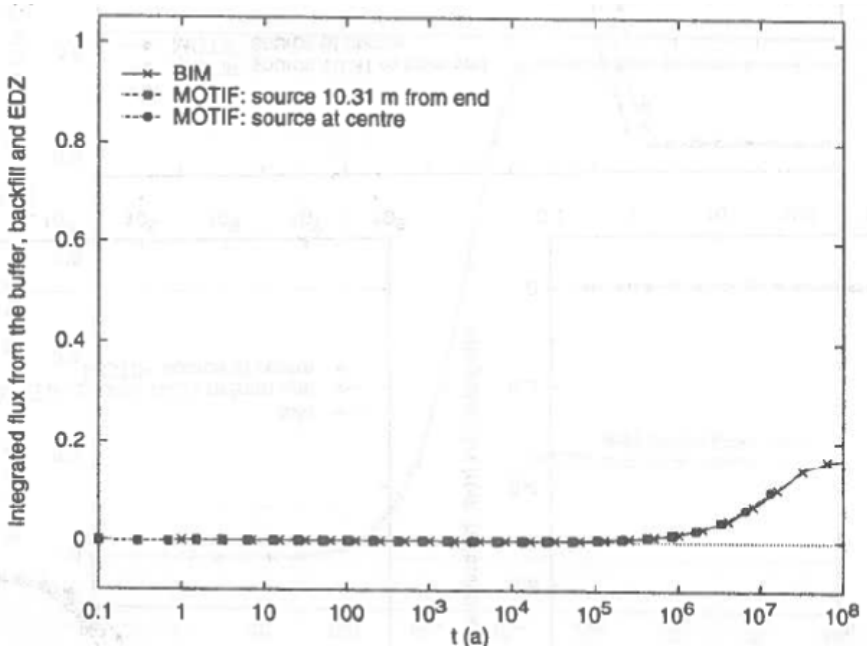

Figure 3-11: Comparison of INROC (formerly BIM) and MOTIF results for the case with zero groundwater velocities in all media

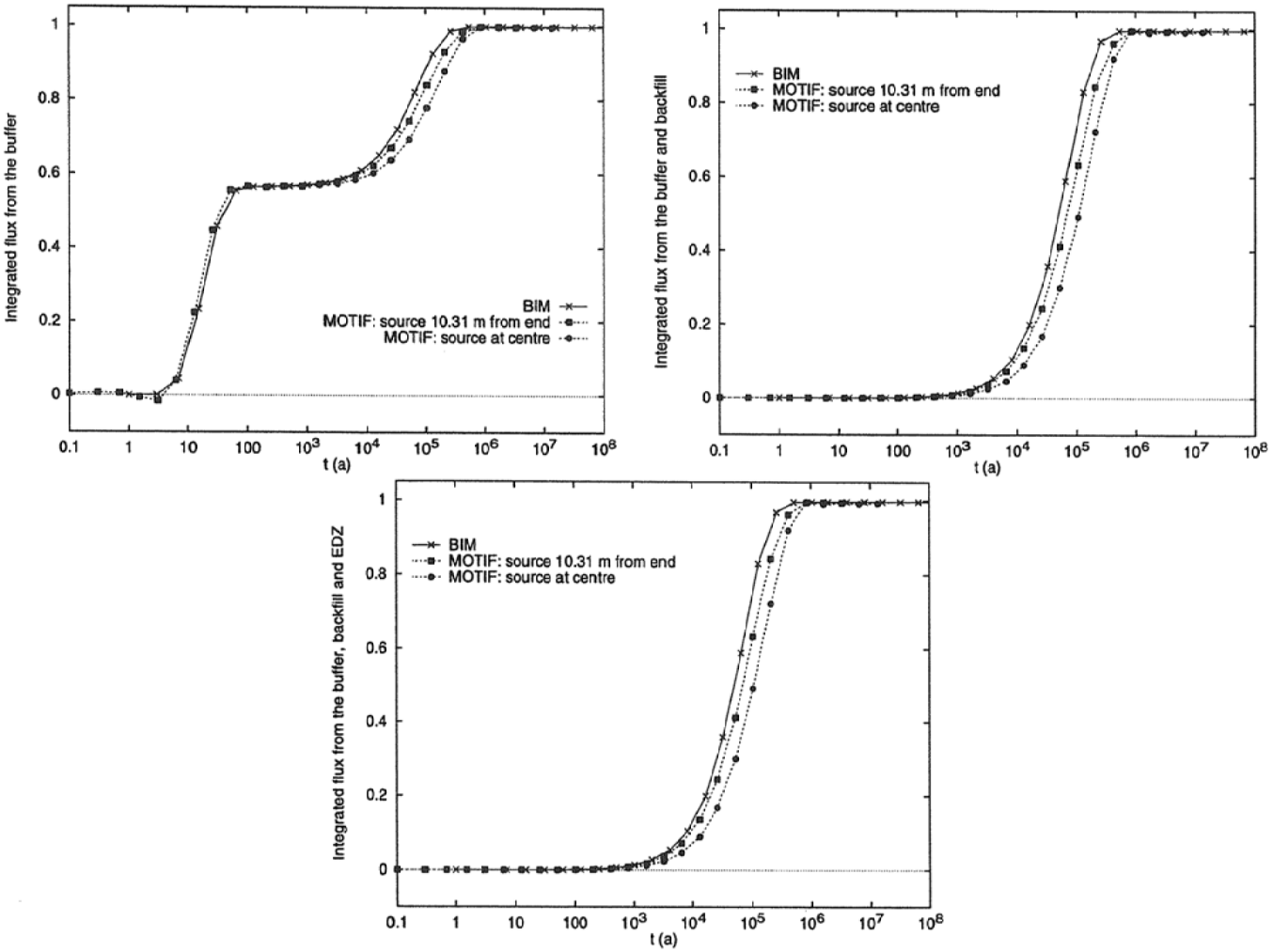

Note: Horizontal Darcy velocities are as follows: buffer V_y =0, backfill V_y = 2.04x10^{-5} m/a, EDZ V_y = 9.83x10^{-6} and rock V_y = 8.36x10^{-6} m/a.

Figure 3-12: Comparison of INROC (formerly BIM) and MOTIF results

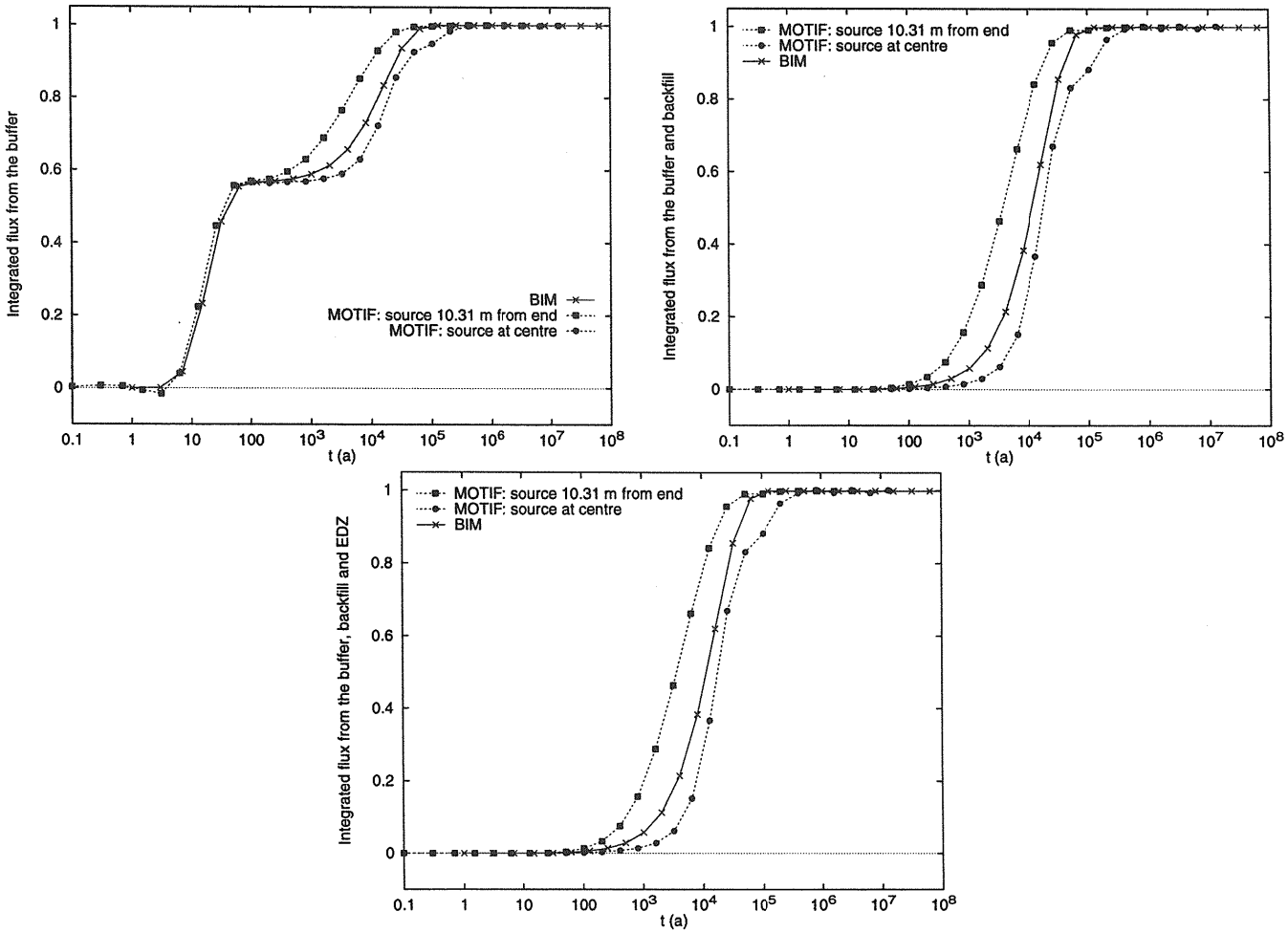

Note: Horizontal Darcy velocities are as follows: EDZ V_y = 8.36x10^{-4} m/a, buffer V_y =0, backfill V_y = 1.98x10^{-5} m/a and rock V_y = 8.36x10^{-6} m/a.

Figure 3-13: Comparison of INROC (formerly BIM) and MOTIF results for large horizontal Darcy velocities in the EDZ

3.7.2 COMSOL Comparison

In this section, radionuclide transport in the repository near-field as determined by SYVAC3-CC4 (Version SCC4.09.1) is compared to the corresponding results from COMSOL. Several test cases were run. In some tests, the COMSOL model repository geometry was identical to that used in INROC, the CC4 repository transport model; whereas, in others, the COMSOL model had a more exact representation of the repository geometry than INROC. The tests and test results are described below.

3.7.2.1 One-to-One Comparison

A COMSOL model was set up to duplicate, as much as possible, the INROC model geometry and boundary conditions. Both models included 3 concentric cylinders consisting of a 1m thick layer of buffer, a 50 cm layer of backfill and a 30 cm layer of EDZ. Beyond the EDZ layer, the COMSOL model included a 10 m thick layer of rock. A zero concentration boundary condition was used on the outer perimeter of the rock layer to approximate the semi-infinite rock layer modelled in CC4. All cylinders are 20 m long. The physical and chemical properties of the buffer, backfill, EDZ, and rock layers were taken from the Fourth Case Study (Garisto et al. 2012) and were identical in the two models. The groundwater flow velocities were very low in all layers, i.e., transport was diffusion dominated. Zero flux boundary conditions were used at the ends of the concentric cylinders in both models. The radionuclide source terms used in the COMSOL model were obtained from the output of the CC4 simulation which assumed that radionuclides do not precipitate in the container. In COMSOL, the radionuclide point sources were located at the mid-point along the central axis of the concentric cylinders.

Calculations were carried out for several radionuclides (Ca-41, I-129 and Cs-135) and a radionuclide decay chain (Pu-242 → U-238 → U-234). The buffer, backfill and EDZ sorption coefficients of these radionuclides vary over a wide range, from non-sorbing (I-129) to strongly sorbing (U-238). The total radionuclide mass flows at the buffer-backfill, backfill-EDZ and EDZ-rock interfaces are compared in Figure 3-14, Figure 3-15, and Figure 3-16, respectively.

Figure 3-14 shows that there is good agreement between the total mass flows calculated by COMSOL and CC4 models at the buffer-backfill interface regardless of the sorption properties of the radionuclide. The small tail seen at early times in the COMSOL results for U-238 is the result of the finite element approached used by COMSOL and could be resolved by further refining the mesh used in the COMSOL simulations.

Figure 3-15 shows the total mass flow of radionuclides at the backfill-EDZ interface. Generally, good agreement is obtained. However, some large differences do exist; most notably for the highly sorbing actinide radionuclides. The mass flows at the backfill-EDZ interface calculated by the CC4 model are generally lower than those from the COMSOL model. Because the nuclide mass flows calculated by CC4 and COMSOL are in good agreement at the buffer-backfill and EDZ-rock interfaces, it is likely that the differences observed between the two models in Figure 3-15 are due to the approximations made in the INROC model; in particular, in INROC, the continuity of flux and concentration, integrated over the interface between the different materials, is used as the interfacial boundary condition rather than continuity of flux and concentration at each point on the boundary. Also, of potential importance, except for I-129, the effective diffusion coefficients of the radionuclides are approximately two orders of magnitude lower in the EDZ than the backfill. For I-129, the difference is only about a factor of 4.

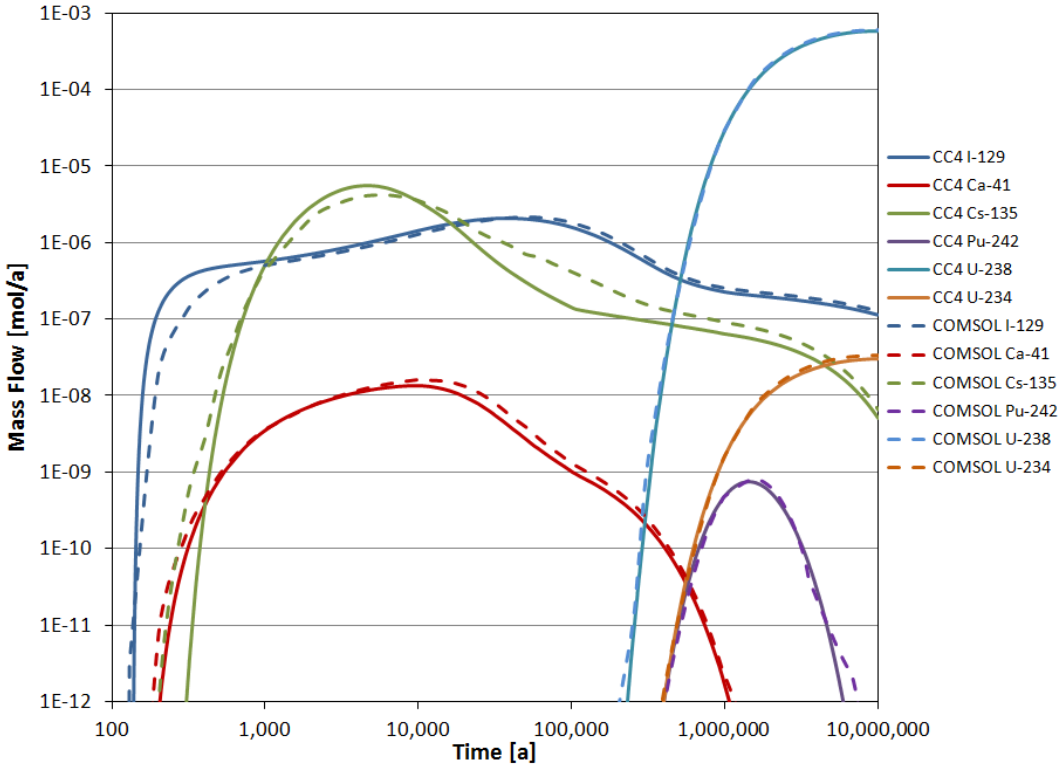

Figure 3-14: Mass flow at the buffer-backfill interface

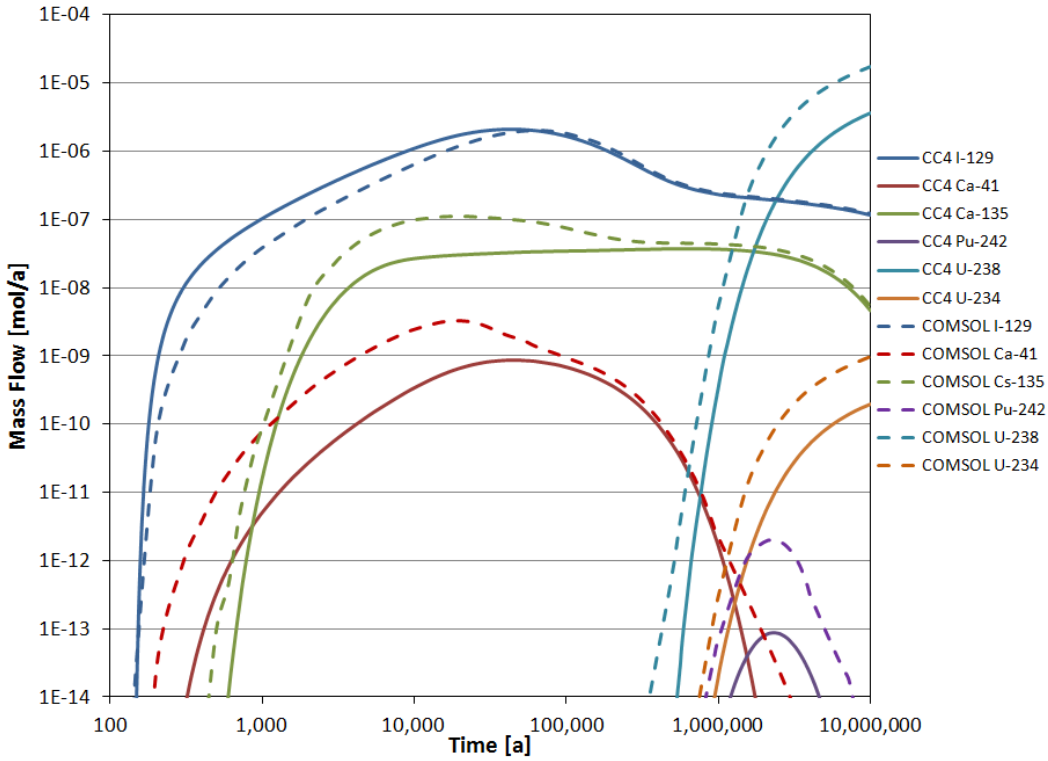

Figure 3-15: Mass flow at the backfill-EDZ interface

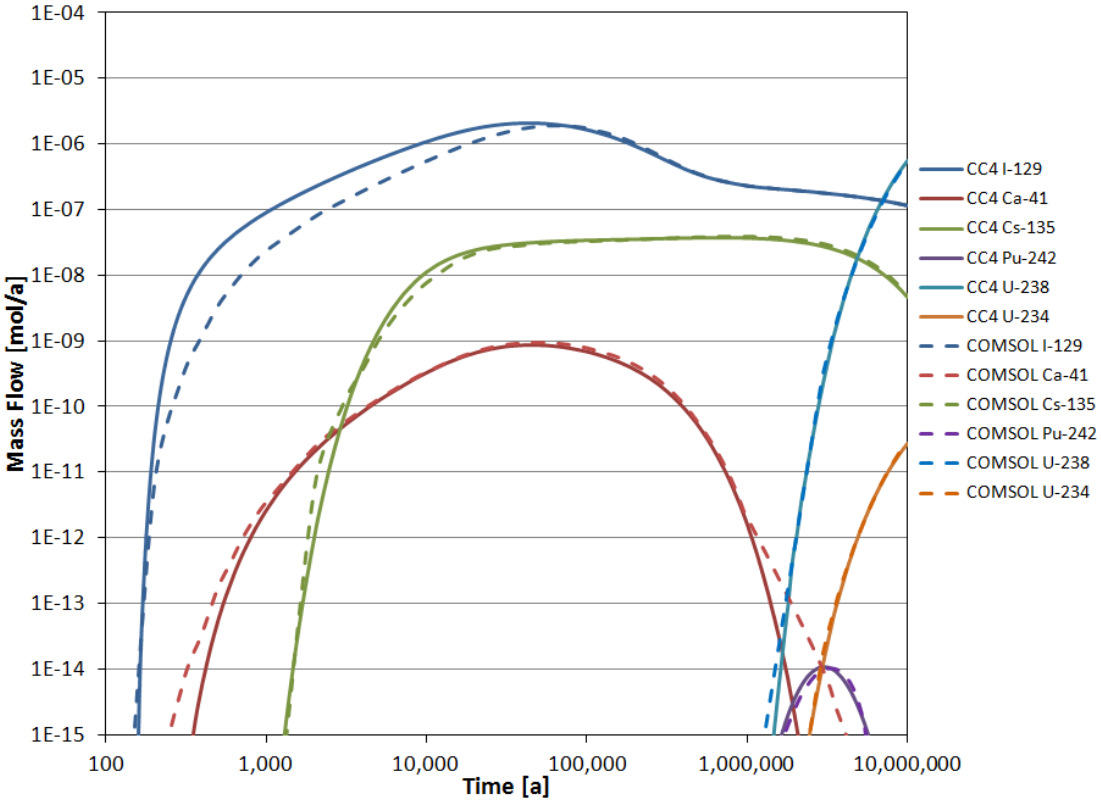

Figure 3-16: Mass flow at the EDZ-rock interface

The radionuclide mass flows entering the rock layer are shown in Figure 3-16. Good agreement between the two models is observed, as was the case for the mass flows at the buffer-backfill interface (see Figure 3-14). Given this good agreement, it is surprising that the radionuclide mass flows at the backfill-EDZ interface calculated by the two models are not in good agreement. The reason for this is not known and will be investigated in the future. However, since the impacts of the repository are determined by the radionuclide mass flows into the rock layer, this comparison gives confidence that the CC4 model correctly calculates these quantities.

Table 3-8 summarizes the peak mass flows and time of the peak calculated by the CC4 and COMSOL models. As expected from the figures shown above, the largest deviations are seen for the mass flows at the backfill-EDZ interface. (Note that the large difference between the two models in the time of the peak mass flow at the backfill-EDZ interface for Cs-135 is due to the different shapes of the calculated mass flow curves, as shown in Figure 3-15.) However, the peak mass flows at the EDZ-rock interface differ by no more than 10%. These latter mass flows determine the calculated impacts of the repository.

Table 3-8: CC4 and COMSOL Repository Transport Comparison

Interface	Nuclide	CC4		COMSOL		Ratio of CC4 to COMSOL Peak Time	Ratio of CC4 to COMSOL Peak Mass Flow
		Time of Peak [a]	Peak Mass Flow [mol/a]	Time of Peak [a]	Peak Mass Flow [mol/a]		
Buffer-Backfill	I-129	3.75×10^{4}	2.10×10^{-6}	5.00×10^{4}	2.15×10^{-6}	0.75	0.97
	Ca-41	1.00×10^{4}	1.35×10^{-8}	1.00×10^{4}	1.60×10^{-8}	1.00	0.84
	Cs-135	4.74×10^{3}	5.48×10^{-6}	6.00×10^{3}	4.21×10^{-6}	0.79	1.30
	Pu-242	1.46×10^{6}	7.38×10^{-10}	1.50×10^{6}	7.87×10^{-10}	0.97	0.94
	U-238	1.00×10^{7}	5.93×10^{-4}	1.00×10^{7}	5.94×10^{-4}	1.00	1.00
	U-234	1.00×10^{7}	2.99×10^{-8}	1.00×10^{7}	3.32×10^{-8}	1.00	0.90
Backfill-EDZ	I-129	4.40×10^{4}	2.07×10^{-6}	6.50×10^{4}	2.00×10^{-6}	0.68	1.04
	Ca-41	4.56×10^{4}	8.76×10^{-10}	2.00×10^{4}	3.25×10^{-9}	2.28	0.27
	Cs-135	6.57×10^{5}	3.78×10^{-8}	2.00×10^{4}	1.10×10^{-7}	32.82	0.35
	Pu-242	2.31×10^{6}	8.82×10^{-14}	2.50×10^{6}	1.95×10^{-12}	0.92	0.05
	U-238	1.00×10^{7}	3.65×10^{-6}	1.00×10^{7}	1.72×10^{-5}	1.00	0.21
	U-234	1.00×10^{7}	1.92×10^{-10}	1.00×10^{7}	9.60×10^{-10}	1.00	0.20
EDZ-Rock	I-129	4.40×10^{4}	2.07×10^{-6}	6.50×10^{4}	1.88×10^{-6}	0.68	1.10
	Ca-41	4.56×10^{4}	8.73×10^{-10}	5.00×10^{4}	9.28×10^{-10}	0.91	0.94
	Cs-135	6.57×10^{5}	3.77×10^{-8}	8.51×10^{5}	3.84×10^{-8}	0.77	0.98
	Pu-242	3.07×10^{6}	1.05×10^{-14}	3.50×10^{6}	9.93×10^{-15}	0.88	1.06
	U-238	1.00×10^{7}	5.45×10^{-7}	1.00×10^{7}	5.31×10^{-7}	1.00	1.03
	U-234	1.00×10^{7}	2.69×10^{-11}	1.00×10^{7}	2.97×10^{-11}	1.00	0.91

3.7.2.2 Impact of the Presence of the Container

One of the main simplifications of the CC4 model of the repository is the absence of the container in the INROC model. In reality, the container would occupy a significant volume of space in the repository. To determine the effect of the container on radionuclide releases from the repository, the COMSOL model described in Sections 3.6.1 and 3.6.2 was used. This model used data from the Fourth Case Study (Garisto et al. 2012).

For the current test, however, the container in the COMSOL model was represented as an impermeable cylinder (of diameter 1.247 m and length 3.842 m) at the centre of the concentric buffer, backfill and EDZ cylinders. The radionuclide source node was located on the side of the container a few centimeters below the top of the container, indicative of a through defect along the weld securing the lid to the body of the container. The buffer layer in this COMSOL model extended 1 m beyond the perimeter of the container, meaning that the buffer "cylinder" had a

diameter of 3.247 m in the region of the placement room between containers. The backfill and EDZ layers were an additional 0.5 m and 0.3 m thick, respectively.

In the CC4 model, the buffer, backfill and EDZ had a thickness of 1 m, 0.5 m and 0.3 m, respectively. The radionuclide source in the CC4 model was placed, as usual, on the axis of the concentric cylinders. The same radionuclide source terms were used in the COMSOL and CC4 models.

The radionuclide mass flows leaving the repository (i.e., the mass flow at the EDZ-rock interface) calculated by the COMSOL and CC4 models are compared in Figure 3-17 and Figure 3-18. The peak mass flows and times of the peak mass flows are shown in Table 3-9.

The results in Figure 3-17 and Figure 3-18 indicate that the mass flows calculated by CC4 are higher than those calculated by COMSOL, particularly for radionuclides that are more strongly sorbed in the buffer and backfill. This may be due to the fact that concentration gradients in the buffer, in particular, would be somewhat higher in the CC4 model because the buffer volume into which the radionuclides can diffuse is smaller in the CC4 model.

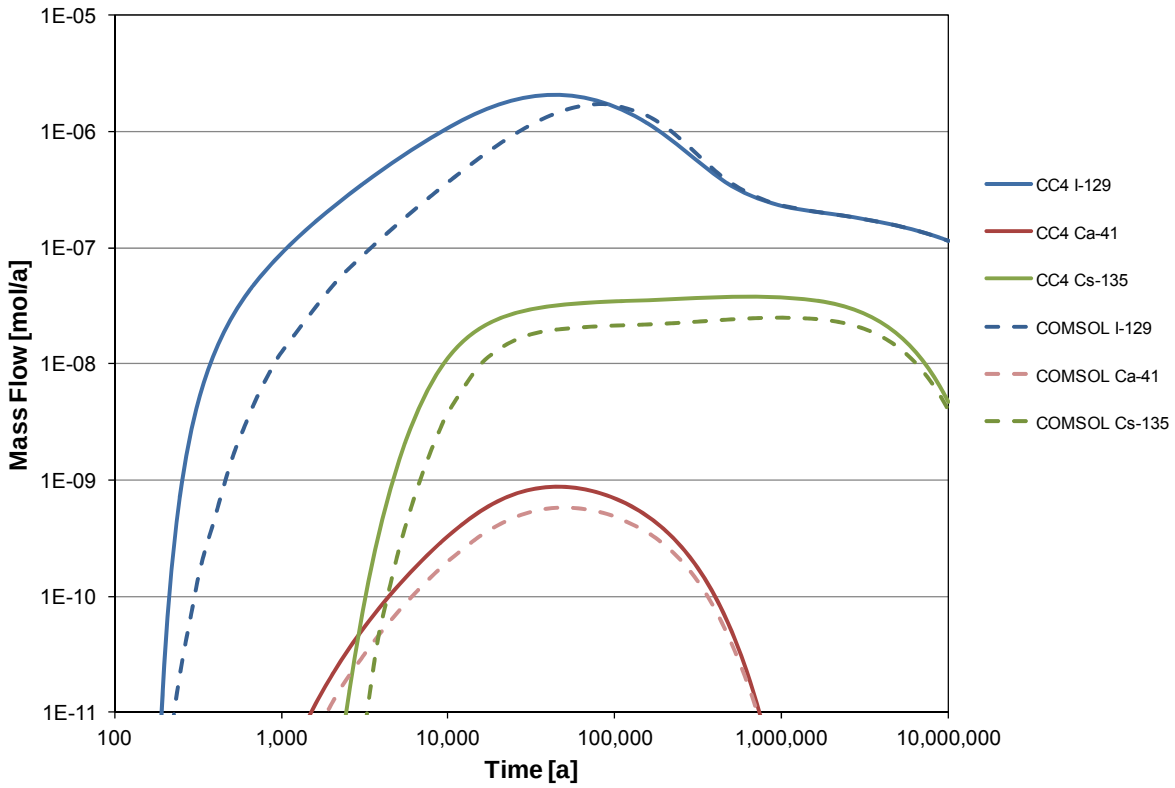

Figure 3-17: CC4 and COMSOL mass flows at the EDZ-rock interface for I-129, Ca-41, and Cs-135

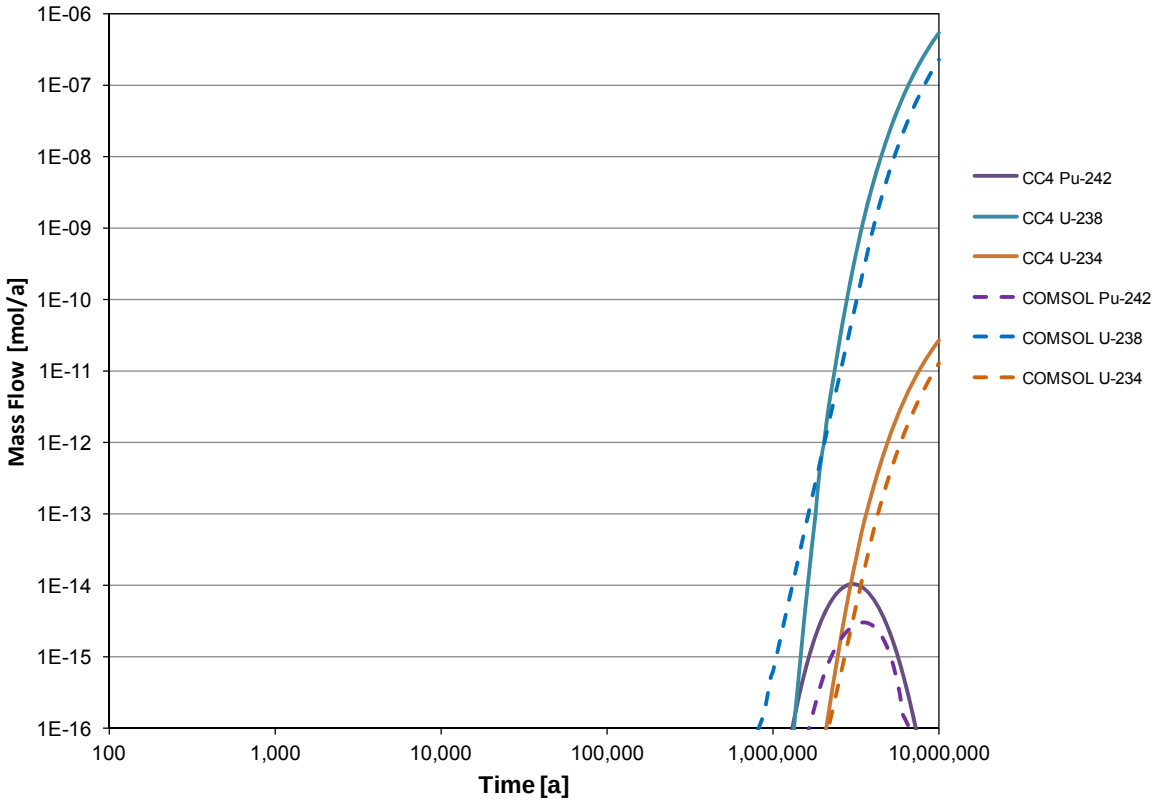

Figure 3-18: CC4 and COMSOL mass flows at EDZ-rock interface for Pu-242, U-238, and U-234

Table 3-9 compares the peak radionuclide mass flows and times of the peak at the buffer-backfill, backfill-EDZ and EDZ-rock interfaces. The agreement between the two models is good for the mass flows at the buffer-backfill and EDZ-rock interfaces, with the CC4 peak mass flows higher than the COMSOL mass flows particularly for strongly sorbing radionuclides. However, at the backfill-EDZ interface, the CC4 peak mass flows are generally lower than the corresponding COMSOL mass flows. The same observations were made in Section 3.7.2.1. The reason why the two models behave so differently at the backfill-EDZ interface is currently not known. However, for a safety assessment of the repository, it is the peak mass flows at the EDZ-rock interface that are important since these affect the calculated impacts of the repository. Hence, based on the current results, it can be concluded that the neglect of the container in INROC, the CC4 repository transport model, is conservative.

Table 3-9: CC4 and COMSOL Peak Mass Flows and Times of Peak

Interface	Nuclide	CC4		COMSOL		Ratio of CC4 to COMSOL Time of Peak	Ratio of CC4 to COMSOL Peak Mass Flow
		Time of Peak [a]	Peak Mass Flow [mol/a]	Time of Peak [a]	Peak Mass Flow [mol/a]		
Buffer-backfill	I-129	3.75E+04	2.10E-06	7.00E+04	1.80E-06	0.54	1.16
	Ca-41	1.00E+04	1.35E-08	1.00E+04	9.88E-09	1.00	1.37
	Cs-135	4.74E+03	5.48E-06	7.00E+03	3.00E-06	0.68	1.83
	Pu-242	1.46E+06	7.38E-10	1.50E+06	2.75E-10	0.97	2.68
	U-238	1.00E+07	5.93E-04	1.00E+07	3.85E-04	1.00	1.54
	U-234	1.00E+07	2.99E-08	1.00E+07	2.15E-08	1.00	1.39
Backfill-EDZ	I-129	4.40E+04	2.07E-06	8.01E+04	1.76E-06	0.55	1.18
	Ca-41	4.56E+04	8.76E-10	2.50E+04	1.54E-09	1.82	0.57
	Cs-135	6.57E+05	3.78E-08	9.01E+03	8.53E-08	72.93	0.44
	Pu-242	2.31E+06	8.82E-14	2.50E+06	1.52E-12	0.92	0.06
	U-238	1.00E+07	3.65E-06	1.00E+07	9.82E-06	1.00	0.37
	U-234	1.00E+07	1.92E-10	1.00E+07	5.49E-10	1.00	0.35
EDZ-Rock	I-129	4.40E+04	2.07E-06	8.01E+04	1.71E-06	0.55	1.21
	Ca-41	4.56E+04	8.73E-10	5.00E+04	5.66E-10	0.91	1.54
	Cs-135	6.57E+05	3.77E-08	1.00E+06	2.51E-08	0.66	1.50
	Pu-242	3.07E+06	1.05E-14	3.50E+06	2.92E-15	0.88	3.60
	U-238	1.00E+07	5.45E-07	1.00E+07	2.32E-07	1.00	2.34
	U-234	1.00E+07	2.69E-11	1.00E+07	1.30E-11	1.00	2.07

3.7.3 FRAC3DVS Comparison: Third Case Study

The Third Case Study (TCS) placement geometry consists of two parallel rows of copper containers in an elliptical placement room, as shown in Figure 3-19(a). The containers are surrounded by a minimum of 0.5 m of buffer (including 100% bentonite and 50% bentonite-sand layers) and 0.5 m of backfill (dense and light backfill layers). Because the inner buffer, outer buffer and gap backfill share similar properties, they were modelled as a single material. This repository-scale geometry was simulated in detail using FRAC3DVS (a 3D finite element groundwater flow and solute transport code) using a 3D triangular finite-element grid with 1.7 million active nodes (Garisto et al. 2004). However, as shown in Figure 3-19(b), the containers were not explicitly included in the FRAC3DVS model, since they occupy a small fraction of the room volume. Hydraulic head boundaries for all sides of the FRAC3DVS repository-scale model were obtained from the local scale flow model.

In the CC4 simulations of this case (which used SYVAC3-CC4, Version SCC404), each room was approximated as a cylindrically nested concentric series of layers of buffer, backfill, EDZ and geosphere near-field rock (see Figure 3-10). All properties are assumed to be symmetric about the cylindrical axis. The source is modelled as a point source located along the central axis of the placement room. The same radionuclide source terms were used in the CC4 and FRAC3DVS models.

The actual thickness of the buffer and backfill layers in the TCS study is approximately 0.5 m and 0.5 m respectively, as shown in Figure 3-19(a), and these thicknesses are used in the FRAC3DVS model (see Figure 3-19(b)). However, the CC4 model of the TCS repository uses the effective thicknesses of the buffer and backfill layers, which are based on the total mass of buffer and backfill in the repository. In this way, the total masses of buffer and backfill in the repository are accounted for in the CC4 radionuclide transport calculations. (Because the container is not present in the CC4 repository model, as shown in Figure 3-10, use of the actual buffer and backfill thicknesses in CC4, although conservative, would mean that the buffer and backfill masses in the repository would be underestimated in CC4.) This approach is appropriate based on the comparisons between the CC4 and MOTIF models presented in Section 3.7.1. The effective thicknesses of the buffer and backfill in the TCS are 1.1 m and 0.9 m, respectively.

Radionuclide releases from the repository into the geosphere calculated by the two codes are compared in Figure 3-20. Mass flow curves for I-129, Cl-36 and Ca-41 from CC4 and FRAC3DVS have similar shapes but the peak release rates produced by CC4 are larger and occur earlier. Actinide release rates from the repository for Np-237 and its daughter U-233 are compared in Figure 3-21. Again, the CC4 repository release rates are generally larger than those calculated by FRAC3DVS release; but, at long times, the ratio of parent to daughter repository release rates are similar in both codes. Similar results were found for U-238 and its daughter U-234, as shown in Figure 3-22.

In summary, for the non-sorbing nuclides (I-129 and Cl-36), the CC4 peak release rates from the repository are within 1.3 times of the FRAC3DVS values. For the sorbing nuclides (Ca-41 and actinides), the release rates from CC4 are 3 to 5 times larger than those from FRAC3DVS.

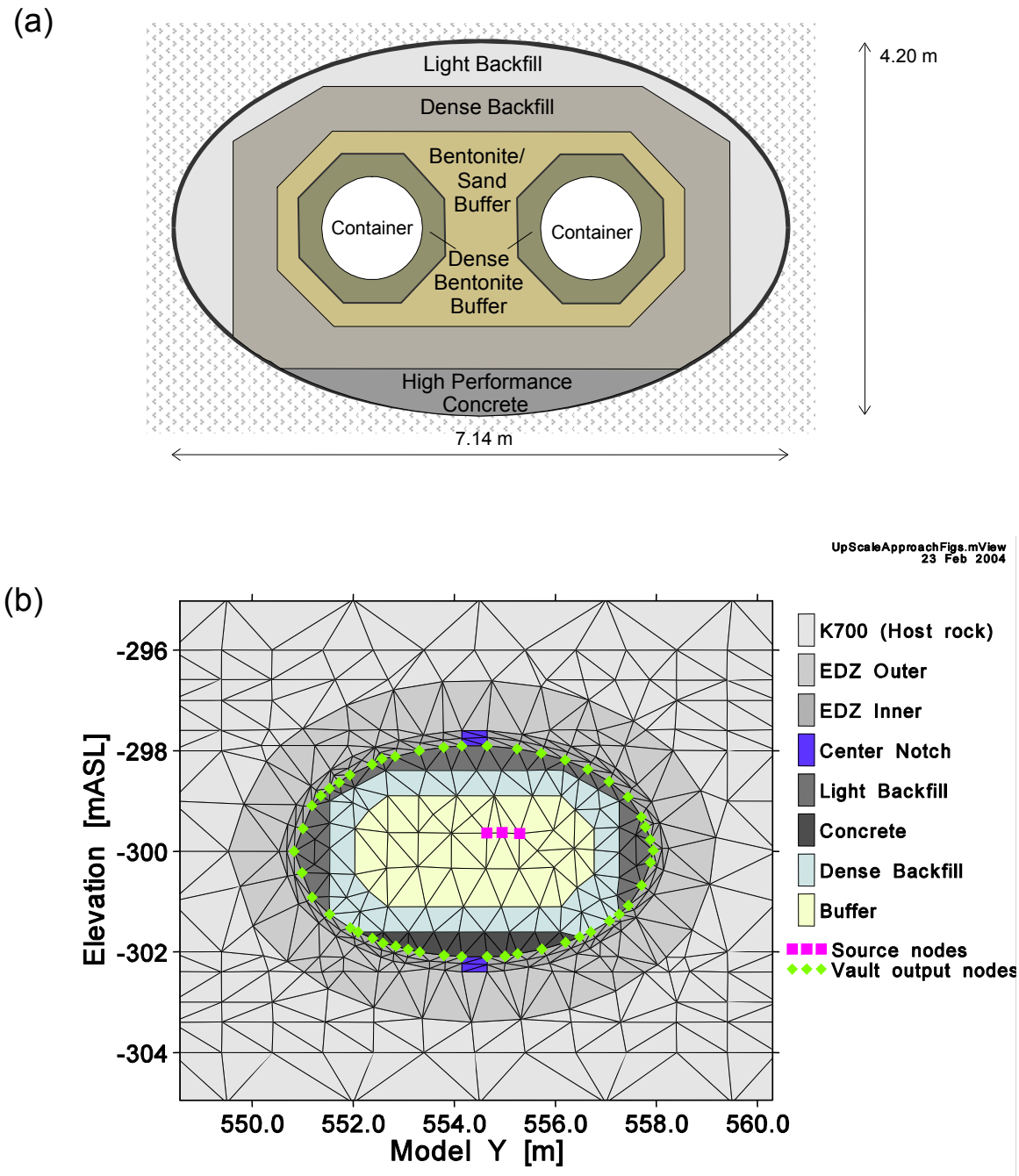

Note: The FRAC3DVS repository model does not explicitly include the fuel containers.

Figure 3-19: Placement room vertical cross-section: (a) General geometry of placement room in repository design and (b) Section of repository-scale model grid showing the location of the source input nodes and mass flux output nodes

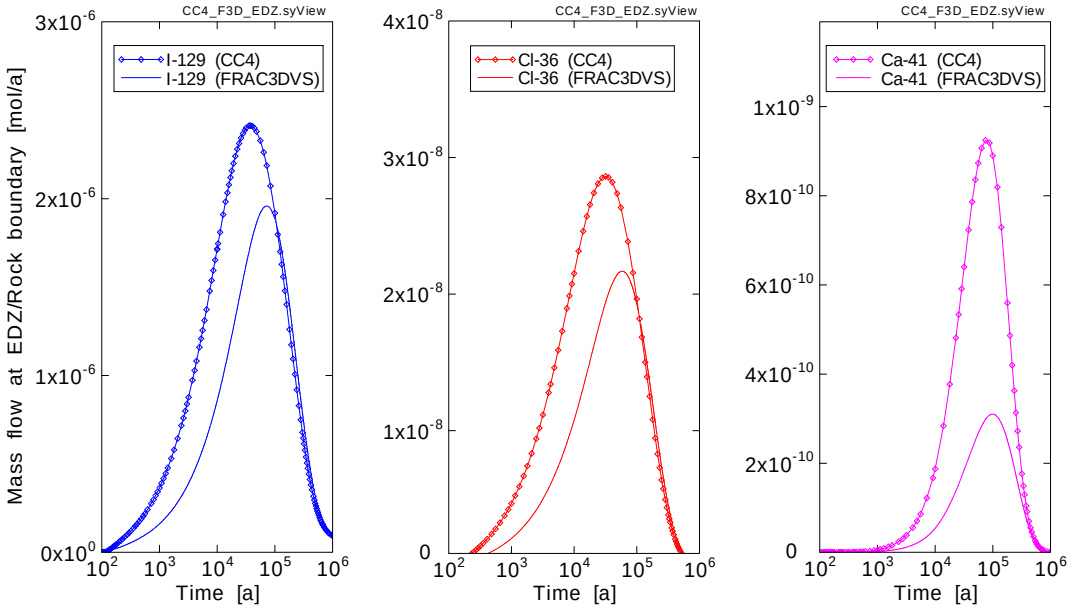

Figure 3-20: Comparison of I-129, Cl-36 and Ca-41 repository releases for CC4 and FRAC3DVS from the Third Case Study

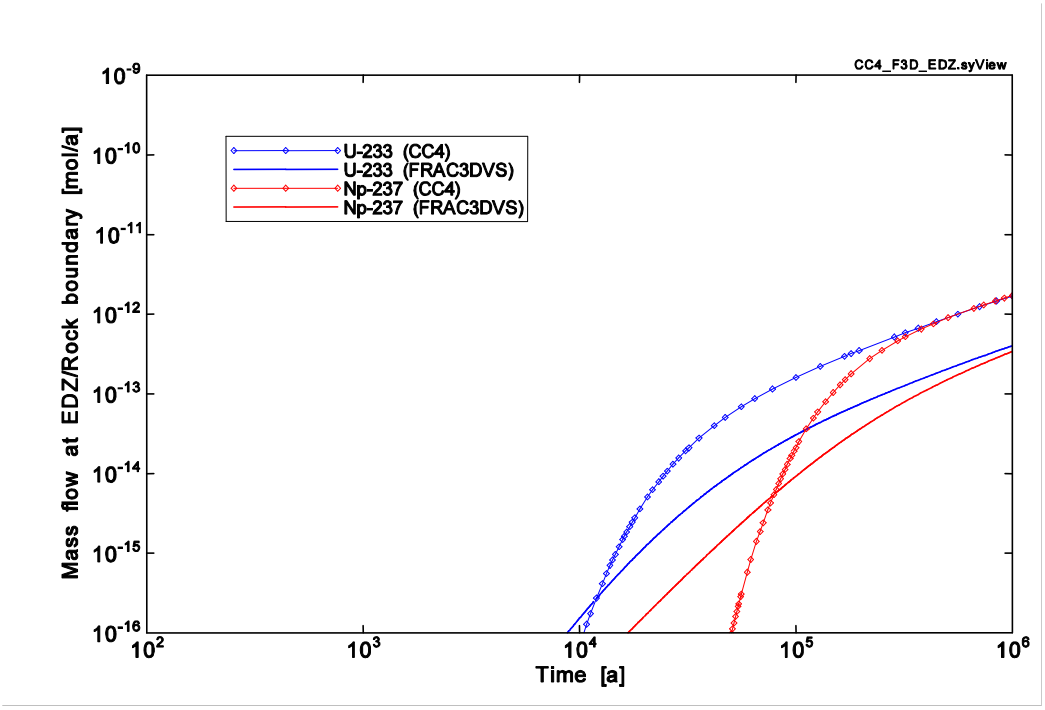

Figure 3-21: Comparison of Np-237 and U-233 repository release rates for CC4 and FRAC3DVS from the Third Case Study

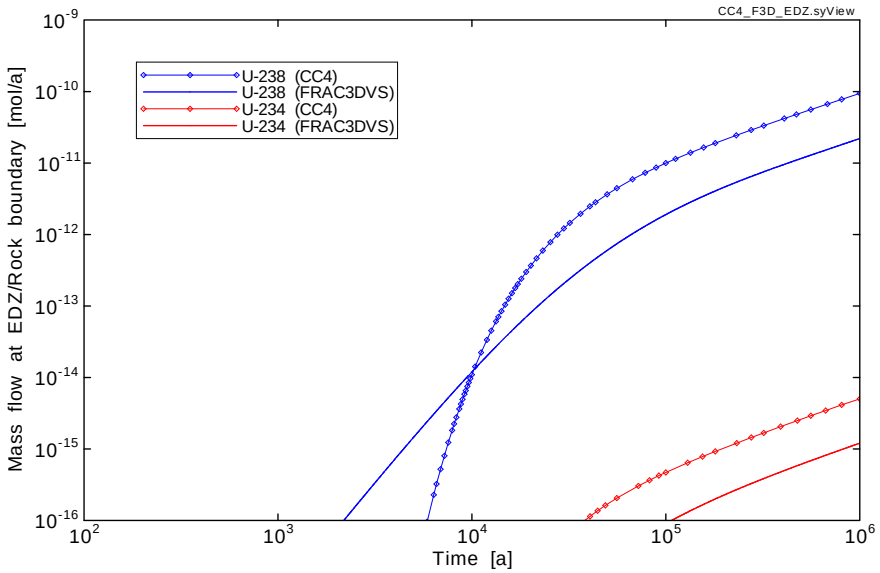

Figure 3-22: Comparison of U-238 and U-234 repository release rates for CC4 and FRAC3DVS from the Third Case Study

3.7.4 FRAC3DVS Comparison: Horizontal Borehole Concept

In the Horizontal Borehole Concept (HBC) study, copper used fuel containers are placed in long horizontal boreholes drilled into the host rock from access tunnels (see Figure 3-9). This geometry was simulated in detail using FRAC3DVS, with a 3D triangular finite-element grid with 1.5 million active nodes (Garisto et al. 2005a). However, in contrast to the Third Case Study, the container was represented in the FRAV3DVS model for the HBC study, as shown in Figure 3-23. Hydraulic head boundaries for all sides of the grid were obtained from the local scale flow model.

In the CC4 simulation of this case (which used SYVAC3-CC4, Version SCC405), each room is approximated as a cylindrically nested concentric series of layers of buffer, EDZ and geosphere near-field rock. All properties are assumed to be symmetric about the cylindrical axis. The source is modelled as a point source located along the central axis. The same source term (flux) was used for both CC4 and FRAC3DVS.

The actual thickness of the cylindrical buffer layer in the HBC study is 0.35 m. However, the effective thickness of the buffer layer, which is based on the total mass of buffer in the repository, is used in the CC4 model of the HBC repository. In this way, the total mass of buffer in the repository is accounted for in the radionuclide transport calculations. (Because the container is not present in the CC4 repository model, as shown in Figure 3-10, use of the actual buffer thickness in CC4, although conservative, would mean that the buffer mass in the repository would be underestimated in CC4.) This approach is appropriate based on the comparisons between the CC4 and MOTIF models presented in Section 3.7.1. The effective thickness of the buffer in the HBC is calculated to be 0.75 m. The EDZ thickness is small (0.03 m) because the horizontal boreholes are drilled rather than excavated.

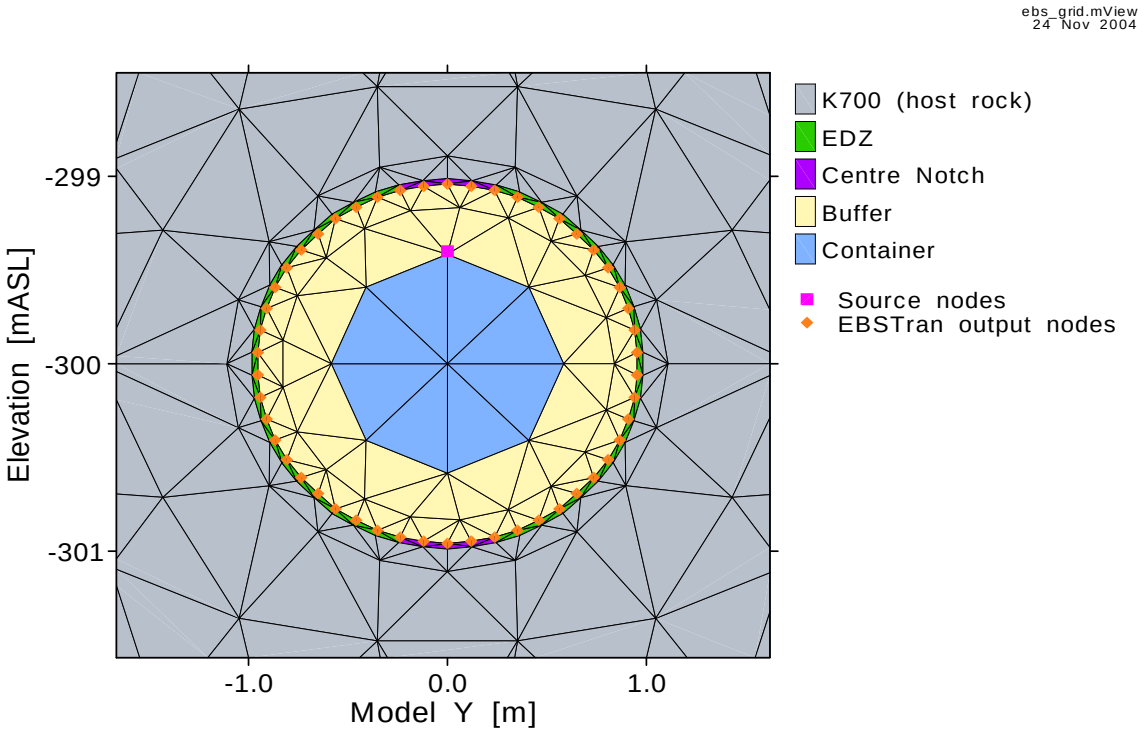

Figure 3-23: Vertical cross-section of the grid in the repository-scale model showing the location of the source input nodes and mass flow output nodes

Radionuclide releases from the placement room into the geosphere calculated by the two codes are compared in Figure 3-24. Mass flow curves for I-129, Cl-36 and Ca-41 from CC4 and FRAC3DVS have similar shapes but the peak release rates from CC4 are larger and occur earlier.

Release rates from the repository for U-238 and its daughter U-234 are compared in Figure 3-25. The release rates for these uranium isotopes are much lower than for the fission products. Again, the CC4 repository release rates are generally larger than those from FRAC3DVS, although the breakthrough seems to occur somewhat earlier in FRAC3DVS. At long times, the ratio of parent to daughter repository release rates are similar in both codes.

In summary, for the non-sorbing nuclides (I-129 and Cl-36), CC4 peak release rates from the repository are within 1.1 times of the FRAC3DVS values. For the moderately sorbing nuclide Ca-41, the peak release rate is about 1.3 time larger in CC4; and, for the uranium isotopes, the CC4 release rates are about 2-fold larger at long times.

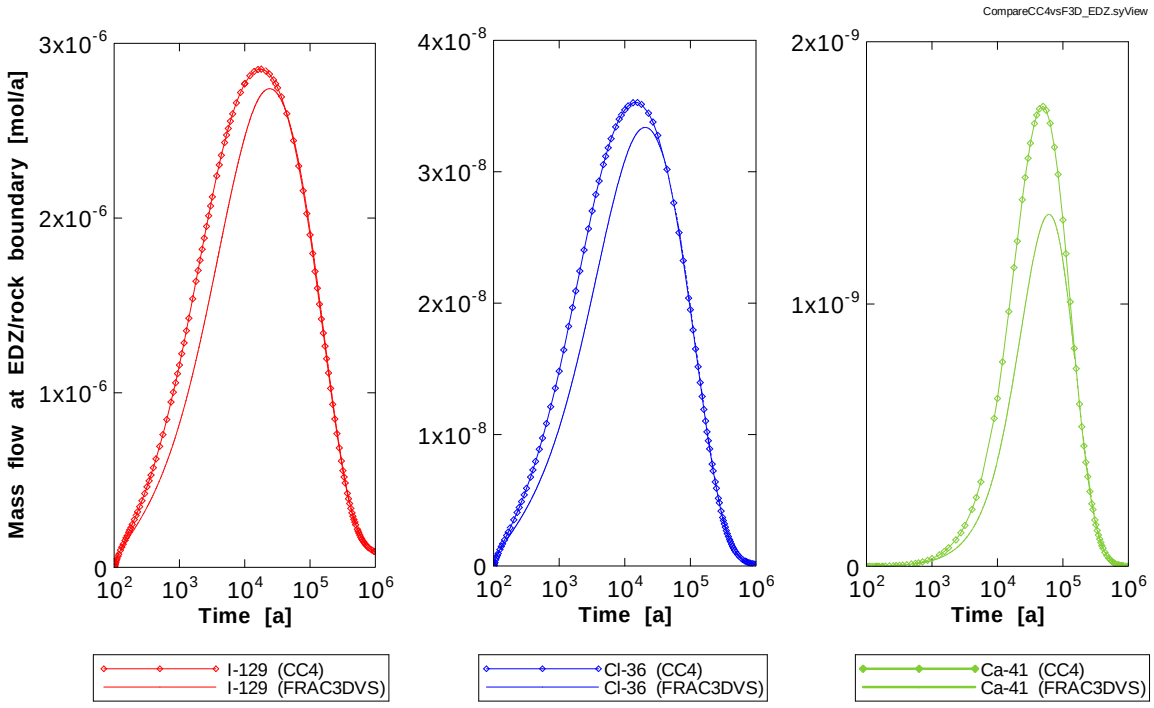

Figure 3-24: Comparison of I-129, Cl-36 and Ca-41 repository release rates for CC4 and FRAC3DVS from the HBC study

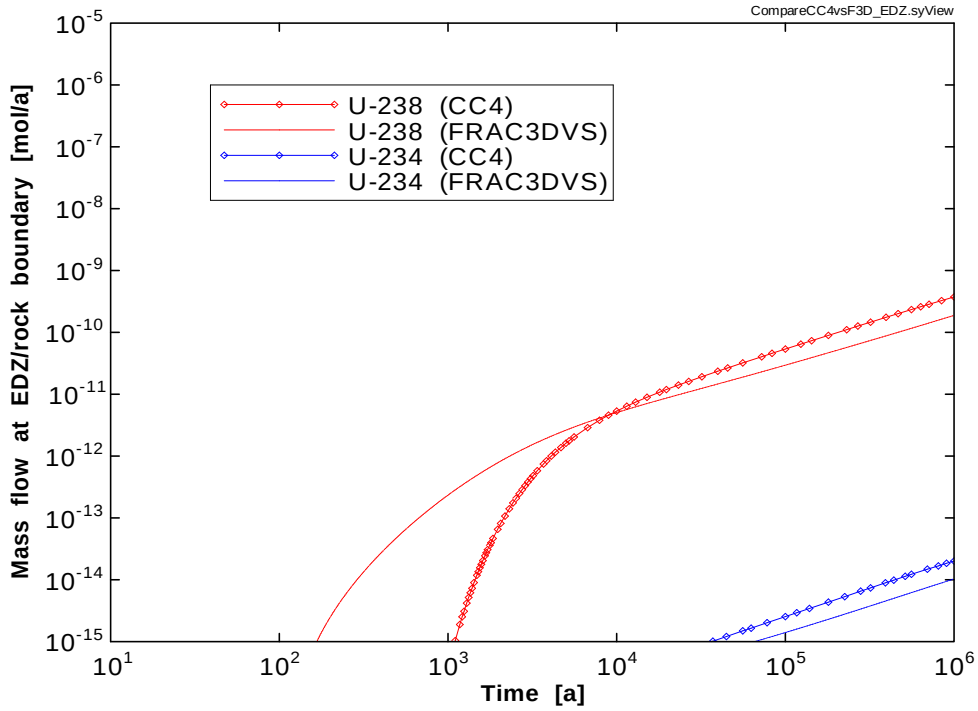

Figure 3-25: Comparison of U-238 and U-234 repository release rates for CC4 and FRAC3DVS from the HBC study

3.7.5 FRAC3DVS Comparison: Fourth Case Study

In the Fourth Case Study (4CS), the copper-clad containers are placed in boreholes drilled into the placement room. The containers are surrounded by a 0.36 m thick bentonite buffer layer. This geometry was simulated in detail using FRAC3DVS with a 3D finite-element grid with about 9.6 million nodes (NWMO 2012a). The container was explicitly represented in the FRAV3DVS model for the 4CS, as shown in Figure 3-26. Hydraulic head boundaries for all sides of the grid were obtained from the local scale flow model.

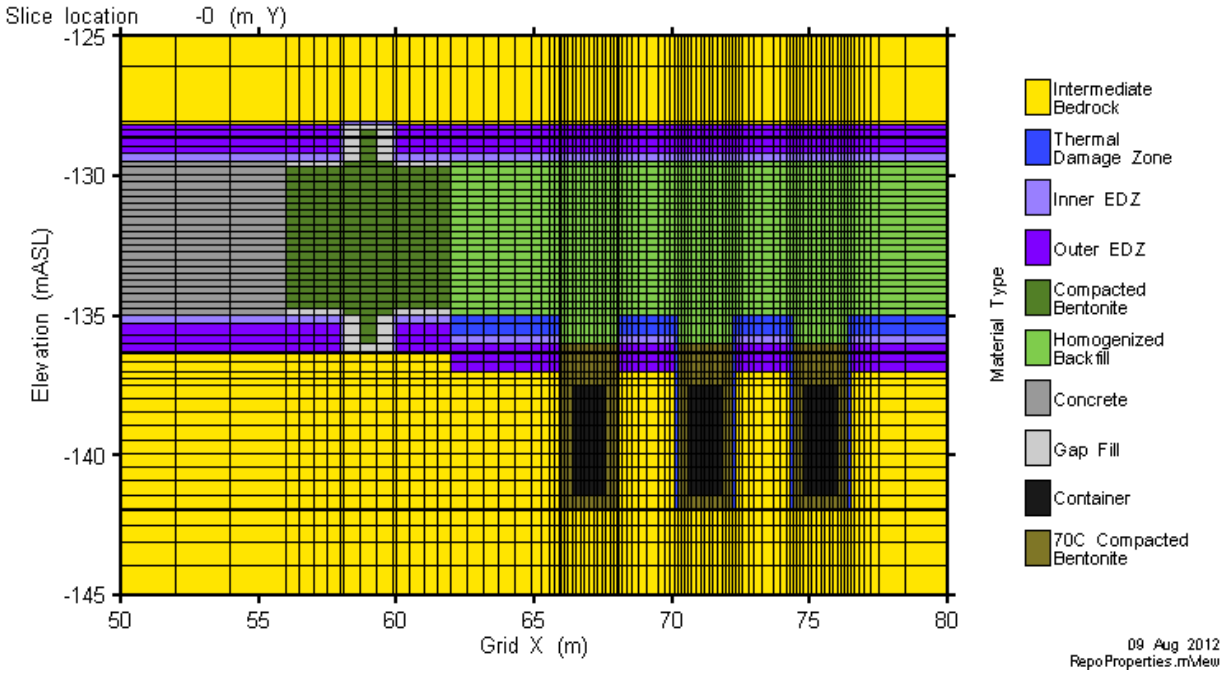

Figure 3-26: Repository-scale model in the 4CS: Vertical slice along placement drift

In the CC4 simulation of this case (which used SYVAC3-CC4, Version SCC409), each borehole is approximated as a cylindrically nested concentric series of layers of buffer, EDZ and geosphere near-field rock. All properties are assumed to be symmetric about the cylindrical axis. The container is not explicitly included in the CC4 model and the radionuclide source is modelled as a point source located along the central axis. The same source term (flux) was used for both CC4 and FRAC3DVS.

In contrast to the Third Case Study, the CC4 model calculations for the 4CS used the actual buffer thickness (0.3 m) rather than the larger effective buffer thickness (of about 1 m). (The effective buffer thickness makes the volume of the buffer material in the CC4 repository model equal to volume of buffer material in an actual borehole). Previous validation studies had indicated that use of the effective buffer thickness leads to good agreement between CC4 and finite element models (Johnson et al. 1996, Kolar and LeNeveu 1995); so, use of the actual buffer thickness is expected to be conservative.

In Figure 3-27, the CC4 transport results for various radionuclides are compared with similar results from detailed FRAV3DVS simulations. The figure shows the radionuclide mass fluxes

from the borehole to the geosphere calculated by the two models, i.e., across the excavation damage zone / rock boundary around the placement borehole. For most radionuclides, the agreement between the two models is fairly good, particularly at longer times. The differences at earlier times are likely due to the fact that the volume of buffer material is about 4-fold larger in the FRAC3DVS simulation, which uses the correct geometry, than in the CC4 simulation in which the container is not modelled. The large difference between the two models for Sn-126 is due to the fact the Sn is very strongly sorbed in the buffer and so, in this case, the significantly larger volume of buffer in the FRAC3DVS model has a much larger influence on the mass flow of Sn-126 into the geosphere from the buffer.

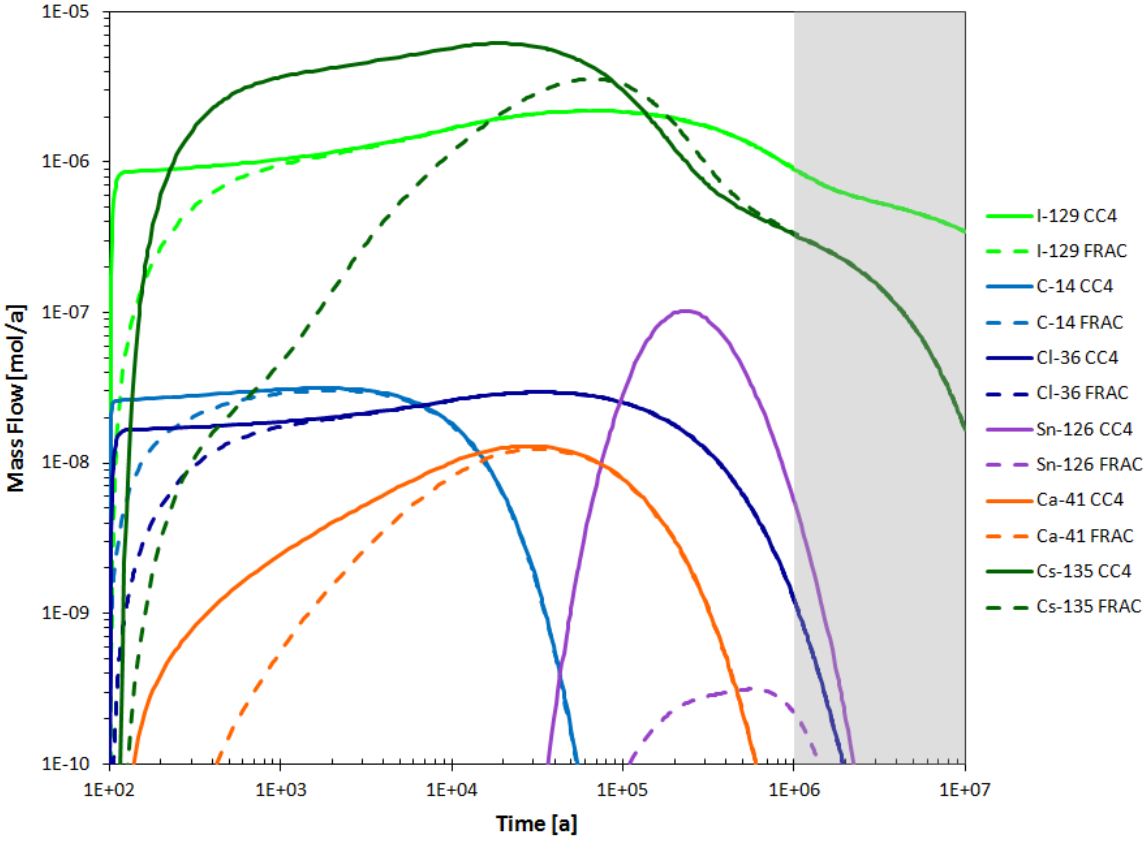

Figure 3-27: Comparison of CC4 and FRAC3DVS transport of I-129, C-14, Cl-36, Ca-41, Sn-126 and Cs-135 into the geosphere for the Fourth Case Study

Results for the peak mass flows and their associated time of occurrence are shown in Table 3-10. The agreement is very close for the non-sorbing radionuclides I-129 and Cl-36 and for the weakly sorbing radionuclides C-14 and Ca-41. The difference is conservative for the sorbing radionuclides in the sense that CC4 calculates higher peak values.

Table 3-10: Comparison of 4CS Peak Mass Flows into the Geosphere

Nuclide	Peak Release Rate (mol/a)			Time of Peak Release (a)		
	CC4	FRAC3DVS	Ratio[1]	SYVAC3	FRAC3DVS	Ratio[1]
I-129	2.21×10^{-6}	2.20×10^{-6}	1.00	6.5×10^{4}	6.5×10^{4}	1.00
C-14	3.15×10^{-8}	3.03×10^{-8}	1.04	1.8×10^{3}	2.1×10^{3}	0.86
Ca-41	1.30×10^{-8}	1.23×10^{-8}	1.06	2.9×10^{4}	3.2×10^{4}	0.91
Cl-36	2.96×10^{-8}	2.99×10^{-8}	1.01	3.2×10^{4}	3.2×10^{4}	1.00
Cs-135	6.16×10^{-6}	3.56×10^{-6}	1.7	1.9×10^{4}	6.8×10^{4}	0.28
Sn-126	1.03×10^{-7}	3.13×10^{-10}	330	2.3×10^{5}	5.8×10^{5}	0.40
U-234	-	-	-	$>10^{7}$	$>10^{7}$	N/A
U-238	-	-	-	$>10^{7}$	$>10^{7}$	N/A

Note: [1] Ratio is the CC4 value divided by the FRAC3DVS value.

3.8 REPOSITORY-GEOSPHERE INTERFACE

Because the repository is large, groundwater flow rates and other repository and geosphere properties may differ from one location to another. Consequently, the CC4 repository model can be discretized into sectors. Each of these sectors is modelled independently of other sectors, with no interaction. All container failures within a given sector occur at the same time, and the effect of multiple failures is treated as additive. This later assumption is considered conservative with respect to nuclide transport.

In CC4, the groundwater flow velocities in the buffer are assumed to be effectively zero, because of the low permeability of compacted buffer and, so, transport in the buffer is diffusion dominated. The groundwater flow velocities in the backfill and excavation damaged zone (EDZ) for a repository sector are calculated based on the groundwater flows in the rock zone near the sector. For a specific repository sector, the properties of the EDZ zone (i.e., Darcy velocity and capacity factors) are taken from the geosphere segment to which the sector is connected.

The magnitude of the transverse velocity in the EDZ and backfill is estimated from the transverse velocity in the host rock by an equivalent resistor model (NWMO 2012b, Section 3.2). It is assumed that the transverse host rock flow is primarily vertical since this would generally be a more unfavourable, i.e., conservative, groundwater flow. The groundwater axial flow velocities in the backfill and EDZ are calculated based on the CC4 groundwater axial flows in the adjacent rock. The formulas used to calculate the groundwater flow velocities in the backfill and EDZ from the adjacent geosphere boundary conditions have been validated over the range of parameters used in the Second Case Study by comparison to the MOTIF code (Johnson et al. 1996). However, there are no published verification studies for other aspects of the repository-geosphere interface, e.g., conservation of mass flow across the interface. These tests will be done in the future.

4. GEOSPHERE MODEL

The CC4 geosphere model, called GEONET, uses the radionuclide flux from the repository (which is calculated by the models described in Section 3), the groundwater flow field, and the rock properties and fracture network to determine how radionuclides move through the geosphere (NWMO 2012b, Melnyk 1995). CC4 passes this geosphere flux onto the biosphere module through an interface with the biosphere that includes lake sediments, surface waters, soil and well.

4.1 GROUNDWATER FLOW FIELD

CC4 does not determine the groundwater flow field. This flow field is calculated with external three-dimensional groundwater flow and transport codes such as FRAC3DVS (Therrien et al. 2010).

The groundwater flow field information is represented within CC4 by a set of one-dimensional (1-D) transport paths or segments that are connected together in three-dimensional (3-D) space to form a transport network from the repository to the groundwater discharges in the biosphere (NWMO 2012b). Radionuclide transport through the 1-D segments is determined using analytical solutions to the 1-D advection-dispersion equations for radionuclide decay chains with sorption (NWMO 2012b). (Thus, the model includes longitudinal dispersion, i.e., along the transport pathway, but not transverse dispersion.) The output (i.e., radionuclide mass flows) from one segment is used as input to the next segment of the network. The transport network may converge and diverge. Convergence occurs, for example, at a well inlet.

Flow data is typically entered into CC4 as hydraulic heads at the nodes of the defined transport segment network. Groundwater velocities within each segment are determined within CC4 from these hydraulic heads, and from the input values of the hydraulic permeability and porosity of the rock or fracture in which the transport segment is located.

The transport network represents a steady-state groundwater flow field, i.e., it is fixed in time and space, but contaminant transport is fully transient. However, in SCC407 and later versions, the transport network can be changed, at specific times, to represent a different steady-state groundwater flow field. This feature was needed to model the effects of glaciation on contaminant transport through the geosphere (Garisto et al. 2010).

Tests of the GEONET model are described below. There are two types of tests. First, specific tests ensure that the various parts of the GEONET model correctly represent their respective processes (see Section 4.3). Second, tests are carried out to demonstrate that the simplified CC4/GEONET model adequately represents the true 3-D groundwater flow and transport through the geosphere (see Section 4.4).

4.2 WELL MODEL

The CC4 GEONET model includes a water supply well, which is generally located within a permeable feature of the geosphere such as a fracture zone (in a crystalline rock environment). Accounting for the influence of the well depth and pumping rate on the geosphere groundwater transport paths and groundwater velocities is an important feature of the GEONET model.

Consequently, GEONET includes an analytical well model that determines the effectiveness of the well in capturing water – and potentially contaminants – with variations in the well parameters such as the pumping rate (NWMO 2012b, Chan and Nakka 1994). This well model is used to calculate the following quantities: the maximum well capacity, the hydraulic head drawdown within the fracture zone intercepted by the well, the quantity of surface water captured by the well, and the fraction of contaminants in the fracture zone captured by the well.

The effects of variations in the well pumping rate on the groundwater flow field are developed by running a range of cases with a groundwater flow field code such as FRAC3DVS, and then providing an empirical calibration factor within the GEONET model to fit the effects of the well on the GEONET parameters such as groundwater heads or velocities.

4.3 TESTS OF ANALYTICAL SOLUTIONS USED IN GEONET

This section summarizes the tests carried out to verify (1) the analytical solutions to the 1-D advection-dispersion equations used in GEONET and (2) the connections between the 1-D segments.

4.3.1 Network tests

Initial testing of the GEONET code was done using cases that include single transport segments and simple networks (Davison et al. 1994). Parameter values, e.g., dispersivity and retardation factor, were varied for the different cases. In all these initial cases, the GEONET code worked as expected, with the changes in the parameter values causing the expected changes to the contaminant break-through curve. Similarly it was demonstrated that the contaminant break-through curve was essentially unaffected by segmentation of the transport path and that branching of the transport network (either convergence or divergence of segments) produced the expected results.

4.3.2 INTRACOIN Comparison

INTRACOIN was an international co-operation project for comparing models for transport of radionuclides in geological media (INTRACOIN 1984). GEONET was used to simulate two of the INTRACOIN cases, namely test cases 1 and 2 of the Level 1 series which tested numerical accuracy. Test cases 1 and 2 involved transport of two radionuclide chains (U-234 $\rightarrow$ Th-230 $\rightarrow$ Ra-226 and Cm-245 $\rightarrow$ Np-237 $\rightarrow$ U-233) through single and multiple layers of media, respectively. Results from GEONET showed very good agreement with corresponding results published in INTRACOIN (1984) for all cases (Davison et al. 1994).

4.3.3 Response Function Solution

Response function solutions to the one-dimensional advection-dispersion equation are used in the CC4 GEONET model (NWMO 2012b). The two main response functions available in CC4 are: RF1, a semi-infinite medium response function (Heinrich and Andres 1985); and, RF3, a zero concentration boundary condition response function (Garisto and LeNeveu 1991).

Chan and Advani (1991) carried out an independent verification of the GEONET response function solutions used in the CC3 code. (The same response functions are still used in the current version of CC4.) The GEONET analytical response function solution was compared with a numerical solution for impulse-flow and constant-concentration input conditions, for all combinations of high/median/low values in the following ranges:

- Barrier layer thickness, d: 0.25 to 1.4 m
- Diffusion coefficient, D: $9x10^{-7}$ to 0.03 m^2/a
- Capacity factor: 0.0001 to $2x10^4$
- Darcy velocity: 0 to 10*D/d
- Radioactive decay constant: 0 to 0.05 a^{-1}

These ranges apply to the tests with the impulse-flow boundary conditions. Slightly different ranges were used for the constant-concentration boundary condition tests.

The numerical results agreed with the CC3 analytical response function within the estimated numerical accuracy of the two solutions for most cases. The remaining discrepancies were small and may have exceeded the estimated numerical accuracy due to errors in estimating the numerical accuracy of the solutions, given that the analysis of the discrepancies produced no pattern with respect to the parameter values.

4.3.4 Comparison to Gureghian and Jansen (1985)

GEONET was used to simulate the transport results reported by Gureghian and Jansen (1985), who analyzed the transport of a three-member decay chain (U-234 $\rightarrow$ Th-230 $\rightarrow$ Ra-226) through a three-layer medium. The GEONET simulations were in very good agreement with the published results (Davison et al. 1994).

4.3.5 SRG check of CC3/GEONET

The Scientific Review Group from the federal Environmental Assessment Panel conducted two checks of the SYVAC3-CC3 GEONET code (SRG 1995). Specifically, one set of manual calculations analyzed the transport of I-129 through a fracture zone and into a well. The second analysis used a one-dimensional closed form diffusion model to compare with the SYVAC3-CC3 calculations for the behaviour of the most significant barrier in the EIS case study, i.e., the intact lower rock zone. Both checks closely agreed with the SYVAC3-CC3 results.

4.3.6 Response Function Solution for a Diffusive Geosphere

In 2013, the response function solution to a diffusion dominated sedimentary geosphere was analysed in support of the Fifth Case Study (NWMO 2013) and compared to two independent codes: FRAC3DVS and COMSOL. The sedimentary geosphere consisted of a sequence of sedimentary rocks with a variety of properties as shown in Table 4-1. The repository is located in the Cobourg formation. A complete description of the sedimentary rock properties can be found in Gobien et al. (2013).

Table 4-1: Sedimentary Rock Layers and Properties

Formation[1] (Listed from top to bottom)	Thickness (m)	Hydraulic Conductivity (m/s)	Porosity (-)	Tortuosity (-)
Guelph	71.57	3×10^{-8}	0.057	0.0061
Fossil Hill	6.86	5×10^{-12}	0.031	0.0017
Cabot Head	15.82	9×10^{-14}	0.116	0.032
Manitoulin	15.53	9×10^{-14}	0.028	0.0064
Queenston	77.52	2×10^{-14}	0.073	0.016
Georgian Bay	154.40	4×10^{-14}	0.070	0.014
Cobourg	46.32	2×10^{-14}	0.015	0.030

[1]The repository is located approximately 26 m below the top of the Cobourg formation.

The FRAC3DVS model is a complete 3D finite element groundwater and transport code that models the geosphere and repository in complete detail and accurately models the transport of radionuclides such as I-129. The model incorporates continuity boundary conditions between the various geosphere layers and applies head boundary conditions at the surface. No flow boundary conditions are applied to the bottom and sides of the model.

The COMSOL model is a one dimensional model similar to the SYVAC3-CC4 GEONET model; however, the model includes downward diffusion and accurately models interfaces between the rock layers with continuity of concentration and flux at the boundaries.

SYVAC3-CC4 (Version SCC409) only models upward diffusion and includes a mix of response function solutions to properly model the sedimentary formations: RF1, a solution for a semi-infinite layer, and RF3, a solution for a finite layer with a zero concentration at the exit of the layer. Transport through a rock layer that precedes a layer with a higher diffusion coefficient was conservatively represented using the RF3 response function. Alternatively, transport through a rock layer that precedes a layer with a lower diffusion coefficient was conservatively represented using the RF1 response function.

Figure 4-1 shows the comparison of the I-129 mass flows calculated by the three models at the interface of the top of Cobourg and Georgian Bay layers and at a well located in the Guelph layer. Although there are apparent differences between the three models at the top of Cobourg layer, the differences decrease with elevation above the Cobourg and the models agree well at the well location. The I-129 mass flow at the well calculated by CC4 is approximately two times higher than that calculated by FRAC3DVS or COMSOL mainly because CC4 doesn't model downward diffusion.

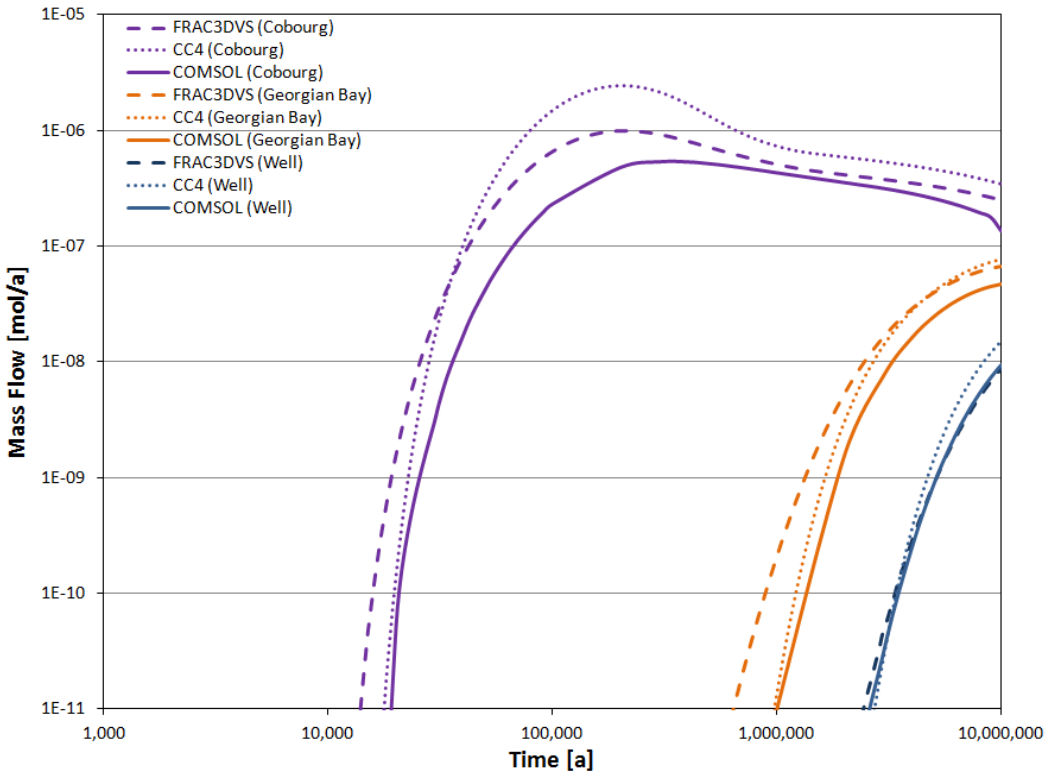

Figure 4-1: Comparison of I-129 mass flows from FRAC3DVS, COMSOL and CC4

4.4 TESTS OF GEONET METHODOLGY

This section describes the tests carried out to demonstrate that the simplified GEONET model adequately represents the true 3-D groundwater flow and transport through the geosphere. Many of these tests were done as part of the case studies carried out using SYVAC3-CC4, e.g., the Third Case Study and the Fourth Case Study. The tests are presented in chronological order.

4.4.1 MOTIF Comparison

A comparison was made between the solute transport calculations using GEONET and detailed solute transport calculations using MOTIF. The modelled system was a cross-section through the Whiteshell Research Area in the vicinity of the Underground Research Laboratory with a hypothetical repository located adjacent to a fracture zone (Chan et al. 1991). The study compared the transport of a non-sorbing solute in a 2-D region of space using MOTIF and GEONET. In the GEONET simulation, a network of 1-D segments extending over the 2-D region was used. Comparison of the spatial distribution of solute flow and the total mass flow into the fracture zone showed good agreement between the two models, with the agreement being best where the GEONET discretization was finest. It was also found that the GEONET network could be adjusted to give conservative results, at least at early times, by choosing the

shortest possible segment lengths, i.e., a transport length equal to the closest distance between the repository and the adjacent fracture zone.

4.4.2 PSACOIN Comparison

GEONET was compared to other contaminant mass-transport codes as part of the international PSACOIN Level 1a Intercomparison, as discussed in Section 6 (Davison et al. 1994). The specification for the Level 1a case contained a relatively complex repository, transport through a two-layer geosphere, and a simple well-based biosphere interface with a drinking water dose pathway (NEA 1990).

The test case specification included linear decay chains, a simple release rate from fuel, advective transport through the geosphere, water dilution, and a drinking water dose pathway. There were 100 input parameters, with specified probability distributions of normal, lognormal, uniform or loguniform for about half of these. The main conclusions of the Level 1a intercomparison were again very positive (NEA 1990). For example, the different modelling codes, including SYVAC3/GEONET, all calculated peak mean dose rates that were in excellent agreement (Davison et al. 1994, Figure 6.8.11).

4.4.3 FRAC3DVS Comparison: Third Case Study

For the Third Case Study (TCS), radionuclide releases out of the geosphere calculated by CC4 were compared to those calculated using the FRAC3DVS code (Garisto et al. 2004). In the TCS, radionuclides are released from the two defective containers in the repository. The radionuclide release rates from the defective containers are the same in the two models.

In CC4, the total nuclide flow out of the placement room at the EDZ/rock interface (which is calculated by INROC, see Section 3.7) is used as input to the appropriate node of the geosphere transport network. In FRAC3DVS, nested models are used to model transport in the repository and geosphere, with the mass flow out of the repository scale model used as input to the site scale model, as described in Garisto et al. (2004).

In the TCS, the defective containers are in repository Sector 1. The groundwater flow modelling indicates that groundwater from this repository sector is mainly discharged to the surface via the well. In development of the GEONET model for the TCS, for conservatism, it was assumed that all groundwater and contaminants from repository Sector 1 would be captured by the well. That is, in the GEONET model, there is a single groundwater pathway from repository Sector 1 and, when the well is operating, this pathway discharges to the surface via the well. In contrast, in the FRAC3DVS model, groundwater and contaminants from repository Sector 1 can enter the surface biosphere at several discharge locations (e.g., well, lake or river).

The radionuclide discharges from geosphere to the surface, as calculated by CC4 and FRAC3DVS for the Third Case Study, are compared in Figure 4-2, Figure 4-3, and Figure 4-4. Figure 4-2 shows the components of the nuclide mass flows out of the geosphere for I-129. In FRAC3DVS, there are I-129 releases to the well, lake and river discharge points, while, in CC4, all I-129 releases are to the well. Thus, CC4 overestimates the I-129 mass flow to the well. However, Figure 4-2 also shows that the total I-129 mass flow to the biosphere, i.e., summed over all discharge points, is similar in the two cases.

Figure 4-3 compares the total geosphere mass discharges for I-129, Cl-36 and Ca-41. The total mass flow curves for CC4 and FRAC3DVS have similar shapes. For all three nuclides, the peak mass flows are larger in CC4 and occur at a later time. Table 4-2 summaries this comparison.

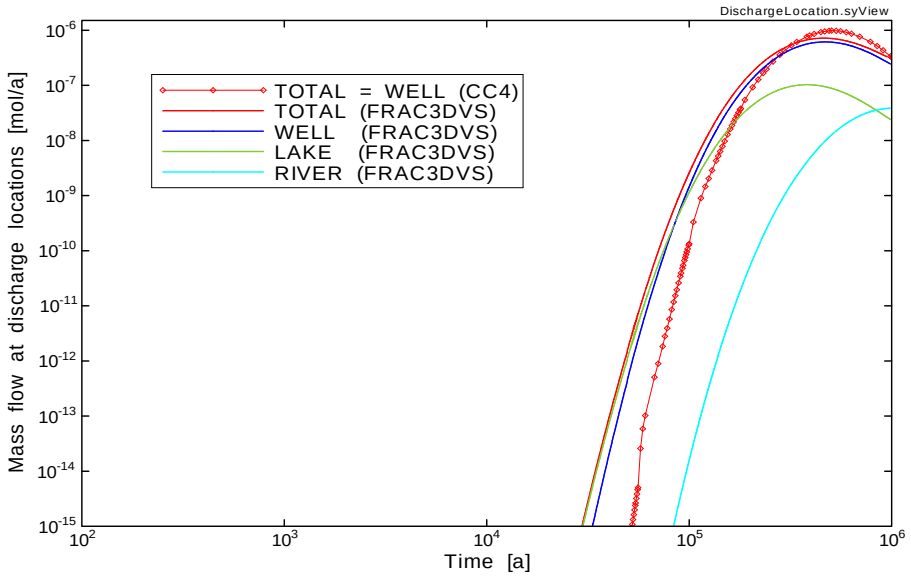

Figure 4-2: Comparison of the geosphere releases of I-129 for CC4 and FRAC3DVS, by discharge zone, for the Third Case Study

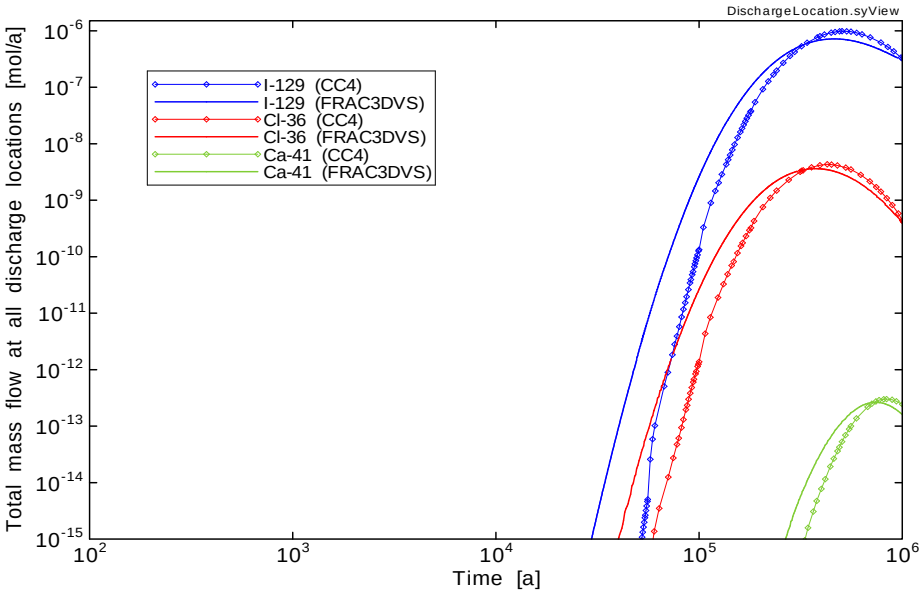

Figure 4-3: Comparison of the total geosphere releases of I-129, Cl-36 and Ca-41 for CC4 and FRAC3DVS for Third Case Study

Table 4-2: Comparison of CC4 and FRAC3DVS TCS Results: Geosphere Releases

Nuclide	Peak mass flow [mol/a]			Peak time [a]		
	CC4	FRAC3DVS	Ratio[1]	CC4	FRAC3DVS	Ratio[1]
I-129	9.8×10^{-7}	7.2×10^{-7}	1.36	5.1×10^{5}	4.6×10^{5}	1.10
Cl-36	4.3×10^{-9}	3.6×10^{-9}	1.19	4.3×10^{5}	3.8×10^{5}	1.13
Ca-41	3.0×10^{-13}	2.6×10^{-13}	1.15	8.4×10^{5}	7.5×10^{5}	1.12

[1]Ratio is the CC4 value divided by the FRAC3DVS value.

The agreement between CC4 and FRAC3DVS seem fairly good for these radionuclides, considering the differences in the two models. However, for Ca-41, the good agreement could be partially fortuitous, given that the peak mass flows of Ca-41 out of the repository are 3-fold higher in CC4 than FRAC3DVS, as shown in Table 4-3.

Table 4-3: Comparison of CC4 and FRAC3DVS TCS Results: Repository Releases

Nuclide	Peak mass flow [mol/a]			Time of peak flow [a]		
	CC4	FRAC3DVS	Ratio[1]	CC4	FRAC3DVS	Ratio[1]
I-129	2.4×10^{-6}	1.9×10^{-6}	1.3	3.8×10^{4}	7.2×10^{4}	0.53
Cl-36	2.9×10^{-8}	2.2×10^{-8}	1.3	3.2×10^{4}	5.8×10^{4}	0.55
Ca-41	9.2×10^{-10}	3.1×10^{-10}	3.0	7.5×10^{4}	9.9×10^{4}	0.76

[1]Ratio is the CC4 value divided by the FRAC3DVS value.

The calculated CC4 geosphere releases for the actinide nuclides Np-237, U-233, U-238 and U-234 are compared to the FRAC3DVS results in Figure 4-4 over the one million year FRAC3DVS simulation time. In both models, the total geosphere release rates are very low for all actinide nuclides because the actinides are strongly sorbed in the repository and geosphere. The FRAC3DVS actinide releases from the geosphere occur earlier and are, consequently, much larger than the corresponding CC4 releases during the 10^6 simulation period. This is particularly true for the progeny nuclides U-233 and U-234. These early releases are consistent with the results shown in Figure 4-3 for the fission product nuclides.

The dependence of the I-129 releases out of the geosphere on the longitudinal dispersivity was also examined in the Third Case Study. Longitudinal dispersivity values of 25 m, 50 m and 80 m were examined, with 50 m being the value used in the Reference Case. The transverse dispersivity is 10% of the longitudinal dispersivity. Transverse dispersion is included in the FRAC3DVS model but not the CC4 model.

The dependence of the geosphere releases on the dispersivity is shown in Figure 4-5. The same I-129 source term is used for all cases shown in Figure 4-5. For both models, the peak total discharge rate from the geosphere decreases as the dispersivity increases. This is expected because a larger dispersivity produces a wider plume (i.e., the peak occurs earlier but is lower). Also, the effect of dispersivity is more pronounced in CC4, likely because CC4 models transport in the geosphere using a network of one-dimensional flow tubes whereas FRAC3DVS is a true 3D transport code.

Based on these results it can be concluded that the radionuclides release rates to the biosphere calculated by CC4 are conservative relative to those calculated by FRAC3DVS for mobile, i.e., non-sorbing or weakly sorbing, radionuclides.

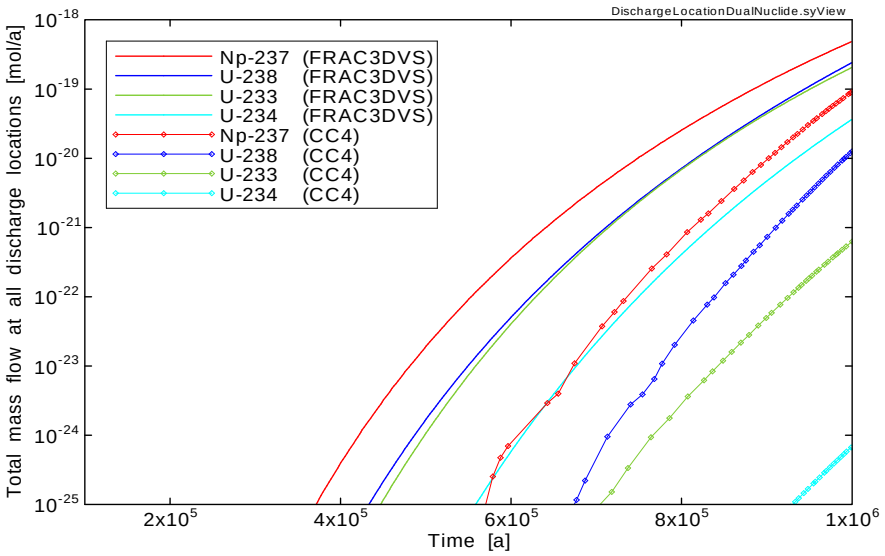

Figure 4-4: Comparison of total geosphere releases of actinide nuclides for CC4 and FRAC3DVS in the Third Case Study

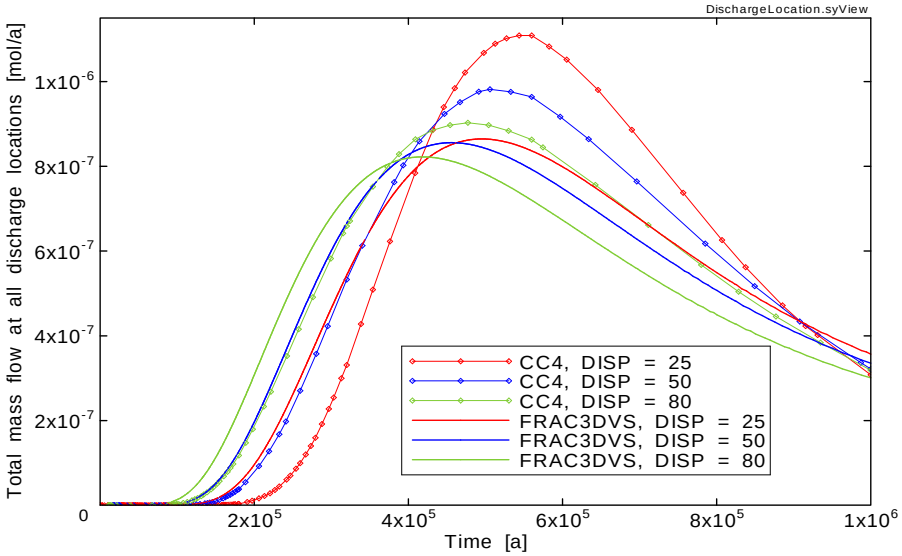

Figure 4-5: Comparison of the total I-129 release rates from the geosphere for different dispersivity values as calculated by CC4 and FRAC3DVS for the TCS

4.4.4 FRAC3DVS Comparison: Horizontal Borehole Concept Study

In the Horizontal Borehole Concept (HBC) (Garisto et al. 2005a), copper used fuel containers are placed in long horizontal boreholes drilled into the host rock from access tunnels (see Figure 3-9). The repository site is the same as that used in the Third Case Study. Groundwater flow simulations were carried out using FRAC3DVS, and radionuclide transport calculations were carried out using both FRAC3DVS and CC4. The GEONET model used in the CC4 calculations was developed using the groundwater modelling results from FRAC3DVS as described in Garisto et al. (2005a, Appendix B).

As in the Third Case Study, the two defective containers in the HBC study are in repository Sector 1. These containers are assumed to fail early, leading to early releases of radionuclides. The radionuclide release rates from the defective containers are the same in the two models.

The FRAC3DVS groundwater flow modelling indicates that groundwater from this repository sector is mainly discharged to the surface via the well, when the well is operating. However, in development of the GEONET model for the HBC, for conservatism, it was assumed that all groundwater and contaminants from repository Sector 1 would be captured by the well. That is, in the GEONET model, there is a single groundwater pathway from repository Sector 1 and, when the well is operating, this pathway discharges to the surface via the well. In contrast, in the FRAC3DVS model, groundwater and contaminants from repository Sector 1 can enter the surface biosphere at several discharge locations (e.g., well, lake or river).

The radionuclide discharges from geosphere to the surface for the HBC study, as calculated by CC4 and FRAC3DVS, are compared in Figure 4-6 and Figure 4-7. Figure 4-6 shows the components of the nuclide mass flows out of the geosphere for I-129. In FRAC3DVS, there are I-129 releases to the well, lake and river discharge points, while, in CC4, all I-129 releases are to the well. Thus, CC4 overestimates the peak I-129 mass flow to the well. However, Figure 4-6 also shows that the total I-129 mass flow to the biosphere, i.e., summed over all discharge points, is similar in the two models.

Figure 4-7 compares the total geosphere mass discharges for I-129, Cl-36 and Ca-41. The total mass flow curves for CC4 and FRAC3DVS have similar shapes. For all three nuclides, the peak mass flows are larger in CC4 and occur at a later time. Table 4-4 summaries this comparison. Given that the radionuclide mass flows out of the repository calculated by the two models are similar (see Table 4-5), this indicates that the peak release rates through the geosphere are larger in CC4 but occur on a similar time scale for non-sorbing and weakly sorbing radionuclides.

The results of these comparisons are similar but not identical to the corresponding comparisons between CC4 and FRAC3DVS for the Third Case Study (see Table 4-2 and Table 4-3). Differences are apparent for Ca-41, which is weakly sorbed by the buffer and backfill materials. These differences are likely due to the fact that the TCS placement room contains larger volumes of buffer and backfill materials than the HBC placement room. (In fact, there is no backfill in the HBC placement room.)

The calculated U-238 and U-234 mass flows out of the geosphere are very low for both the CC4 and FRAC3DVS models. For these nuclides, the differences between the two models are similar to those observed previously in the Third Case Study (see Section 4.4.3) and so are not shown here.

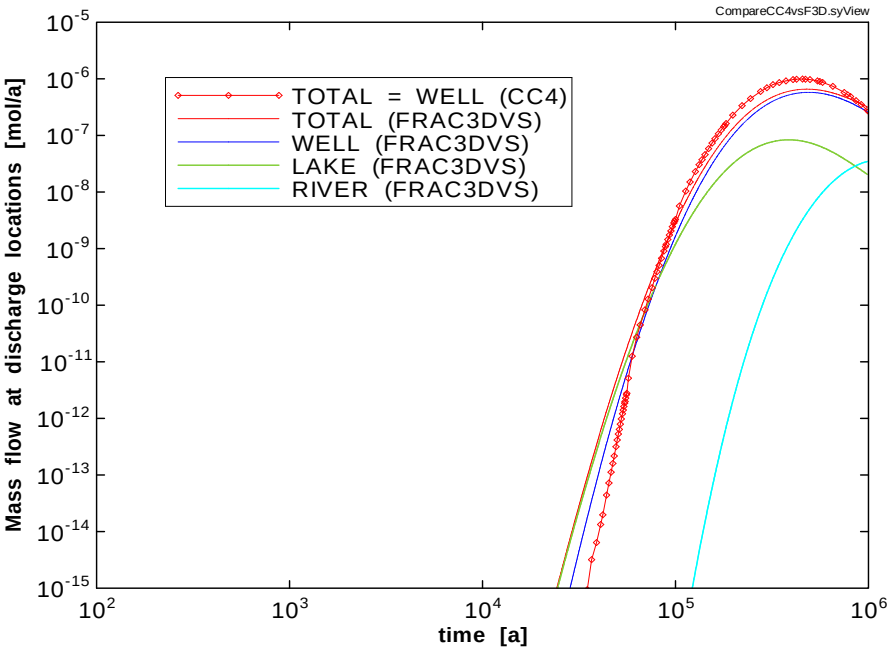

Figure 4-6: Comparison of the geosphere releases of I-129 for CC4 and FRAC3DVS, by discharge zone, for the HBC study

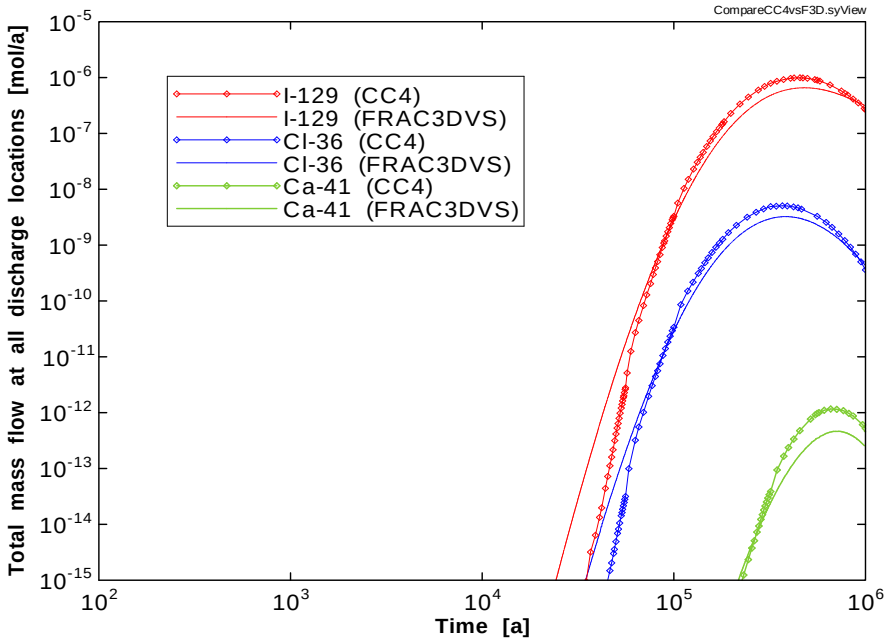

Figure 4-7: Comparison of the total geosphere releases of I-129, Cl-36 and Ca-41 for CC4 and FRAC3DVS in the HBC study

Table 4-4: Comparison of CC4 and FRAC3DVS Results for HBC: Geosphere Releases

Nuclide	Peak mass flow [mol/a]			Peak time [a]		
	CC4	FRAC3DVS	Ratio[1]	CC4	FRAC3DVS	Ratio[1]
I-129	9.92×10^{-7}	6.59×10^{-7}	1.51	4.56×10^{5}	4.82×10^{5}	0.946
Cl-36	5.08×10^{-9}	3.25×10^{-9}	1.56	3.68×10^{5}	3.83×10^{5}	0.961
Ca-41	1.17×10^{-12}	4.65×10^{-13}	2.52	6.58×10^{5}	7.25×10^{5}	0.908

[1]Ratio is the CC4 value divided by the FRAC3DVS value.

Table 4-5: Comparison of CC4 and FRAC3DVS Results for HBC: Repository Releases

Nuclide	Peak mass flow [mol/a]			Time of peak flow [a]		
	CC4	FRAC3DVS	Ratio[1]	CC4	FRAC3DVS	Ratio[1]
I-129	2.85×10^{-6}	2.74×10^{-6}	1.04	1.80×10^{4}	2.44×10^{4}	0.738
Cl-36	3.53×10^{-8}	3.34×10^{-8}	1.06	1.57×10^{4}	2.05×10^{4}	0.766
Ca-41	1.75×10^{-9}	1.34×10^{-9}	1.31	5.00×10^{4}	6.20×10^{4}	0.806

[1]Ratio is the CC4 value divided by the FRAC3DVS value.

Based on these results it can be concluded that the radionuclides release rates to the biosphere calculated by CC4 are conservative relative to those calculated by FRAC3DVS for mobile, i.e., non-sorbing or weakly sorbing, radionuclides.

4.4.5 FRAC3DVS Comparison: Fourth Case Study

In the Fourth Case Study (NWMO 2012a), copper used fuel containers are placed in boreholes drilled into the floor of the placement rooms. The repository site is the same as that used in the Third Case Study. However, the repository is larger since it contains more used fuel bundles. Groundwater flow simulations were carried out using FRAC3DVS, and radionuclide transport calculations were carried out using both FRAC3DVS and CC4. The GEONET model used in the CC4 calculations was developed using the groundwater modelling results from FRAC3DVS as described in NWMO (2012a).

The three defective containers in the Fourth Case Study are in repository Sector 8. The defective containers are assumed to fail early, leading to early releases for radionuclides. The radionuclide source terms are the same in the CC4 and FRAC3DVS models.

The FRAC3DVS groundwater flow modelling indicates that groundwater from repository Sector 8 is mainly discharged to the surface via the well, when the well is operating. However, in the development of the GEONET model for the Fourth Case Study, for conservatism, it was assumed that all groundwater and contaminants from repository Sector 8 would be captured by the well. That is, in the GEONET model, there is a single groundwater pathway from repository Sector 8 and, when the well is operating, this pathway discharges to the surface via the well. In contrast, in the FRAC3DVS model, groundwater and contaminants from repository Sector 8 can enter the surface biosphere at several discharge locations (e.g., well or wetland).

The radionuclide mass flows out of the geosphere and into the surface biosphere for the two models are compared in Figure 4-8, with Table 4-6 summarizing the peak values. (Note that, for Sn-126, the releases into the biosphere from repository Sector 8 are very low.) The agreement is best for I-129, a non-sorbing radionuclide with a long half-life.

The comparisons in Table 4-6 should be viewed in light of the results in Table 3-10, which shows that the peak radionuclide releases into the geosphere from the repository calculated by the two models are in good agreement, except for Cs-135 and Sn-126. This indicates that the peak release rates through the geosphere are larger and the transport times through the geosphere are shorter in CC4 than in FRAC3DVS. The shorter transport time in CC4 would affect the peak release rates for shorter-lived radionuclides because there is less time for radionuclide decay.

For U-238 and U-234, the release rates are effectively zero in both models due to the highly sorbing nature of these radionuclides.

In summary, this comparison indicates that the radionuclide releases from the geosphere (to the biosphere) calculated by CC4 are conservative when compared to FRAC3DVS (i.e., the peak values are greater than those from FRAC3DVS while the time of the peak is earlier).

Table 4-6: Comparison of Peak Release Rates to the Surface for the 4CS

Nuclide	Peak Mass Flow (mol/a)			Time of Peak Release (a)		
	CC4	FRAC3DVS	Ratio[1]	CC4	FRAC3DVS	Ratio[1]
I-129	2.15×10^{-6}	1.98×10^{-6}	1.08	1.00×10^{5}	1.02×10^{5}	0.98
C-14	6.16×10^{-10}	1.62×10^{-10}	3.79	2.24×10^{4}	2.92×10^{4}	0.77
Ca-41	9.02×10^{-9}	2.41×10^{-9}	3.74	5.60×10^{4}	1.25×10^{5}	0.45
Cl-36	2.71×10^{-8}	1.52×10^{-8}	1.78	5.60×10^{4}	1.43×10^{5}	0.39
Cs-135	3.93×10^{-7}	8.28×10^{-8}	4.75	1.00×10^{6}	2.86×10^{6}	0.35

Note: [1] Ratio is the CC4 value divided by the FRAC3DVS value.

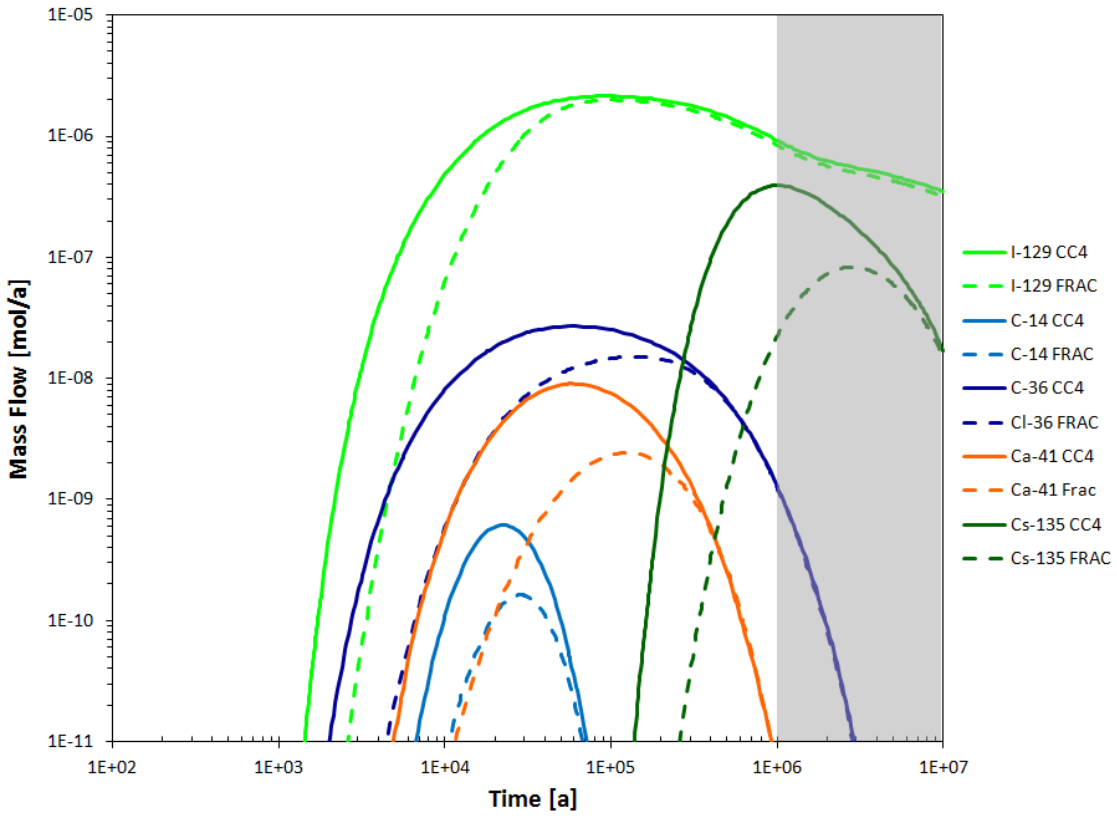

Note: Sn-126 results are off scale low

Figure 4-8: Comparison of CC4 and FRAC3DVS transport of I-129, C-14, Cl-36 Ca-41 and Cs-135 to the surface for the 4CS

4.4.6 FRAC3DVS Comparison: Glaciation Scenario Study

4.4.6.1 Introduction

During past glacial cycles, much of Canada was covered by kilometre-thick ice sheets. The movement of ice sheets over a repository site represent a large potential perturbation on time scales of interest to long-term safety assessment. Thus, the NWMO has quantitatively assessed the long-term safety implications of glacial cycles for a deep geological repository at the hypothetical Third Case Study (TCS) site on the Canadian Shield (Garisto et al. 2011, Walsh and Avis 2010, Garisto et al. 2010). This is referred to as the Glaciation Scenario study (GSS). The repository layout at ≈670 m depth is based on the Horizontal Borehole Concept (HBC) study (Garisto et al. 2005a).

To explore the possible impacts of glaciation, a representative future glacial cycle was defined using models of the past glacial cycle (Peltier 2003, 2006). In particular, in the Glaciation Scenario study, it was assumed that the present interglacial (temperate) period lasts a further 50,000 years; after which, the climate at the repository site is assumed to be described by repeating cycles of a simplified version of Simulation nn2778 from Peltier (2006). The ice sheet height at the repository site, during the first 180,000 years, is illustrated in Figure 4-9. Other

properties of the glacial cycle, e.g., permafrost depth, are described in Table 4-7. A total of 8 glacial cycles would occur over the next million years.

The study area is a hypothetical watershed of about 150 km^2 (see Figure 4-10). The area is characterized by mild topographic change with a topographic high along the northern boundary. There are two major lakes within the model domain, the North and South lakes. The North Lake was identified as a discharge zone and was the terminus of the shortest flow pathline from the radionuclide source (i.e., the defective containers, which are located at the east corner of the repository). For the current study, the two lakes have been designated as open taliks, under which permafrost conditions will not occur during the glacial cycle.

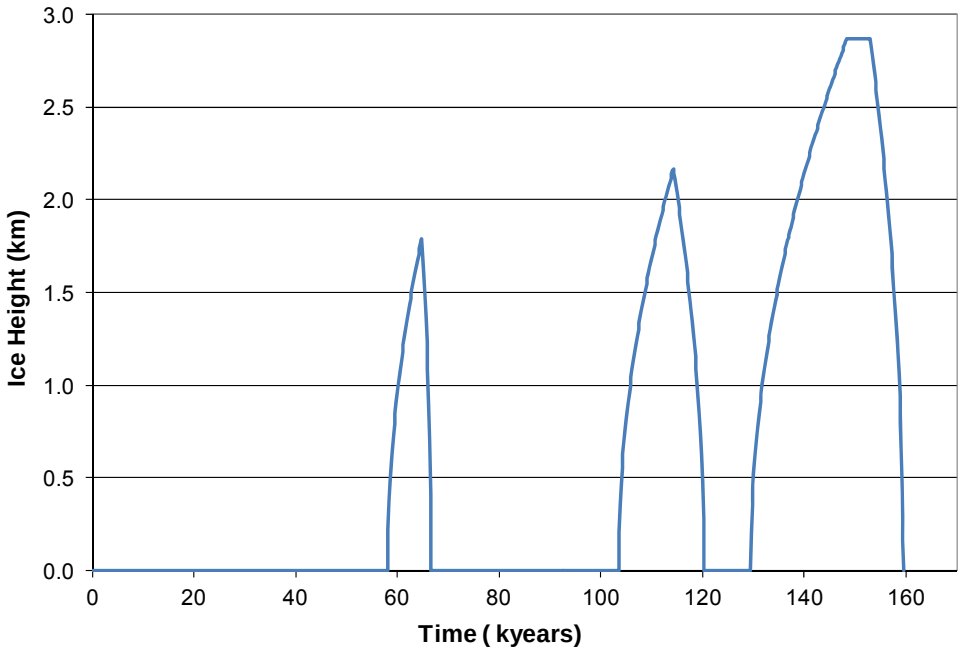

Figure 4-9: Ice sheet height at the repository site during the first cycle of reference glacial cycle

Because of the movement of ice sheets over the repository site, which affects hydrogeological boundary conditions, the groundwater flow fields are transient during the Glaciation Scenario study. The numeric transient groundwater flow modeling was performed using FRAC3DVS (Therrien et al. 2010, Therrien and Sudicky 1996). FRAC3DVS includes a hydromechanical (HM) coupling module, which is based on the work of Neuzil (2003) and assumes purely vertical strain. This module was included in the FRAC3DVS groundwater and I-129 transport simulations.

Table 4-7: Time History of Simplified Glacial Cycle and Geosphere State Names

Climate State Description[1]	Geosphere State Name	Permafrost Depth (m)	Start Time[2] (a)	End Time (a)	Duration (a)
Temperate (boreal)	TEMPR	0	0	50,300	50,300
Permafrost 1	PERM1	100	50,300	5,8100	7,800
Ice Sheet 1 Advancing - Cold Based	ISCB1	100	58,100	64,800	6700
Ice Sheet 1 Retreating - Cold Based	ISCB1	100	64,800	66,700	1,900
Permafrost 2	PERM2	250	66,700	103,500	36,800
Ice Sheet 2 Advancing - Cold based	ISCB2	150	103,500	114,300	10,800
Ice Sheet 2 Retreating - Warm Based	ISWB1	0	114,300	120,300	6,000
Permafrost 3	PERM2	250	120,300	129,500	9,200
Ice Sheet 3 Advancing - Cold based	ISCB3	200	129,500	136,900	7,400
Ice Sheet 3 Advancing - Warm Based	ISWB2	0	136,900	153,000	16,100
Ice Sheet 3 Retreating - Warm Based	ISWB1	0	153,000	159,500	6,500
Proglacial Lake	PROLA	0	159,500	160,700	1,200
Temperate (boreal)	TEMPR	0	160,700	171,500	10,800

[1]A well (738 m^3/a) operates during all temperate states. There is a talik beneath the lakes during permafrost states but no taliks during cold based ice sheet states.

[2]The current interglacial extend 50,000 years into the future and immediately precedes the start of the first glacial cycle at 50,300 years. The glacial cycle repeats itself starting at 171,500; 292,700; etc. years.

Because the groundwater flow field is transient, it was necessary to develop a new version of SYVAC2-CC4 (i.e., SYVAC3-CC4, Version SCC407) in which the geosphere and biosphere states could be varied, at selected time points, according to the changing climate. The climate states used to define the future climate in the Glaciation Scenario study are described in Table 4-7. The current-day glacial cycle is assumed to end following a long Temperate State (i.e., today's climate) and then a new glacial cycle begins. The new cycle begins at a Permafrost State and proceeds through a sequence of climatic states finishing with a temperate climatic state. The glacial cycle is 121,200 years long. After the first glacial cycle is complete, the climate will cycle over the same sequence of climatic states, starting at the Permafrost 1 state, until the end of the approximately one million year simulation period. Eight complete glacial cycles occur during the one million year simulation period.

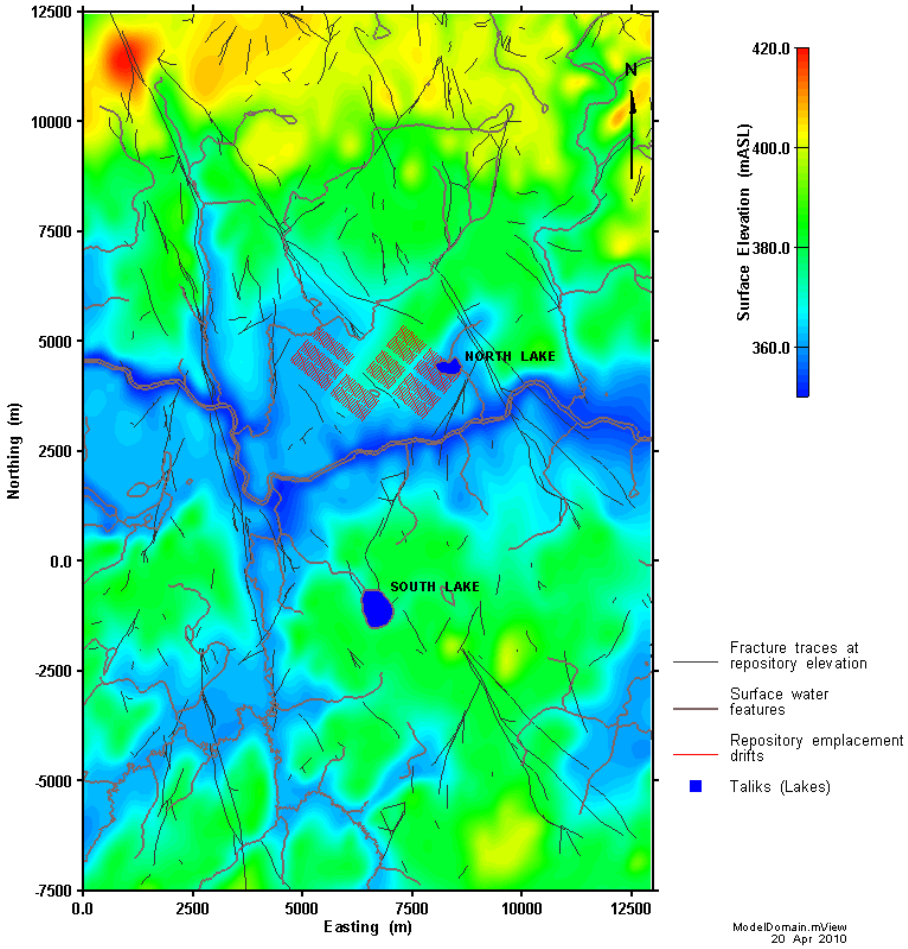

Figure 4-10: Hydrogeological and transport model domain, illustrating the model extent, surface water features, fracture zones at repository depth, and repository placement drifts

Based on the characteristics of the climatic states in Table 4-7, it was possible to define a set of unique geosphere and biosphere states for use in CC4. Each unique geosphere state and biosphere state has different properties. For example, the groundwater flow field is different for each geosphere state. These properties remain constant for the duration of the state. All Permafrost States have two open taliks. These are referred to as the North and South talik or, during Temperate States, the North and South lake.

Figure 4-11 shows the colour scheme used in many of the figures presented below. The green sections are Temperate States, the tan sections are Permafrost States, the blue sections are Ice Sheet States and the grey section is the Proglacial Lake State. The colour bars show the relative duration of the states, e.g., the first Temperate State lasts 50,300 years compared to the other Temperate States which last 10,800 years.

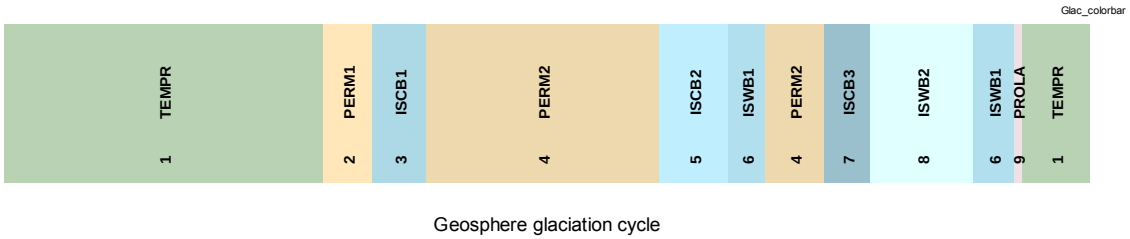

Figure 4-11: Colour scheme for geosphere glaciation states showing both the geosphere state name and geosphere state index (see Table 4-7)

4.4.6.2 Overview of CC4 and FRAC3DVS Comparisons

The CC4 geosphere model has a simplified description of the repository site geometry, relative to the FRAC3DVS model. The geosphere in CC4 is represented by a network of 1-dimensional transport segments, whereas FRAC3DVS uses a three dimensional numerical model to represent the geosphere (Walsh and Avis 2010)). Furthermore, CC4 uses a series of (fixed) groundwater flow fields to represent the transient groundwater flow field during a glacial cycle. Generally, CC4 uses a "snapshot" of the transient groundwater field at the midpoint of a geosphere or climatic state to represent the groundwater flows during that geosphere state.

The FRAC3DVS model does not include a representation of the repository in the geosphere model; rather the nuclide mass flows out of the repository previously developed for the Horizontal Borehole Concept study (Garisto et al. 2005a) were used as source terms for the FRAC3DVS transport modelling (Garisto et al. 2010). In contrast, the CC4 model includes a representation (albeit appropriately simplified) of the repository (Garisto et al. 2005a). In addition, a larger longitudinal dispersivity value of 80 m was used in the FRAC3DCS transport calculations, to maintain numerical stability, instead of the 50 m value used in CC4.

In the following sections, the CC4 and FRAC3DVS model results for I-129 are compared as a consistency check between these two numeric models. (FRAC3DVS transport results are only available for I-129.) In particular, we compare the I-129 release rates from the geosphere to the biosphere. The I-129 release rates from the repository cannot be compared because the repository is not explicitly represented in the FRAC3DVS transport model and, hence, I-129 release rates out of the repository are not calculated by FRAC3DVS.

The comparisons between the CC4 and FRAC3DVS are first done for the Constant Climate cases and then for the Glaciation Scenario Study cases.

4.4.6.3 Comparison of FRAC3DVS and CC4 for Constant Climate Cases

In this section, we compare the CC4 and FRAC3DVS results for the following Constant Climate cases:

1. The DC1 Temperate case, in which the defective containers are located at source location DC1 (see Figure 4-12). Except for the constant climate, this calculation case is identical to the reference case of the Glaciation Scenario Study.
2. The DC3 Temperate case, in which the defective containers are located at source location DC3 (see Figure 4-12). Except for the constant climate and source location, this calculation case is identical to the reference case of the Glaciation Scenario Study.

Groundwater from location DC1 discharges to the surface via the well or North Lake, whereas groundwater from location DC3 discharges to the Stream (or Wetland) located directly to the west of the repository location, at approximately 3000 northing and 4000 easting on Figure 4-10.

Groundwater travel times to the surface are shorter for the DC1 location than the DC3 location. For the DC3 location, the groundwater travel time to the Well or Lake is so long (i.e., much longer than the simulation time) that this groundwater pathway was not modelled in CC4.

The total I-129 mass flow rates to the biosphere are presented in Figure 4-13 for the DC1 and DC3 Temperate cases. Overall the agreement between the two models is fairly good for these cases; although, in FRAC3DVS, the peak I-129 mass flows occur earlier because the FRAC3DVS model uses a larger longitudinal dispersivity value (80 m in FRAC3DVS versus 50 m in CC4).

For the DC1 Temperate case, all I-129 is discharged to the biosphere via the well in CC4; whereas, in FRAC3DVS, only a portion of the I-129 plume is captured by the well and some I-129 is also discharged to the North Lake. This difference arises because the CC4 geosphere transport network was conservatively constrained, by the choice of data values for well capture, so that the well captures the entire contaminant plume from location DC1. Thus, for this case, CC4 overestimates the contaminant mass flows to the well relative to FRAC3DVS. For the DC3 Temperate case, the FRAC3DVS and CC4 releases are to the Stream.

Figure 4-12: Defective container source locations. Only DC1 and DC3 were assessed for the complete performance period

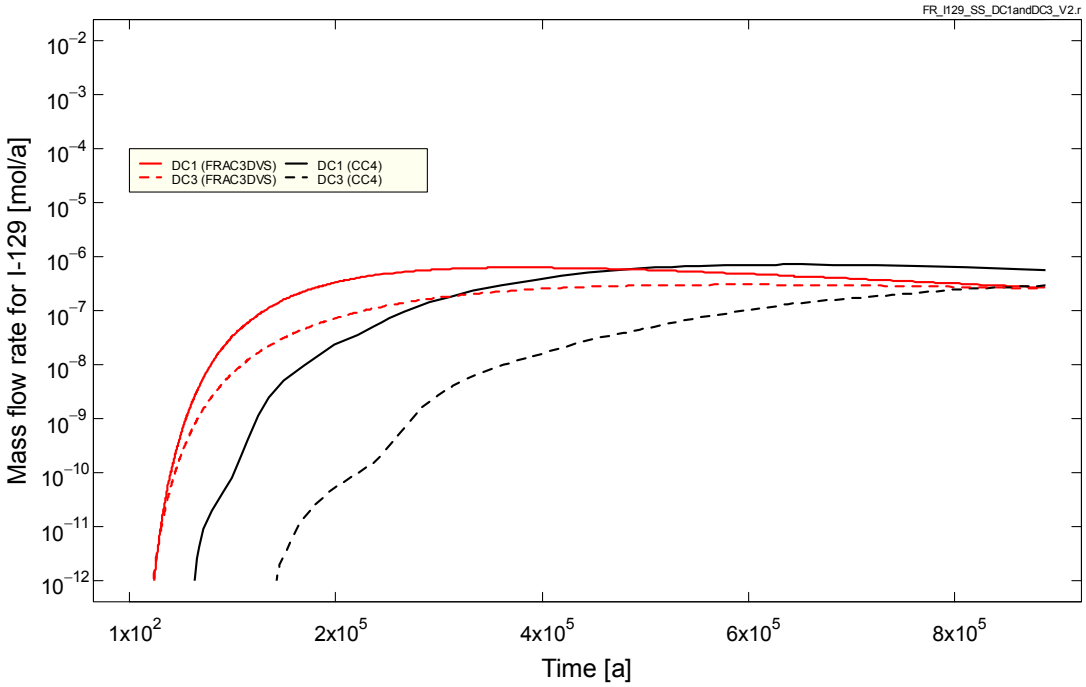

Figure 4-13: Comparison of I-129 geosphere releases to the biosphere for CC4 and FRAC3DVS for the DC1 Temperate and DC3 Temperate cases of the Constant Climate Scenario

Table 4-8 summarizes the calculated peak I-129 mass flows to the surface for the DC1 and DC3 Temperate cases. The peak mass flow rates to the well and stream are similar in CC4 and FRAC3DVS, although the peak mass flow rates occur earlier in FRAC3DVS. The earlier arrival time in FRAC3DVS is mainly due to the higher longitudinal dispersivity value used in the FRAC3DVS transport model.

Table 4-8: Comparison of CC4 and FRAC3DVS I-129 Releases to the Biosphere for the DC1 Temperate and DC3 Temperate Cases

Nuclide	Peak mass flow rate [mol/a]			Time of Peak [a]		
	CC4	FRAC3DVS	Ratio[1]	CC4	FRAC3DVS	Ratio[1]
DC1 Source						
Well	7.4×10^{-7}	4.7×10^{-7}	1.2[#]	6.2×10^{5}	4.0×10^{5}	1.5
Lake	0.0	1.7×10^{-7}		NA	3.5×10^{5}	NA
DC3 Source						
Stream	2.8×10^{-7}	3.1×10^{-7}	0.9	8.9×10^{5}	6.0×10^{5}	1.5
Lake.	0.0	8.4×10^{-17}	NA	NA	1.0×10^{6}	NA

[1]Ratio is the CC4 result divided by the FRA3DVS result.
[#]This is the ratio of the peak total mass flow to well and lake.

4.4.6.4 Comparison of FRAC3DVS and CC4 for Glaciation Cases

In this section, we compare the CC4 and FRAC3DVS results for various Glaciation Scenario cases. We consider the following two Glaciation Scenario cases:

1. The reference case, in which the defective containers are in the DC1 source location (see Figure 4-12).
2. The DC3 Glaciation case, in which the defective containers are in the DC3 source location (see Figure 4-12). Except for the source location, this calculation case is identical to that for the reference case.

In Figure 4-14, the I-129 mass flows from the geosphere to the biosphere from CC4 and FRAC3DVS are compared for the reference case of the Glaciation Scenario. (The colour scheme used for the geosphere glaciation states is shown in Figure 4-11.)

Initially, the FRAC3DVS mass flow rates to the biosphere are larger than those from CC4, because the contaminant plume reaches the surface faster in FRAC3DVS, as was the case in the constant climate cases. However, the agreement becomes better after about 3×10^5 years and, at longer times, the CC4 I-129 geosphere releases generally exceed the FRAC3DVS releases except at particular times during each glacial cycle (such as at the beginning of the long Permafrost State).

A prominent difference between the two models occurs at the beginning of the second and longest Permafrost State (PERM2 or geosphere state 4, see Figure 4-11) in the glacial cycle. In FRAC3DVS, a pulse of I-129 mass is released into the biosphere at the start of this Permafrost State because groundwater flow velocities are generally higher (and upwards) at the beginning of the second Permafrost State (Garisto et al. 2010, Section 6) due to pressurization of the

groundwater flow system during the Ice Sheet State preceding this Permafrost State. In CC4, the I-129 release rate increases rapidly at the start of this Permafrost State and reaches a fairly constant value after several thousand years.

This difference is likely due to the fact that the two codes use different approaches to handle the time-dependent groundwater flow field. In FRAC3DVS, the groundwater flow field is transient. In contrast, in CC4, a (fixed) snapshot of the groundwater flow field is selected for use during each unique geosphere state. (For PERM2, the snapshot is taken near the end of the state.) Thus, the CC4 model does not include a complete representation of the transient groundwater flow field. In particular, the higher groundwater flows into the North talik, which occur at the beginning of the second Permafrost State, are absent in the CC4 model. In FRAC3DVS, these high flows carry a pulse of I-129 mass into the North talik at the start of the second Permafrost State. Similar, but more muted, differences are also noticeable during the start of the other Permafrost States.

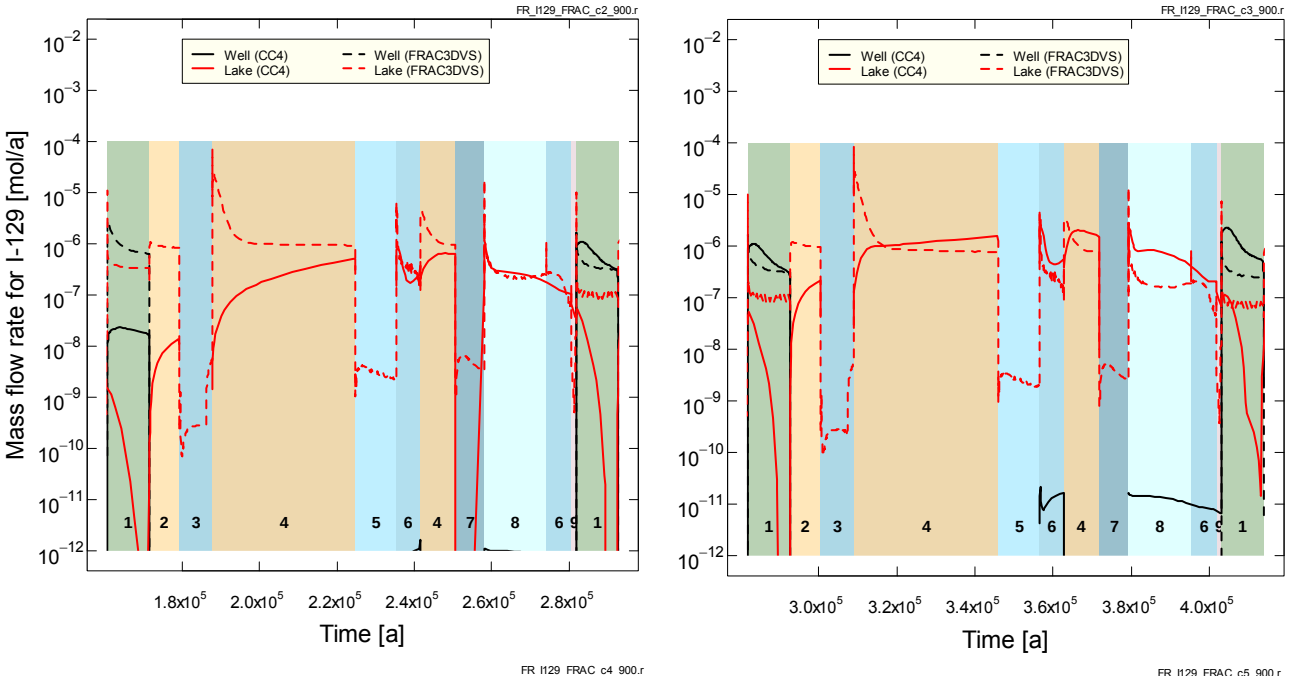

Figure 4-14: Comparison of the I-129 geosphere releases to the biosphere for CC4 and FRAC3DVS for the Reference Case and glacial cycles 2 and 3; for the other glacial cycles, the I-129 releases to the biosphere are similar to those for cycle 3

Another apparent difference between the two models occurs during cold-based ice sheet states (geosphere states 3, 5 and 7). In FRAC3DVS, the I-129 mass flow rate into the biosphere is lower during these stated (compared to preceding or subsequent states); but, in CC4, it is zero. This difference arises because the properties of the permafrost zone are different in the two models. In CC4, the permafrost is considered impermeable and so there is no mass transport through the permafrost. In contrast, in FRAC3DVS, permafrost has an unrealistically high water filled porosity (similar to granite), allowing radionuclides to be transported (both by advection and diffusion) through the permafrost.

In summary, although there are differences, the comparisons indicate that, even though the peak I-129 mass flows occur earlier in FRAC3DVS, these two significantly different models predict similar trends for the I-129 mass flow rates into the biosphere.

The I-129 mass flow rates to the biosphere from FRAC3DVS and CC4 are compared in Figure 4-15 for the DC3 Glaciation case. For the DC3 source location, the I-129 discharges to the biosphere are mainly to the Stream. The results in Figure 4-15 indicate that the I-129 plume reaches the biosphere much earlier in FRAC3DVS than in CC4 for the DC3 source location. This larger difference (compared to the Reference Case) is likely due to the larger dispersivity values used in the FRAC3DVS model.

The major difference between the FRAC3DVS and CC4 models for the DC3 Glaciation case occurs during Permafrost and cold-based Ice Sheet States. During these periods, permafrost exists below the Stream discharge location. Therefore, the differences in the two models during these periods arise because the permafrost (transport) properties are different in the two models. In CC4, the permafrost is impermeable and so there is no mass transport through the permafrost. Therefore, in CC4, I-129 discharges to the Stream are zero during Permafrost and cold-based Ice Sheet States. In FRAC3DVS, the permafrost is conservatively assigned the same transport properties as granite, so although I-129 mass flows to the Stream discharge are much reduced during these periods they are not zero.

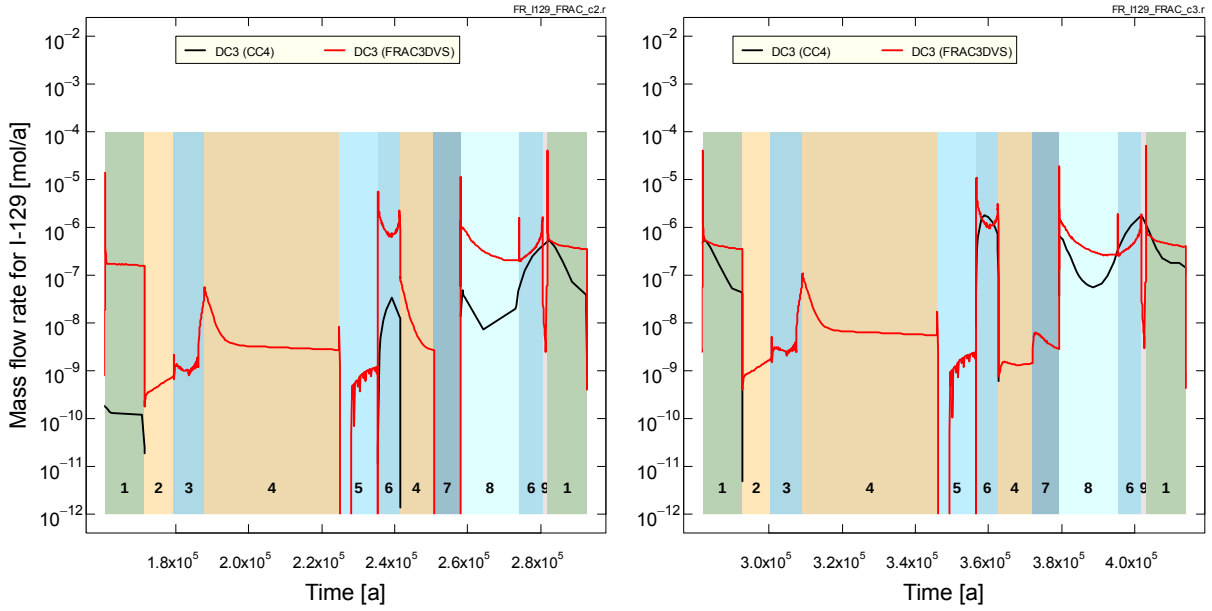

Figure 4-15: Comparison of the I-129 geosphere releases to the stream discharge for CC4 and FRAC3DVS for the DC3 Glaciation case for glacial cycles 2 and 3; for the other glacial cycles, the I-129 releases to the biosphere are similar to those for cycle 3

4.5 CONCLUSIONS OF GEONET TESTS

The tests of the GEONET model described in this section indicate that (1) the solutions of the advection-dispersion equations used in the GEONET model are correct, (2) the solutions are properly treated at the intersection of the line segments in the GEONET network, and (3) the GEONET methodology can be used to adequately represent the true 3-D steady-state groundwater flow and radionuclide transport in the geosphere. However, for complex groundwater flow fields, a more refined GEONET network may be required to for this task.

Furthermore, the comparisons made for the Glaciation Scenario study, in which the groundwater flow field is transient, indicate that the CC4 system model generally reproduces the key results from FRAC3DVS. This suggests that the approach taken to represent the transient groundwater flow field (generated by FRAC3DVS) in CC4, by using “snapshots” of the transient groundwater flow field at particular times during the glacial cycle, is acceptable.

4.6 GEOSPHERE - BIOSPHERE INTERFACE

In addition to the well, the SYVAC3-CC4 model allows for transport of nuclides, via groundwater, from the geosphere into other biosphere regions, such as lake sediments and garden soils. The testing of these interfaces is discussed in the next section as part of the biosphere model validation tests.

5. BIOSPHERE MODEL VALIDATION

The CC4 biosphere model is comprised of four main submodels: the surface water submodel; the soil submodel; the atmospheric submodel; and the food chain and dose submodel. The four submodels are considerably different with respect to their treatment of time-dependence.

The biosphere model assumes that the watershed containing the repository site includes a major surface water body that intercepts radionuclides released from the repository directly or through various groundwater discharge areas within the watershed. The critical group is a self-sufficient farmer household that lives near the repository site, raises animals and grows plants near the site and uses water from a well or the surface water body.

It is not possible to directly validate the main submodels of the biosphere for long-term safety assessments because of the long time periods of interest. However, it is possible to make comparisons with real data over short periods (months to years). Furthermore, code comparisons help ensure that the models perform as expected.

5.1 Surface Water Submodel

In the surface water model, a single, well-mixed compartment represents the water column of the surface water body and a second compartment represents the surficial sediments. The model explicitly includes the principal mass flows into and out of the surface water body that control the behaviour of contaminants in aquatic systems (NWMO 2012b). Most other processes are implicitly incorporated in the values of the net hydrological or biogeochemical parameters (e.g., sediment resuspension).

Processes that affect contaminants in surface water systems are dilution, losses to lake outflow, degassing to the atmosphere, transfer from water to sediment, sedimentation, and radioactive decay and ingrowth. Other processes that are rapid, seasonal or exceedingly slow have been excluded from the model (e.g., variations in lake discharge due to spring snowmelt, lake stratification during summer, in-filling of the lake due to sedimentation, etc.) because they will have little impact on long-term model predictions. However, the implications of slow processes are included by using a distribution of parameter values (e.g., lake depth) and by assuming that sediments are available for farming.

Various datasets are available describing the fate of radionuclides entering lakes from atmospheric fallout and from experimental additions to the epilimnion of lakes (Bird et al. 1992 and references therein). However, for disposal of used fuel in a repository, contaminants released from the repository would mainly enter the bottom waters of a surface water body with groundwater discharging into the water body. Thus, to be able to use much of the literature data to validate the surface water model, it was important to test the hypothesis that the ultimate fate of radionuclides added to an anaerobic hypolimnion and the epilimnion is the same. This was carried out by Bird et al. (1999, 1998, 1997) by determining, over a five year period, the fate of (redox-sensitive) Co-60 and (redox-insensitive) Cs-134 added to the anaerobic hypolimnion of Lake 226 at the Experimental Lakes Area, Ontario. They concluded that there was little difference in the fate of these radionuclides when their addition is to the anaerobic hypolimnion versus the epilimnion; and, consequently, literature data from epilimnetic additions can be used to validate the surface water model.

The surface water submodel has been validated with field data from studies in Canadian Shield lakes that lasted over several years (Bird et al. 1992). The studies involved both relatively reactive (phosphorous) and nonreactive (calcium) elements as well as various radionuclides (Co-60, Cs-134 and H-3). The duration of the aquatic studies was long compared to the time required for the water concentrations to reach steady state. Thus, parts of the surface water model can also be assumed to perform well over long periods of time relative to a biosphere time scale.

Details of these tests can be found in Bird et al. (1992) and a summary of the results is provided in Table 5-1. (Note that the parameter values used in the model calculations were selected *a priori*, unless otherwise specified.) The predicted water and sediment concentrations were found to be in reasonable agreement with the observed values when uncertainties were taken into consideration.

Table 5-1: Surface Water Model Validation Tests Described in Bird et al. (1992)

Validation Test	Test Results
Phosphorus in Haliburton-Kawartha Lakes, Ontario	Tributary annual input of phosphorus into the different lakes varied widely. Calculated phosphorus concentrations in lake water were generally within a factor of two of the observed concentrations.
Phosphorus in Shield wetlands (including beaver ponds), Ontario	Annual input of phosphorus into different wetlands varied widely. Calculated phosphorus concentrations in water agreed well with observations for two wetlands but were 2 to 5 times lower than observed values for three wetlands. The underpredictions were likely due an internal source of phosphorous in these wetlands. Calculated phosphorus concentrations in sediments were about one to two orders of magnitude lower than the observed values. This may be because phosphorus concentrations in the peat sediments reflect the phosphorus content of decaying vegetation.
Calcium in Experiment Lakes Area Lake 239, Ontario	Calcium aqueous concentration and budget of Lake 239 measured over a 3 year period. Calculated Ca concentrations in water were approximately 70 to 80% of observed values. Calculated Ca concentrations in sediment were approximately 35% of the measured value, but well within the 95% confidence limits of the calculated concentrations.
Cadmium in Batchawanda Lake South, Ontario	Atmospheric deposition is major source of cadmium in this lake. The calculated Cd concentration in water is 3-fold higher than the observed value in the lake but within the range of measured values for central Ontario lakes. The calculated sediment concentration is 3-fold lower than the observed value.

Co-60 in Perch Lake, Ontario	Based on a fitted Co transfer rate from water to sediment, the model accurately described the behaviour of aqueous Co-60 over an eleven year period, during which the Co-60 concentrations varied by over an order of magnitude. Calculated sediment concentrations of Co-60 were within a factor of two of values measured in 1969 and 1982.
Co-60, Cs-134 and H-3 in Experiment Lakes Area Lake 226, Ontario	Nuclide concentrations in water and sediment were measured one year following addition of nuclides to the anaerobic hypolimnion. Lake-specific data were not used for element transfer to sediment. The calculated aqueous concentration of H-3 was in good agreement with observations but the aqueous Co-60 and Cs-134 concentrations were about 4-fold larger than the observed values. The total activities of Co-60 and Cs-134 in sediment were in good agreement with measured values.
Cadmium in Experiment Lakes Area Lake 382, Ontario	Cd was added to Lake 382 over a four-year period. Calculated Cd concentrations in water, calculated for a three year period, were up to an order of magnitude greater than observed values (using geometric mean parameter values); but, the observed values fall within the range of calculated values. The calculated total amount of Cd in sediment was approximately 60% of the observed amount.

A model of the carbon cycle in Canadian Shield lakes was developed by Stephenson and Reid (1996) and tested using field observations on the fate of experimentally added spikes of C-14 to Lake 226 and Lake 224 at the Experimental Lakes Area, Ontario, Canada. C-14 data were collected over a 16 year period. The field data were also used to test the CC4 surface water model.

It was found that the short-term (0.1 to 1.0 a) behaviour of aqueous C-14 in the lakes, which is described by relatively rapid transport to the sediment, could be adequately predicted (see Figure 5-1). However, the long-term behaviour of aqueous C-14 was not well predicted. This is because the surface water model, which was developed to simulate the long-term net exchange between water and sediment assuming a continuing source flux into the water, fails to account for internal C-14 fluxes (e.g., from sediment to water) following a single pulse addition of C-14. Nevertheless, it was found that under steady state conditions, i.e., assuming a continuous source of C-14 into Lake 224, the surface water model gave predictions that agreed well with the carbon cycle model. This convergence indicates that the surface water model is adequate for predicting the fate and concentrations of C-14 in lakes, if the sources are sufficiently long that steady state is attained.

A C-14 validation study in BIOMOVSII employed the same data used by Stephenson and Reid (1996), see above, to validate their model of the carbon cycle in Canadian Shield lakes (BIOMOVSII 1996a, Bird et al. 1999). The study concluded that the surface water model provided reasonable predictions of C-14 retention in lake sediments but was too simplistic to provide realistic predictions of water concentrations over the long-term following an acute release of C-14. More complex models are required to simulate the internal recycling of

contaminants between the water body and sediments under non-equilibrium conditions. The comparison between calculated aqueous concentrations and field data are shown in Figure 5-1.

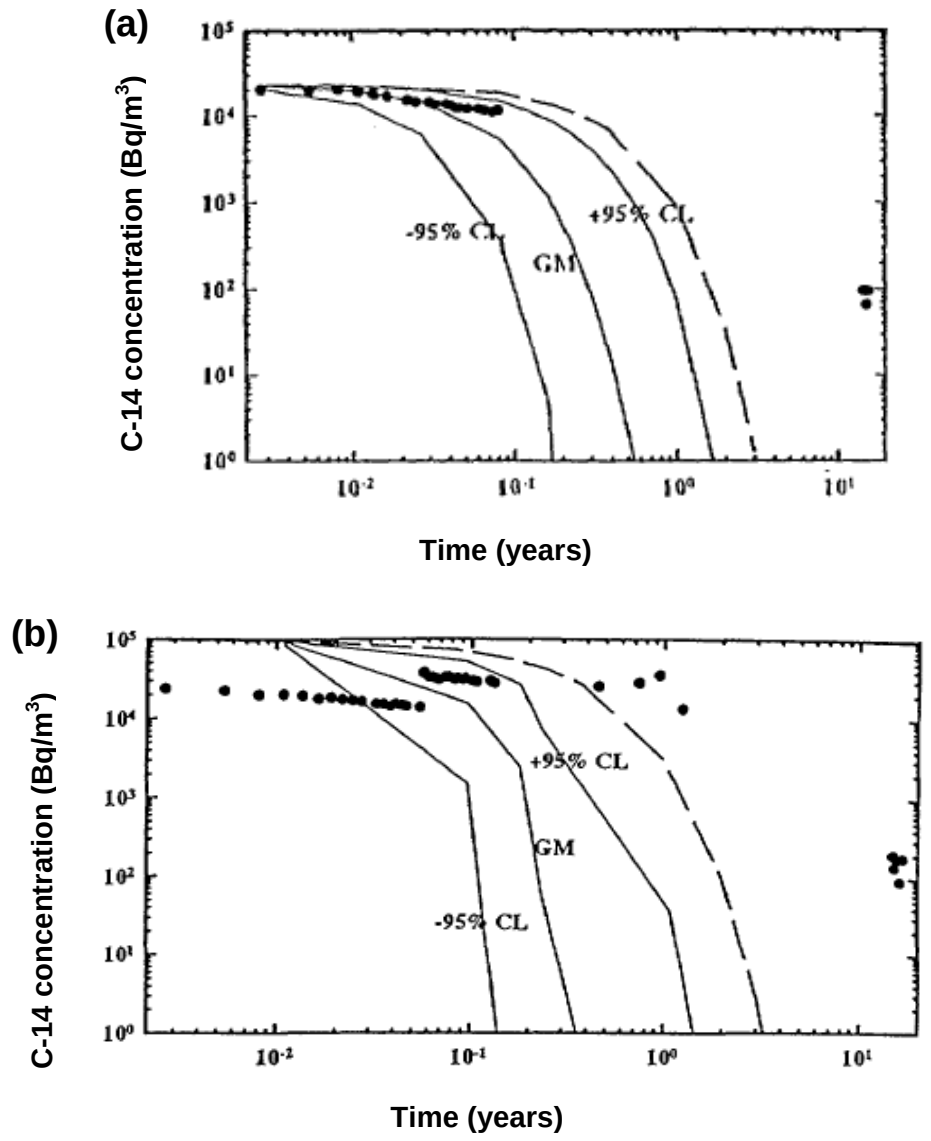

Note: Calculations using the geometric mean (GM) and the +95% and -95% confidence limits (CL) of the parameter values are shown. Note that for Lake 226 north the four spikes were modelled as a single spike.

Figure 5-1: Observed (•) and C-14 concentrations calculated by the surface water model in water of (a) Lake 226 South and (b) Lake 226 North following the C-14 spike(s) to the epilimnion (from BIOMOVSII 1996a)

The predictions of the CC4 surface water submodel were compared to those of other models that participated in BIOMOVS Scenario B3 (Bergström 1988), which considered the behaviour of Ra-226 and Th-230 in a lake. AECL did not participate directly in the BIOMOVS Scenario 3 exercise but performed the BIOTRAC calculations afterwards (Bird et al. 1992). The only parameter that was varied was the nuclide-specific transfer rate from water to sediment.

The concentrations predicted for Ra-226 and Th-230 in water and sediment did not differ appreciably from those predicted by the other six assessment models, as shown in Figure 5-2 (Bird et al. 1992). The mostly fair agreement between the concentrations predicted by the surface water submodel with those of the other independently developed models suggests that the predictions of the surface water model are appropriate.

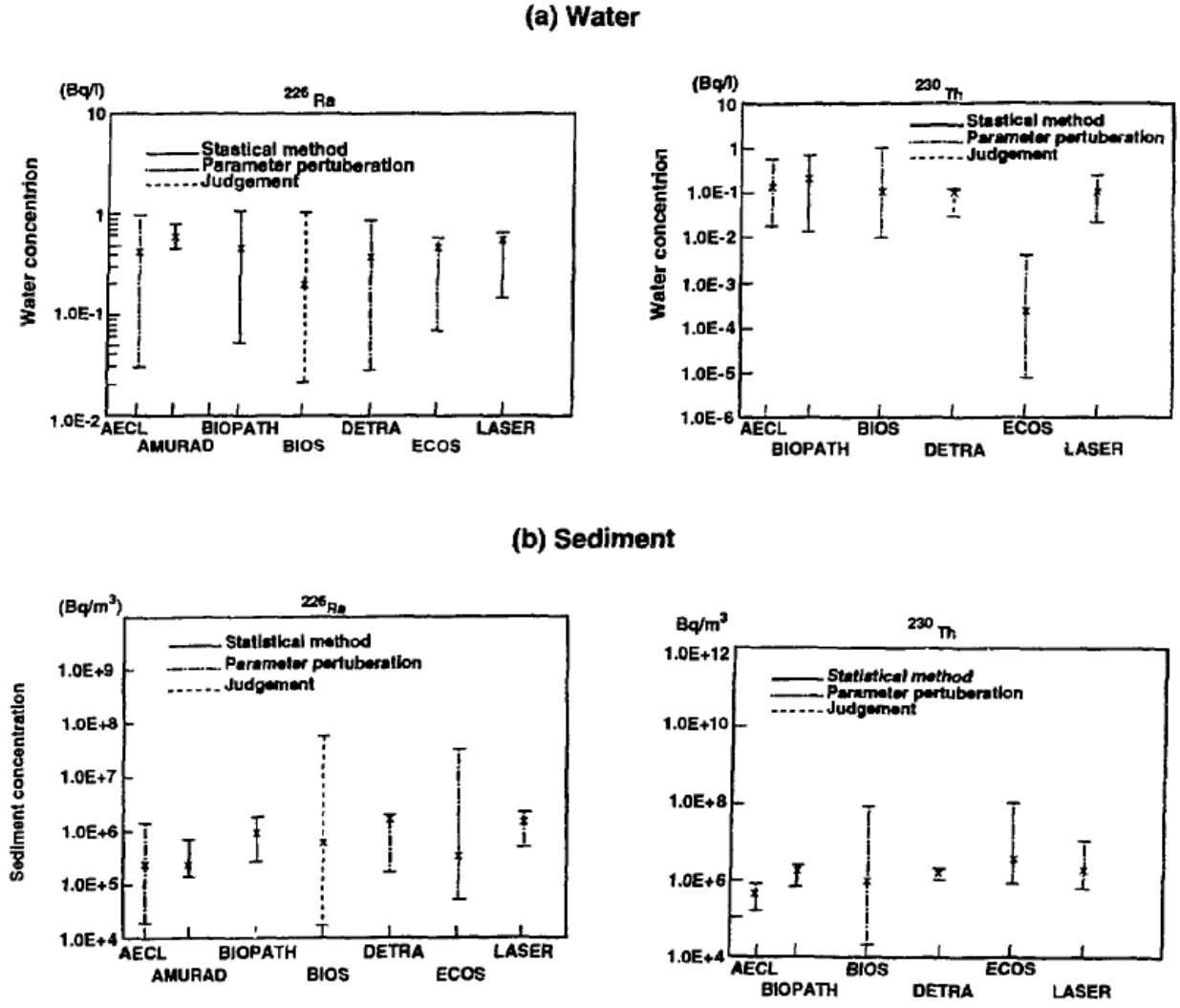

Note: AECL = CC4 surface water model; AMURAD = Oak Ridge National Laboratory, U.S.; BIOPATH = Studsvik Nuclear AB, Sweden; BIOS = National Radiation Protection Board, U.K.; DETRA = Technical Research Centre of Finland, Finland; ECOS = Department of Environment, U.K.; and LASER = Riso National Laboratory, Denmark.

Figure 5-2: BIOMOVS Scenario B3 model predictions (mean ± 95% confidence limits) after 100 years of radionuclide input to a lake (Bergström 1988) (from Bird et al. 1992)

5.2 Soil Model

The soil model calculates the concentrations of contaminants in the surface (rooting or cultivated) soil layer. The soil layer is assumed to be well-mixed. The soil model includes contaminant input from irrigation water, atmospheric deposition, groundwater discharge and ingrowth due to radioactive decay. The contaminant loss terms from the soil layer include: radioactive decay, leaching, volatilization, crop removal and bioturbation.

There are two soil models in SYVAC3-CC4: (1) an upland soil model, with the water table somewhat below the surface soil layer, and (2) a shallow soil model, which is appropriate when the water table extends into the surface soil on a regular and extended basis, e.g., wetland soils. Upland soil is the usual case.

The CC3 upland soil model, called SCEMR1, was very complicated and not easily adapted to alternative climate scenarios (Davis et al. 1993). Consequently, in 2002, it was replaced by a simpler root-zone compartment model that includes capillary rise from the groundwater table as well as irrigation (NWMO 2012b). This upland soil model is similar to the CSA Soil Model (CSA 2008). SYVAC3-CC4, Version SCC403 was the first version of CC4 to include the new soil model.

Consequently, many of the tests of the upland soil model carried out by AECL and described by Sheppard (1992) are not applicable to the current version of CC4 and, so, only one test of the current soil model is available. In the future, some of the previous tests of the upland soil model will be redone using the current version of CC4. However, it will not be possible to repeat all the tests because the soil model SCEMR1 was a multi-compartment model which could predict radionuclide concentrations in soil as a function of depth. In contrast, the upland soil model in the current version of CC4 only predicts radionuclide concentrations in a single layer, i.e., the root zone, so it does not give concentrations as a function of soil depth.

The shallow soil model in the current version of CC4 is the same as that used in CC3 (Davies et al. 1993).

5.2.1 Tests of Upland Soil Model

The current soil model was compared to two other models in a BIOPROTA scenario (Limer 2012). This scenario examined the behaviour of U-238 series radionuclides at the former Los Ratones uranium mine in Spain. The calculated surface soil concentrations are compared in Table 5-2.

The NDA RWMD and CC4 soil models agree fairly well. The large differences between these two models and the (ANDRA) SAMM model reflect the different assumption made for the source of contamination. The SAMM model calculated initial soil concentrations using groundwater radionuclide concentrations, whereas the other models assumed the river was the source of contaminants. Groundwater concentrations are up to three orders of magnitude larger than river concentrations.

After accounting for the different source strengths, the calculated soil concentrations vary within about a factor of three, with the exception of the NDA RWMD result for Th-230, downstream of the mine.

Table 5-2: Comparison of Calculated 2010 Surface Soil Concentrations for the Los Ratones Scenario

Location	Radionuclide	Soil Concentrations (Bq kg^{-1} dry weight)		
		SAMM*	NDA NWMD[1]	SYVAC3-CC4
Upstream of mine	U-238	380	0.78 (0.39, 1.5)	0.81 (0.44, 1.1)
	U-234	380	0.92 (0.47, 1.8)	0.88 (0.50, 1.1)
	Th-230	410	0.38 (0.13, 0.85)	0.69 (0.10, 1.8)
	Ra-226	470	0.40 (0.38, 0.42)	1.3 (0.64, 1.6)
Downstream of mine	U-238	16,000	30 (11, 60)	16 (16, 17)
	U-234	16,000	33 (12, 58)	19 (18, 19)
	Th-230	15,000	1.0 (0.74, 1.3)	10 (6.6, 13)
	Ra-226	18,000	14 (12, 16)	8.7 (4.8, 13)

*Source term assumptions were much higher, see text for explanation. SAMM = SCM-Andra-Multtilayer Model

[1]Nuclear Decommissioning Authority, Radioactive Waste Management Directorate

5.2.2 Tests of Shallow Soil Model

There have been no tests of the shallow soil model.

5.3 Atmosphere Submodel

The atmosphere is a potential recipient of radionuclides that escaped from the repository. It receives its radionuclide load via suspension from contaminated water bodies, soils and vegetation. The atmosphere dilutes radionuclides reaching it, but is also very effective at redistributing them.

The atmosphere submodel considers three main processes: suspension of radionuclides into the atmosphere from soil, surface waters and vegetation (via agricultural and land clearing fires); dispersion of radionuclides by atmospheric turbulence; and deposition back to the underlying surface. Only local atmospheric transport within the air compartment that overlies the local biosphere near the repository site is considered. Furthermore, only air concentrations fairly close to the ground, where the critical group and other biota are located, are calculated.

The atmosphere submodel is simple and assumes equilibrium conditions (Amiro 1992, Amiro and Davis 1991). Most of the parameter values in the atmosphere submodel can be derived from long-term measurements at the repository site (Canadian Shield for a crystalline rock site

and Southern Ontario for a sedimentary rock site). Furthermore, the dispersion relationships in the atmosphere submodel are based on a widely accepted numerical dispersion theory which agrees well with experimental data (Wilson 1982a,b).

There have been no direct validation studies of the atmosphere submodel. A comparison of the atmosphere submodel was invoked in the BIOMOVS B6 scenario (BIOMOVS 1990). Here the concentrations for I-129 and Np-237 in the air were compared with those of seven other models. These air concentrations were calculated from the radionuclide concentrations in soil using a dust loading factor. Since the dust loading factor used by most of the participants in the study were similar, the differences in the calculated air concentrations reflect more the differences in the soil models used by the participants than the atmosphere models. Hence, this study cannot be considered a test of the atmosphere submodel.

5.4 Food Chain and Dose Submodel

Nuclides from the repository that reach the biosphere (surface water, sediment, soil and atmosphere) may be taken up by living organisms, both plants and animal. These nuclides may affect the organisms and may move along the food chain and eventually be ingested by humans. All biota, including humans, that live in the contaminated environment may be exposed internally and externally to radiation fields. The food chain and dose submodel traces radionuclides through the food chain to humans and calculates doses from both internal and external exposure pathways (Zach and Sheppard 1992, 1991).

The food chain and dose submodel in SYVAC3-CC4 is called CALDOS. CALDOS is a standard food chain and dose submodel with impacts calculated using the diet habits of the critical group, environmental transfer factors and concentration ratios, and dose conversion factors. The critical group is assumed to be a self-sufficient farming household. This model is consistent with CSA N288.1 (CSA 2008) and other international practice.

Radiological environmental assessment models are difficult to validate (Hoffman et al. 1984, NCRP 1984) because of the extremely low environmental radionuclide concentrations and the very long time periods. Further, it is difficult to obtain test data on radionuclide concentrations in human tissues and organs. For this reason, confidence in CALDOS was gained through other means, including scientific consensus, peer review and model intercomparisons (Davies et al. 1993, Zach and Sheppard 1992). The international code comparisons involving the BIOTRAC food chain and dose model are described below.

5.4.1 Code Comparisons

<u>BIOMOVS</u>

The food chain and dose submodel was compared with independently developed codes in the BIOMOVS code comparisons (Haegg and Johansson 1988) involving a number of specific scenarios. BIOMOVS was an international co-operative study to test models designed to calculate the environmental transfer and bioaccumulation of radionuclides and other trace substances. These comparisons showed that the CALDOS predictions closely agreed with models used in several other countries (Zach and Sheppard 1992).

BIOMOVSII

The BIOMOVSII (1996b) biosphere model intercomparison compared the calculated annual dose rates from I-129, Np-237, U-233 and Th-229 for three biosphere discharge scenarios: release to a river, release to an irrigation source and release to deep soil. It extracted and compared the results of ten international contributors for each of the major pathways for each radionuclide. AECL participated in this BIOMOVSII exercise using the BIOTRAC model from SYVAC3-CC3.

The I-129 doses calculated by the AECL code in BIOMOVSII (1996b) were one to two orders of magnitude higher than those calculated by other codes for two of the scenarios. This was attributed mainly to the use of an I-129 specific activity model in CC3 (Davis et al. 1993), the SCEMR1 soil model and different approaches to modelling the scenarios.

The doses calculated by BIOTRAC for the actinide nuclides were in fair agreement with those calculated by the other codes. However, this may have been fortuitous given the large differences in the calculated concentrations of the actinide nuclides in various media (soil and sediment) and the different approaches for modelling the scenarios. Furthermore, additional tests indicated that the differences in calculated doses for the actinide nuclides could be traced to differences in modelling transport through the biosphere rather than differences in the food chain and dose model.

Since the current version of SYVAC3-CC4 biosphere model does not use the SCEMR1 soil model (which was replaced in 2002 by a simpler model in SYVAC3-CC4, Version SCC403) and no longer uses the I-129 specific activity model (which was replaced in 2009 by the dose model used for most other nuclides in SYVAC3-CC4, Version SCC406) the BIOMOVSII (1996b) intercomparison is not a suitable verification test for the CALDOS model.

SKB SR97

The SYVAC3-PR4 code was compared with the results of the SKB SR97 safety assessment study (SKB 1999) by Garisto et al. (2001). PR4 was the version of the AECL system model used in the AECL Second Case Study, and it subsequently was converted to CC4 after code quality assurance was completed. In the PR4 simulations of the SR97 well scenario (with bioturbation and weeding soil losses), the radionuclides with the largest peak doses over the 10^6 year simulation time are: I-129, Cl-36, Se-79, Sn-126, Sb-126 and Ni-59 in order of decreasing peak doses. The peak doses for the other nuclides are orders of magnitude smaller. This ranking of radionuclides is the same as that found in SR97, i.e., I-129, Cl-36, Se-79 and Sn-126. (The nuclide Ni-59 does not reach the biosphere in SR97 and Sb-126 was not explicitly included in the SR-97 simulations).

The comparisons of doses calculated by SYVAC3-PR4 and SR97 are shown in Table 5-3, for the Peat Scenario, and Table 5-4, for the Ceberg Well Scenario. To remove differences due to differences in the repository and geosphere models, we compare the calculated dose rates per unit release (Bq/a) of the nuclide from the geosphere. This quantity is equivalent to the SR97 ecosystem-specific dose conversion factors (EDFs) for the scenarios.

In the peat scenario, groundwater from the repository discharges to a peat bog. Crops are grown on the peat bog. For the peat scenario, PR4 uses the shallow soil model (which remains unchanged in the current version of CC4). For this comparison, the specific activity models for Cl-36 and I-129 were not used in the PR4 calculations since they are not used in SR97.

Table 5-3: Comparison of SR97 and PR4 EDF Values for the Peat Scenario (Garisto et al. 2001)

Nuclide	SR97 EDF[1] (Sv/Bq)	PR4 EDF[2] (Sv/Bq)	Ratio of PR4 to SR97 EDF Values
C-14	4.6×10^{-15}	1.7×10^{-15}	0.37
Cl-36	1.5×10^{-11}	8.3×10^{-12}	0.55
I-129	2.1×10^{-11}	8.1×10^{-12}	0.39
Nb-94	1.5×10^{-12}	7.8×10^{-13}	0.52
Ni-59	1.9×10^{-13}	8.3×10^{-14}	0.44
Ra-226	9.4×10^{-10}	1.1×10^{-9}	1.2
Se-79	1.2×10^{-9}	2.1×10^{-9}	1.8
Sn-126	6.1×10^{-11}	6.2×10^{-11}	1.0
Tc-99	2.9×10^{-13}	5.5×10^{-13}	1.9
Th-230	3.7×10^{-9}	6.0×10^{-9}	1.6

[1]Lindgren and Lindström (1999). The SR97 EDF factors are calculated assuming a constant release rate into the biosphere for 10000 years.
[2]The maximum dose rate (Sv/a) in the PR4 simulation divided by the maximum release rate into the biosphere (Bq/a).

For the peat scenario, the agreement between the two models is good. The PR4 doses are higher for Ra-226, Se-79, Sn-126, Tc-99 and Th-230; but lower for C-14, Cl-36, I-129 and Ni-59. PR4 underestimates the dose rates for radionuclides, e.g., C-14, for which the animal ingestion pathways are important, because the forage field in the PR4 simulation was 2.5-fold larger than in SR97. This parameter is calculated internally by PR4 from the number of dairy cows and beef cattle needed to supply the animal products ingested by the critical group.

In the well scenario, water from a well is used as drinking water for humans and cattle and to irrigate a garden plot. The irrigation rate could not be adjusted to the SR97 value in the PR4 simulations since it is not an input parameter and, so, the irrigation rate in the PR4 calculations was 4.8 times larger than in SR97. To account for this difference, the calculated PR4 doses for the air inhalation, plant ingestion, groundshine and soil ingestion pathways were reduced by a factor of 4.8. Finally, for this comparison, the specific activity models for Cl-36 and I-129 were not used in the PR4 calculations since they are not used in SR97.

As shown in Table 5-4, except for Cl-36, Se-79 and Tc-99, the agreement between the two models was rather good considering the differences in the models (Garisto et al. 2001). Because the soil-plant-man pathway is the dominant contributor to the total Cl-36, Se-79 and Tc-99 doses, the large differences in the predicted doses for these nuclides were attributed to differences in the SR97 and PR4 soil models. Interestingly, for these three nuclides, the soil K_d values are low: Cl (0.001 m^3/kg), Se (0.01 m^3/kg) and Tc (0.005 m^3/kg). (Note that C-14 is also weakly adsorbed in soil. However, for this nuclide, the most important exposure pathways are water-man, water-animal-man and water-plant-man.) The major difference in the PR4 and SR97 soil models is in the treatment of soil leaching. Hence, the leaching model used in PR4 is likely too conservative for radionuclides that are weakly adsorbed by the soil (Garisto et al. 2001).

However, as noted earlier, the PR4 soil model SCEMR1 was replaced with a simpler model in SYVAC3-CC4, Version SCC403. The SKB SR97 code comparison has not been repeated using the latest version of the SYVAC3-CC4 code.

Table 5-4: Comparison of SR97 and PR4 EDF Values for the Ceberg Well Scenario (Garisto et al. 2001)

Nuclide	SR97 EDF[1] (Sv/Bq)	SYVAC3-PR4 EDF[2] (Sv/Bq)	Ratio of PR4 to SR97 EDF Values
C-14	2.4×10^{-13}	2.0×10^{-13}	0.83
Cl-36	6.3×10^{-13}	9.8×10^{-12}	7.5
I-129	7.7×10^{-11}	5.2×10^{-11}	0.68
Nb-94	2.8×10^{-12}	1.9×10^{-12}	0.68
Ni-59	5.1×10^{-14}	3.7×10^{-14}	0.73
Ra-226	1.1×10^{-10}	1.1×10^{-10}	1.0
Se-79	2.1×10^{-12}	7.0×10^{-11}	33.3
Sn-126	3.1×10^{-12}	3.4×10^{-12}	1.1
Tc-99	4.7×10^{-13}	1.6×10^{-11}	34.0
Th-230	2.0×10^{-10}	5.9×10^{-11}	0.3

[1]Lindgren and Lindström (1999). The SR97 EDF factors are calculated assuming a constant release rate into the biosphere for 10000 years.
[2]The maximum dose rate (Sv/a) in the PR4 simulation, corrected for differences in the irrigation rate (see text), divided by the maximum release rate into the biosphere (Bq/a).

5.4.2 Tritium Specific Activity Model

Predictions of the tritium specific activity model in BIOTRAC were compared with those of UNSCEAR (1982) and NCRP (1979) for a number of chronic exposure scenarios. UNSCEAR (1982) estimated the surface water concentration of cosmically produced H-3 at 0.4 Bq/L and the corresponding dose to man of 10^{-8} Sv/a. For the same situation, CALDOS predicted a slightly higher dose of 1.3×10^{-8} Sv/a. Based on a water concentration of 37×10^{3} Bq/L, NCRP (1979) estimated to dose to man at about 1 mSv/a. The CALDOS model predicted a dose of 1.2 mSv/a. These comparisons show that the tritium specific activity model in CALDOS generally agrees well with other models although it is consistently conservative.

There may be another opportunity to validate the H-3 transport model in BIOTRAC using the BIOMOVSII experimental study at Chalk River (BIOMOVSII 1996c). If relevant, this test will be done using the current version of SYVAC3-CC4.

5.4.3 Non-Human Biota

The biosphere model includes a submodel for calculating doses to non-human biota. This model has not been subjected to any validation tests.

6. SYSTEM MODEL VALIDATION

This section of the report discusses the test carried out on the SYVAC3 executive module and the SYVAC3-CC4 system model as a whole, rather than the performance of specific CC4 submodels. This includes, for example, tests of mass conservation in the SYVAC3-CC4 system model and tests of the tasks carried out by SYVAC3, e.g., input/output, random number generation and parameter sampling from various probability density functions.

6.1 Mass Balance

Conservation of mass is a fundamental principle that can be used as a form of validation.

Two different types of validation tests are considered for conservation of mass. One, called the system mass balance test, deals with the entire CC4 repository model. The second, called the biosphere mass balance test, examines in more detail the conservation of mass within the various compartments used to represent the biosphere in CC4.

SYVAC3-CC4 tracks radionuclide flow rates, but not generally the accumulated mass in any repository component. For the validation tests (Goodwin et al. 2002), code was added to the CC4 model to determine the accumulated mass at any time in four compartments of interest: the used fuel container (including the fuel bundles), the repository (includes the buffer, the backfill and the EDZ rock), geosphere, and biosphere. These code changes were implemented as part of SYVAC3-CC4, Version SCC4.02.

The results of the system model tests show that nuclide masses were conserved within the test criteria (Goodwin et al. 2002). The biosphere-level test showed, as expected, that contaminant mass is overestimated in most cases - that is, the biosphere models were designed to be simpler and conservative. The maximum mass balance deviation seen in these test runs was 70%, and this apparent increase in mass is deemed to be an acceptable consequence of model simplification. One case displayed a mass loss of 6% for C-14, although this is likely due to the fact that the mass balance calculation did not account for downwind atmospheric mass loss (Goodwin et al. 2002). This deficiency in the mass balance calculation was corrected in SYVAC3-CC4, Version SCC4.04.

6.2 THE PSACOIN Code Intercomparison

The SYVAC3 executive code and the used fuel disposal system model elements were compared with codes and models developed by other international groups in the PSACOIN code intercomparisons co-ordinated by the Nuclear Energy Agency (NEA/OECD) over the period 1987-1993.

The PSACOIN exercise was carried out by the NEA Probabilistic System Assessment Code User Group. This consisted of representatives from various groups that were developing probabilistic-based codes for nuclear waste disposal safety assessments. The main features of each intercomparison exercise are listed in Table 6-1.

Each code intercomparison exercise helps confirm that a given code correctly implements a specific model. The reference results are either an analytic solution or the results of other

codes. In the latter case, although each of the codes is not necessarily any better validated than any other, the fact that there were several such independently developed codes in the comparison helps verify that the results from any given code are correct.

Table 6-1: Main Features of Each PSACOIN Code Intercomparison Exercise

Intercomparison	Main features
Level 0	- Test the executive modules of the probabilistic codes - Test post-processing codes - Test sensitivity analysis techniques - Simple analytic system model, but no analytic solution when input parameters have a probability distribution
Level E	- As with Level 0, except that a special system model was chosen for which an analytic solution is available even when input parameters have a probability distribution
Level 1a	- More complex system repository and geosphere model, simple biosphere model
Level 1b	- More complex biosphere model, with several exposure pathways - Constant release rate to biosphere from initial inventory
Level S	- Sensitivity analysis of probabilistic results

The SYVAC3-CC3/PR4 code was under development during this period, and was not directly verified or validated in these tests. However, portions of the codes tested in PSACOIN did eventually become part of the SYVAC3-PR4 code.

Level 0

One of the main purposes of the Level 0 intercomparison exercise was to compare the executive modules of the probabilistic codes. These modules control such aspects as input/output, parameter sampling, and run execution. The Level 0 exercise tested the executive modules using a simple disposal system model.

The disposal system model was a time-dependent but analytic model - single nuclide decay, simple release rate from fuel, time delays in different barriers, water dilution, and drinking water dose pathway. There were 25 input parameters, with specified probability distributions of normal, lognormal, uniform or log uniform. The dose rate results were recorded at 10^4 to 10^7 years. The reference results were assumed to be those from a 1,000,000 case run using an AEA Harwell (UK) code.

Twelve different groups participated in the final iteration. AECL participated using the SYVAC3, Version 03 executive code with a special LZ (Level 0) system model. The combined code was called SYVAC3-LZ. The intercomparison concluded that all the participating codes were very consistent in their results (NEA 1987). The SYVAC3-LZ results agreed with the reference code results to within their 95% confidence bounds.

This provides confidence in the following features of the SYVAC3 executive code:

- input and output file reading and writing;
- input parameter sampling from constant, uniform, log uniform, normal and lognormal distributions;
- control and execution of multiple runs;
- generation of random numbers;
- handling of time series for arithmetic operations.

Virtually all of these functions have been adopted, frequently with no substantive code changes, in the corresponding code used in SYVAC3-CC4.

Level E

The Level E exercise was similar to the Level 0 exercise. However, a particular transport model was defined which possessed a semi-analytic solution for the mean dose rate when input parameters had a uniform or log-uniform distribution.

The system model used a finite inventory with a constant depletion rate source, followed by two 1-D advection/diffusion layers, leading to a drinking water pathway. There were 33 input parameters, with 12 having uniform or log-uniform probability distributions. The dose rates were calculated at 10^4 to 10^6 years. The nuclides modelled were I-129, and the Np-237 $\rightarrow$ U-233 $\rightarrow$ Th-229 chain.

A total of 10 codes were compared. AECL participated with the SYVAC3 executive code with a special LE disposal system model. The intercomparison concluded that "...the results from the 10 participating codes show a high degree of consistency for both deterministic and stochastic analyses, despite the use of different codes, sampling schemes and sampling sizes...results from most of the PSA codes also agree well with the exact solution" (NEA 1989).

For the SYVAC3-LE code, the code convergence parameters were set to a 0.1% target error in each time-series operation. The deterministic results (3 cases) agreed within 0.3% and 1.6% for the peak doses and peak times, respectively (the error was less for cases with later peaks). For the probabilistic test case, the 1000-run mean dose rates were in agreement with the exact values within the 95% confidence intervals.

This provides confidence in the following features of the tested SYVAC3-LE code, which were largely retained in the current SYVAC3-CC4 version:

- input parameter sampling from constant, uniform and log uniform distributions;
- control and execution of multiple runs;
- handling of time series for arithmetic operations;
- the solution to the decay chain equations;
- solution of the 1-D advective-diffusive equation with chains using semi-infinite response functions.

The test also helped verify the random number generator used in this version of SYVAC3. However, this generator was later replaced with an improved generator in SYVAC Version 3.10.

Level 1

These exercises verified the following functions of the tested SYVAC3 special code, which were largely retained in the SYVAC3-PR4 version:

- input parameter sampling from uniform, log-uniform, normal and log-normal distributions;
- control and execution of multiple runs;
- generation of random numbers;
- handling of time series for arithmetic operations;
- solution of compartment models;
- portions of the biosphere modules for nuclide transport and dose pathways.

The details of the Level 1a intercomparison are given in Section 4.4.2.

The PSACOIN Level 1b exercise mainly focussed on the biosphere (NEA 1993b). The system model was based on a leach rate source term, with four biosphere compartments (deep soil, top soil, river water and river sediment) and seven dose pathways (drinking water, fish, grain, meat, milk, dust inhalation and external irradiation). The radionuclides studied were C-14 and the U-235 → Pa-231 → Ac-227 chain. The model had 115 input parameters, of which 26 were sampled probabilistically. Seven codes participated in the comparison.

AECL developed a system model, called L1B201, specifically for use in this PSACOIN test as well as a new SYVAC routine called MULTIC for solving the equations for a linear multi-compartment system. The system model L1B201 included a nuclide source term model and a biosphere transport and dose model. The MULTIC routine was incorporated into SYVAC3, Version 09. The complete executable code used in this PSACOIN test was called SYVAC309-L1B201.

Intermediate results (compartment accumulation and pathway doses) were compared between the codes for a median-value deterministic case (at 1, 10^3 and 10^5 years). The AECL code results for the compartment inventories agreed to much better than 10% with the "all-code average" for the dominant nuclides and to within about 10% for the Pa-231 and Ac-227 daughters. The corresponding dose results for each of the several pathways modelled agreed to much better than 10% with the "all-code" average.

For the probabilistic exercise (1000 runs), the results of interest were the mean total doses from C-14 and from the U-235 chain. The AECL model mean dose results agreed well with the average results from the other codes and were within the Chebyshev 95% confidence interval of one of the participants.

Level S

The Level S exercise examined different approaches to analyzing a set of probabilistic results to determine sensitivities and confidence intervals (NEA 1993a). However, the results of this exercise do not contribute to the verification or validation of the SYVAC3-PR4 code. Rather, they test post-processing tools that are outside the scope of this report.

6.3 Comparisons with NUTP

The Canadian National Uranium Tailings Program produced a computer code called UTAP to simulate the movement of radionuclides and chemically toxic elements from uranium mine tailings. The SYVAC3 code with a special system model was used to simulate the same scenario to check the UTAP code. The results showed acceptable agreement (Goodwin and Andres 1986). Since the system model was different from CC4, this comparison primarily helps provide confidence in SYVAC3.

7. SUMMARY AND CONCLUSIONS

In this report, the verification and validation studies that have been carried out on the SYVAC3-CC4 computer program or its submodels have been summarized. Most of these tests have been previously published, so this document serves primarily as a single reference summary report.

Full validation of models for long-term assessment of nuclear fuel disposal is not possible for several reasons, notably the long time periods involved. Rather, verification and validation is an ongoing process to improve confidence in the results - that the code correctly implements a given model, and that the model adequately (or conservatively) represents reality for the intended use of the model.

Direct comparison of the SYVAC3-CC4 results with experimental data is presently only available for some aspects of the system model. A variety of tests can be used to contribute to this confidence, with some being stronger tests than others.

Hence, many of the validation tests involve code comparisons. These are valuable when a number of models have been independently developed to treat the same situation and the scenarios to be simulated are defined in detail (e.g., PSACOIN). Code comparisons have been used with the repository, geosphere and biosphere models. Appendix A presents a simple categorization of the processes included in the SYVAC3-CC4 model, and the types of validation undertaken, as discussed in this report.

Overall, the results summarized in this report indicate that at least partial validation tests have been done for a large number of the models in SYVAC3-CC4. The model results are sufficiently reliable for use in safety assessment of a deep geological repository, where the calculated safety margins are significant. Further tests are needed to extend the range of confidence in the results.

REFERENCES

Amiro, B.D. 1992. The atmosphere submodel for the assessment of Canada's nuclear fuel waste management concept. Atomic Energy of Canada Limited Report AECL-9889. Chalk River, Canada.

Amiro, B. D. and P.A. Davis. 1991. A pathways model to assess transport of radionuclides from terrestrial and aquatic surfaces to the atmosphere. Waste Management 11, 41-57.

Andres, T.H. 1999. SYVAC3 Manual. Atomic Energy of Canada Limited Report AECL-10982. Chalk River, Canada.

Bateman, H. 1910. The solution of a system of differential equations occurring in the theory of radioactive transformations. Proceedings of Cambridge Philosophical Society 15, 423.

Beauregard, Y., M. Gobien and F. Garisto. 2010. The dissolution and transport of radionuclides from used nuclear fuel in an underground repository. COMSOL Conference 2010, Boston, USA, Oct. 7-9.

Bergström, U. 1988. BIOMOVS Scenario B3. Release of radium-226 and thorium-230 to a lake. BIOMOVS Technical Report 1. Swedish National Institute of Radiation Protection. Stockholm, Sweden.

BIOMOVS. 1990. Scenario B6, Transport of radionuclides to root-zone soil from contaminated groundwater. BIOMOVS Technical Report 9. Swedish National Institute of Radiation Protection. Stockholm, Sweden.

BIOMOVSII. 1996a. Validation test for carbon-14 migration and accumulation in a Canadian Shield lake. BIOMOVS Technical Report 14. Swedish Radiation Protection Institute. Stockholm, Sweden.

BIOMOVSII. 1996b. Biosphere modeling for dose assessments of radioactive waste repositories. BIOMOVS Technical Report 12. Swedish Radiation Protection Institute. Stockholm, Sweden.

BIOMOVSII. 1996c. Tritium in the food chain. BIOMOVS Technical Report 13. Swedish Radiation Protection Institute. Stockholm, Sweden.

Bird, G.A., M. Stephenson and R.J. Cornett. 1992. The surface water submodel for the assessment of Canada's nuclear fuel waste management concept. Atomic Energy of Canada Limited Report AECL-10290. Chalk River, Canada.

Bird, G.A., U. Bergstrom, S. Nordlinder, S.L. Neal and G.M. Smith. 1999. Model simulations of the fate of C-14 added to a Canadian Shield lake. 1999. Journal of Environmental Radioactivity 42: 209-223.

Bird, G.A., W.J. Schwartz and M. Motycka. 1998. Fate of Co-60 and Cs-134 added to the hypolimnion of a Canadian Shield lake: accumulation in biota. Can. J. Fish. Aquat. Sci. 55: 987-998.

Bird, G.A., W.J. Schwartz, M. Motycka and J. Rosentreter. 1997. Behaviour of Co-60 And Cs-134 in a Canadian Shield lake over five years. Atomic Energy of Canada Limited Technical Record, TR-781, COG-97-166-I. Chalk River, Canada.

Chambre, P.L., W.W.-L. Lee, C.L. Kim and T.H. Pigford. 1986. Steady-state and transient radionuclide transport through penetrations in nuclear waste containers. Lawrence Berkeley Laboratory Report LBL-21806. Berkeley, USA.

Chan, A. and A. Advani. 1991. Verification of vault response function solution. Ontario Hydro Research Division Report 91-26-K. Toronto, Canada.

Chan, T. and B.W. Nakka. 1994. A two-dimensional analytical well model with applications to groundwater flow and convective transport modelling in the geosphere. Atomic Energy of Canada Limited Report, AECL-10880. Chalk River, Canada.

Chan, T., Y.C. Jin, C. Kitson, T. Melnyk and P.A. O'Connor. 1991. Comparison of a 2-D finite element solute transport model with a 1-D network solute transport model. In Joint International Waste Management Conference, 1991 Oct. 21-26, Seoul, ASME/KNS Volume 2, pp. 283-290.

Chan, T., N.W. Scheier and F.W. Stanchell. 2000. MOTIF Version 3.2 Verification and validation report. Ontario Power Generation Report 06819-REP-01200-10026-R00. Toronto, Canada.

Clarens, F., J. Gimanez, J.D. Pablo, I. Casas, M. Sevilla and J. Dies. 2003. Effect of beta radiation on non-irradiated $UO_{2(s)}$ dissolution. Mat. Res. Soc. Symp. Proc. 757, 415.

Clarens, F., J. Gimanez, J.D. Pablo, I. Casas, M. Rovira, and J. Dies. 2005. Influence of beta-radiation on UO_2 dissolution at different pH values. Radiochimica Acta 93, 533-538.

Cramer, J.J. 1994. Natural analogs in support of the Canadian concept for nuclear fuel waste disposal. Atomic Energy of Canada Limited Report AECL-10291. Chalk River, Canada.

Cramer, J. and J.A.T. Smellie (eds.). 1994. Final report of the AECL/SKB Cigar Lake analog study. SKB Technical Report TR-94-04. Stockholm, Sweden.

CSA (Canadian Standards Association). 1999. Quality assurance of analytical, scientific, and design computer programs for nuclear power plants. Canadian Standards Association Standard N286.7-99. Toronto, Canada.

CSA (Canadian Standards Association). 2008. Guidelines for calculating derived release limits for radioactive material in airborne and liquid effluents for normal operation of nuclear facilities. Canadian Standards Association N288.1-08. Toronto, Canada.

CSA (Canadian Standards Association). 2012. Guideline for the application of N286.7-99, Quality assurance of analytical, scientific, and design computer programs for nuclear power plants. Canadian Standards Association Report CSA-N286.7.1-09. Toronto, Canada.

Davis, P.A., R. Zach, M.E. Stephens, B.D. Amiro, G.A. Bird, J.A.K. Reid, M.I. Sheppard and M. Stephenson. 1993. The disposal of Canada's nuclear fuel waste: The biosphere model,

BIOTRAC, for postclosure assessment. Atomic Energy of Canada Limited Report, AECL-10720. Chalk River, Canada.

Davison, C.C., T. Chan, A. Brown, M. Gascoyne, D.C. Kamineni, G.S. Lodha, T.W. Melnyk, B.W. Nakka, P.A. O'connor, D.U. Ophori, N.W. Scheier, N.M. Soonawala, F.W. Stanchell, D.R. Stevenson, G.A. Thorne, T.T. Vandergraaf, P. Vilks and S.H. Whitaker. 1994. The disposal of Canada's nuclear fuel waste: The geosphere model for postclosure assessment. Atomic Energy of Canada Limited Report AECL-10719. Chalk River, Canada.

Dolinar, G.M., R.H. Rowat, M.E. Stephens, B.A. Lange, R.W.D. Killey, D.S. Rattan, S.R. Wilkinson, J.R. Walker, R.P. Jategaonkar, M. Stephenson, F.E. Lane, S.L. Wickware, K.E. Philipose. 1996. Preliminary safety analysis report (PSAR) for the intrusion resistant underground structure (IRUS). Atomic Energy of Canada Limited Report AECL-MISC-295 (Rev.4). Chalk River, Canada.

Duro, L., V. Montoya, E. Colàs and D. García. 2010. Groundwater equilibration and radionuclide solubility calculations. Nuclear Waste Management Organization Technical Report NWMO TR-2010-02. Toronto, Canada.

Eckerman, K.F. and R.W. Leggett. 1996. DCFPAK: Dose coefficients data file package for Sandia National Laboratory. Oak Ridge National Laboratory ORNL/TM-13347.

Flavelle, P. 1987. Regulatory perspectives of concept assessment. In Proceedings of the Conference on Geostatistical, Sensitivity, and Uncertainty Methods for Ground-Water Flow and Radionuclide Transport Modeling, San Francisco, USA (1987). Battelle Press. pp.111-119.

Garisto, F., J. Avis, N. Calder, A. D'Andrea, P. Gierszewski, C. Kitson, T. Melnyk, K. Wei and L.C. Wojciechowski. 2004. Third Case Study – Defective container scenario. Ontario Power Generation Report 06819-REP-01200-10126-R00. Toronto, Canada.

Garisto, F., J. Avis, N. Calder, P. Gierszewski, C. Kitson, T. Melnyk, K. Wei and L. Wojciechowski. 2005a. Horizontal borehole concept case study. Ontario Power Generation report 06819-REP-01200-10139-R00. Toronto, Canada.

Garisto, F., J. Avis., T. Chshyolkova, P. Gierszewski, M. Gobien, C. Kitson, T. Melnyk, J. Miller, R. Walsh and L. Wojciechowski. 2010. Glaciation scenario: Safety assessment for a deep geological repository for used fuel. Nuclear Waste Management Organization Technical Report NWMO TR-2010-10. Toronto, Canada.

Garisto, F., D.H. Barber, E. Chen, A. Inglot and C.A. Morrison. 2009. Alpha, beta and gamma dose rates in water in contact with used CANDU fuel. Nuclear Waste Management Organization Technical Report NWMO TR-2009-27. Toronto, Canada.

Garisto, F., P. Gierszewski, B. Goodwin, A. D'Andrea and M. Da Silva. 2001. Simulations of the SR97 Safety Assessment Case Using the NUCTRAN, RSM, DSM and PR4 Codes. Ontario Power Generation Report 06819-REP-01200-10057-R00. Toronto, Canada.

Garisto, F., M. Gobien, E. Kremer and C. Medri. 2012. Fourth Case Study: Reference data and codes. Nuclear Waste Management Organization Report NWMO TR-2012-08. Toronto, Canada.

Garisto, F., T. Kempe, P. Gierszewski, K. Wei, C. Kitson, T. Melnyk, L. Wojciechowski, J. Avis and N. Calder. 2005b. Horizontal borehole concept case study: Chemical toxicity risk. Ontario Power Generation Report 06819-REP-01200-10149-R00. Toronto, Canada.

Garisto, F., R. Walsh, L. Wojciechowski, J. Avis, T. Chshyolkova, P. Gierszewski, M. Gobien, C. Kitson, T. Melnyk and J. Miller. 2011. Safety assessment for a glaciation scenario. In Proceedings of the International High-Level Radioactive Waste Management Conference; Albuquerque, NM; April 10-14, 2011. American Nuclear Society, Illinois USA.

Garisto, N. and D.M. LeNeveu. 1991. A radionuclide mass-transport model for the performance assessment of engineered barriers in a used nuclear fuel disposal vault. Atomic Energy of Canada Limited Report AECL-10277. Chalk River, Canada.

Garisto, N.C., L.H. Johnson and W.H. Hocking. 1990. An instant release source term model for the assessment of used nuclear fuel disposal. In Second International Conference on CANDU Fuel, Conference Proceedings, Pembroke, Canada, 1989, pp. 352-368.

Gierszewski, P., J. Avis, N. Calder, A. D'Andrea, F. Garisto, C. Kitson, T. Melnyk, K. Wei and L. Wojciechowski. 2004. Third Case Study - Postclosure safety assessment. Ontario Power Generation report 06819-REP-01200-10109-R00. Toronto, Canada.

Gobien, M., F. Garisto and E. Kremer. 2013. Fifth Case Study: Reference data and codes. Nuclear Waste Management Organization Report NWMO TR-2013-05. Toronto, Canada.

Goodwin, B.W. and T.H. Andres. 1986. Comparison of the probabilistic systems assessment codes, UTAP and SYVAC3, applied to the long-term assessment of uranium mill tailings in Canada. Volume 1: Main Report. The National Uranium Tailings Program, Canada Centre for Mineral and Energy Technology, Energy, Mines and Resources Canada. Ottawa, Canada.

Goodwin, B.W., D.B. McConnell, T.H. Andres, W.C. Hajas, D.M. LeNeveu, T.W. Melnyk, G.R. Sherman, M.E. Stephens, J.G. Szekely, P.C. Bera, C.M. Cosgrove, K.D. Dougan, S.B. Keeling, C.I. Kitson, B.C. Kummen, S.E. Oliver, K. Witzke, L. Wojciechowski, and A.G. Wikjord. 1994. The disposal of Canada's nuclear fuel waste: Postclosure assessment of a reference system. Atomic Energy of Canada Limited Report AECL-10717. Chalk River, Canada.

Goodwin, B.W., P. Gierszewski and F. Garisto. 2001. Radionuclide Screening Model (RSM) Version 1.1 - Theory. Ontario Power Generation Report 06819-REP-01200-10045-R00. Toronto, Canada.

Goodwin, B.W., T. W. Melnyk, F. Garisto, J. D. Garroni, C. I. Kitson, S. Stroes-Gascoyne, L.C. Wojciechowski. 2002. Validation of four submodels of SYVAC3-CC4, Version SCC402. Ontario Power Generation Report 06819-REP-01300-10057-R00. Toronto, Canada.

Grambow, B., J. Bruno, L. Duro, J. Merino, A. Tamayo, C. Martin, G. Pepin, S. Schumacher, O. Smidt, C. Ferry, C. Jegou, J. Quiñones, E. Iglesias, N. Rodriguez Villagra, J. M. Nieto, A. Martínez-Esparza, A. Loida, V. Metz, B. Kienzler, G. Bracke (GRS), D. Pellegrini, G. Mathieu, V. Wasselin-Trupin, C. Serres, D. Wegen, M. Jonsson, L. Johnson, K. Lemmens, J. Liu, K. Spahiu, E. Ekeroth, I. Casas, J. de Pablo, C. Watson, P. Robinson, and D. Hodgkinson. 2010. MICADO model uncertainty for the mechanism of dissolution of spent fuel in nuclear waste repository. European Commission Report EUR 24597 EN. Brussels, Belgium.

Gray, W.J. and D.M. Strachan. 1991. UO_2 matrix dissolution rates and grain boundary inventories of Cs, Sr and Tc in spent LWR fuel. Materials Research Society Symposium Proceedings 212, 205-212.

Gureghian, A.B. and G. Jansen. 1985. One-dimensional analytical solutions for the migration of a three-member radionuclide decay chain in a multilayered geologic medium. Water Res. Research 21, 733.

Haegg, C. and G. Johansson. 1988. BIOMOVS: an international model validation study. In Reliability and Radioactive transfer Models, Proceedings of a Workshop, Athens, Greece, 1987, pp. 22-29. Elsevier Applied Science Publishers Ltd., Barking, U.K.

Heinrich, W.F. and T.H. Andres. 1985. Response functions of the convection-dispersion equations describing radionuclide migration in a semi-infinite medium. Annals of Nuclear Energy 12, 685-691.

Hermann, O.W. and R.M. Westfall. 2000. ORIGEN-S: Scale system module to calculate fuel depletion, actinide transmutation, fission product buildup and decay, and associated radiation terms. U.S. Nuclear Regulatory Commission Report NUREG/CR-0200, Revision 6, Volume 2, Section F7. USA.

Hume, H.B. 1995. Technetium diffusion in clay-based materials under oxic and anoxic conditions. Atomic Energy of Canada Limited Report AECL-11419. Chalk River, Canada.

ICRP (International Commission on Radiological Protection). 1983. Radionuclide transformations. Energy and intensity of emissions. ICRP Publication 38. Annals of the ICRP, Volumes 11-13.

INTRACOIN. 1984. International nuclide transport code intercomparison study. Final report level 1: Code verification. Swedish Nuclear Power Inspectorate report SKI-84:3. .Stockholm, Sweden.

Johnson, L.H., D.M. LeNeveu, F. King, D.W. Shoesmith, M. Kolar, D.W. Oscarson, S. Sunder, C. Onofrei, and J.L. Crosthwaite. 1996. The disposal of Canada's nuclear fuel waste: A study of postclosure safety of in-room emplacement of used CANDU fuel in copper containers in permeable plutonic rock. Volume 2: Vault model. Atomic Energy of Canada Limited Report AECL-11494-2. Chalk River, Canada.

Johnson, L.H., D.M. LeNeveu, D.W. Shoesmith, D.W. Oscarson, M.N. Gray, R.J. Lemire and N.C. Garisto. 1994. The disposal of Canada's nuclear fuel waste: The vault model for

postclosure assessment. Atomic Energy of Canada Limited Report AECL-10714. Chalk River, Canada.

Johnson, L., C. Poinssot, C. Ferry and P. Lovera. 2004. Estimates of the instant release fractions for UO_2 and MOX fuel at t=0. NAGRA Technical Report NTB 04-08. Wettingen, Switzerland.

Johnson, L.H., D.W. Shoesmith, G.E. Lunansky, M.G. Bailey and P.R. Tremaine. 1982. Mechanisms of leaching and dissolution of used fuel. Nucl. Technol. 56, 238-253.

Kersch, K. and S. Oliver. 1994. Verification of the AECL total system performance models. In High Level Radioactive Waste Management, Proceedings of the Fifth International Conference, Las Vegas, USA, Vol. 4, pp. 2437-2442.

King, F., C. Lilja, K. Pedersen, P. Pitkanen and M. Vahanen. 2010. An update of the state-of-the-art report on the corrosion of copper under expected conditions in a deep geologic repository. SKB Technical Report TR-10-67. Stockholm, Sweden.

Kitson, C.I., T. W. Melnyk, L.C. Wojciechowski and T. Chshyolkova. 2012. SYVAC3-CC4 user manual, version SCC409. Nuclear Waste Management Organization Technical Report NWMO TR-2012-21. Toronto, Canada.

Kwong, G. 2011. Status of corrosion studies for copper used fuel containers under low salinity conditions. Nuclear Waste Management Organization Report NWMO TR-2011-14. Toronto, Canada.

LeNeveu, D.M. 1994. Analysis specifications for the CC3 vault model. Atomic Energy of Canada Limited Report AECL-10970, COG-94-100. Chalk River, Canada.

LeNeveu, D.M. 1996. Radionuclide mass transfer rates from a pinhole in a waste container for an inventory-limited and constant concentration source. Atomic Energy of Canada Limited Report AECL-11540, COG-96-68. Chalk River, Canada.

LeNeveu, D.M and M. Kolar. 1996. Radionuclide response functions to the convection-dispersion equation for a point source along the axis of nested cylindrical media. Atomic Energy of Canada Limited Report AECL-11549, COG-96-90. Chalk River, Canada.

Limer, L.M.C., A. Albrecht, V. Hormann, M.-O. Gallerand, C. Medr, D. Perez-Sanchez, K. Smith, G. Smith and M. Thorne. 2012. Improving confidence in long-term dose assessments for U-238 series radionuclides. A report prepared within the BIOPROTA international cooperation programme. Final Report Version 3.1, August 2012.

Maak, P., P. Gierszewski and M. Saiedfar. 2001. Early failure probability of used-fuel containers in a deep geologic repository. Ontario Power Generation Report 06819-REP-01300-10022 R00. Toronto, Canada.

Melnyk, T.W.. 1995. Analysis specifications for the CC3 geosphere model, GEONET. Atomic Energy of Canada Limited Report AECL-11077, COG-94-101. Chalk River, Canada.

Muzeau, B., C. Jegou, F. Delaunay, V. Brodic, A. Brevet, H. Catalette, E. Simoni and C. Corbel. Radiolytic oxidation of UO_2 pellets doped with alpha–emitters ($^{238/239}Pu$). J. Alloys and Comps. 467, 578-589.

NCRP (National Council on Radiation Protection and Measurement). 1979. Tritium in the environment. NCRP Report No. 62. USA.

NCRP (National Council on Radiation Protection). 1984. Radiological assessment: Predicting the transport, bioaccumulation and uptake by man of radionuclides released to the environment. National Council on Radiation Protection and Measurements Report, NCRP Report No. 76. USA.

NEA (Nuclear Energy Agency). 1987. PSACOIN Level 0 - An International code intercomparison exercise for radioactive waste disposal assessments, Organization for Economic Co-operation and Development (OECD) report. Paris, France.

NEA (Nuclear Energy Agency). 1989. PSACOIN Level E - An International code intercomparison exercise for radioactive waste disposal assessments, Organization for Economic Co-operation and Development (OECD) report. Paris, France.

NEA (Nuclear Energy Agency). 1990. PSACOIN Level 1a - An International code intercomparison exercise on a hypothetical safety assessment case study for radioactive waste disposal systems, Organization for Economic Co-operation and Development (OECD) report. Paris, France.

NEA (Nuclear Energy Agency). 1993a. PSACOIN Level S - An International code intercomparison exercise for radioactive waste disposal assessments, Organization for Economic Co-operation and Development (OECD) report. Paris, France.

NEA (Nuclear Energy Agency). 1993b. PSACOIN Level 1b - An International code intercomparison exercise for radioactive waste disposal assessments, Organization for Economic Co-operation and Development (OECD) report. Paris, France.

Neal, W.L., S.A. Rawson and W.M. Murphy. 1988. Radionuclide release behavior of light water reactor spent fuel under hydrothermal conditions. Mater. Res. Soc. Symp. Proc. 112, 505-515.

Neuzil, C. 2003. Hydromechancial coupling in geological processes. Hydrogeology Journal, 11, 41-83.

NWMO (Nuclear Waste Management Organization). 2012a. Used fuel repository conceptual design and postclosure safety assessment in crystalline rock. Pre-project report. Nuclear Waste Management Organization Technical Report NWMO TR-2012-16. Toronto, Canada.

NWMO (Nuclear Waste Management Organization). 2012b. SYVAV3-CC4 Theory, version SCC409. Nuclear Waste Management Organization Technical Report NWMO TR-2012-22. Toronto, Canada.

NWMO (Nuclear Waste Management Organization). 2013. Postclosure safety assessment of a used fuel repository in sedimentary rock. Pre-project report. Nuclear Waste Management Organization Technical Report NWMO TR-2013-07. Toronto, Canada.

Oliver, S., K. Dougan, K. Kersch, C. Kitson, G. Sherman, L. Wojciechowski. 1995. Unit testing - A component of verification of scientific modelling software. In Proceedings of the 27th Annual Summer Computing Simulation Conference, Ottawa, Canada. Society of Computer Simulation, pp. 978-983.

Oscarson, D.W., N.G. Sawatsky, W.-J. Cho and J.-W. Choi. 1995. Compacted clays as barriers to radionuclide transport. In Fifth International Conference on Radioactive Waste Management and Environmental Remediation, Berlin, Germany. American Society of Mechanical Engineers, pp. 751-754.

Oscarson, D.W., D.A. Dixon and M.N. Gray. 1990. Swelling capacity and permeability of an unprocessed and processed bentonite clay. Engineering Geology 28, 281-289.

Parkhurst, D.L. and C.A.J. Appelo. 1999. User's guide to PHREEQC (version 2). A computer program for speciation, batch reaction, one dimensional transport and inverse geochemical calculations. U. S. Department of the Interior. U. S. Geological Survey, Water Resources Investigations. Reston, Virginia, USA.

Peltier, W.R. 2006. Boundary conditions data sets for spent fuel repository performance assessment. Ontario Power Generation, Nuclear Waste Management Division Report 06819-REP-01200-10154-R00. Toronto, Canada.

Peltier, W.R. 2003. Long-term climate change – glaciation. Ontario Power Generation, Nuclear Waste Management Division Report 06819-REP-01200-10113-R00. Toronto, Canada.

Poinssot, C., C. Ferry, M. Kelm, B.Grambow, A. Martinez-Esparza, L. Johnson, Z.Andriambololona, J. Bruno, C. Cachoir, J-M. Cavendon, H. Christensen, C.Corbel, C. Jegou, K.Lemmens, A. Loida, P. Lovera, F. Miserque, J. de Pablo, A. Poulesquen, J. Quinones, V. Rondinella, K. Spahiu and D.Wegen. 2005. Final report of the European project spent fuel stability under repository conditions. European Commission Report CEA-R-6093. Brussels, Belgium.

Posiva. 2012. Safety case for the disposal of spent nuclear fuel at Olkiluoto – Synthesis 2012. Posiva Oy Report Posiva 2012-12. Olkiluoto, Finland.

Posiva. 2013. Safety case for the disposal of spent nuclear fuel at Olkiluoto - Formulation of radionuclide release scenarios. Posiva Oy Report Posiva 2012-08. Olkiluoto, Finland.

Pusch, R. 2001. The buffer and backfill handbook, Part 2: Materials and techniques. SKB Technical Report TR-02-12. Stockholm, Sweden.

Pusch, R. and O. Karnland. 1990. Preliminary report on longevity of montmorillonite clay under repository-related conditions. Swedish Nuclear Fuel and Waste Management Co. Report SKB-TR-90-44. Stockholm, Sweden.

Pusch, R. L. Borgesson and M. Erlstrom. 1987. Alteration of isolating properties of dense smectite clay in repository environment as exemplified by seven pre-quarternary clays.

Swedish Nuclear Fuel and Waste Management Co. Report SKB-TR-87-10. Stockholm, Sweden.

Rowat, J.H., D.S. Rattan and G.M. Dolinar. 1996. Source-term model for the SYVAC3-NSURE performance assessment code. Atomic Energy of Canada Limited Report AECL-11321. Chalk River, Canada.

Sheppard, M.I. 1992. The soil submodel, SCEMR1, for the assessment of Canada's nuclear fuel waste management concept. Atomic Energy of Canada Limited Report AECL-9577. Chalk River, Canada.

Sheppard, S.C., W.C. Hajas, C.I. Kitson. D.M. LeNeveu, T.W. Melnyk, K.H. Witzke, L.C. Wojciechowski and D.M. Wuschke. 1997. Second assessment of low- and intermediate-level waste disposal in the Michigan basin. Candu Owners Group Report, COG-97-193. Toronto, Canada.

Shoesmith, D.W.. 2000. Fuel corosion processes under waste disposal conditions. J. of Nucl. Mat. 282, 1-31.

Shoesmith, D.W. 2007. Used fuel and uranium dioxide dissolution studies – A review. Nuclear Waste Management Technical Report NWMO TR-2007-03. Toronto, Canada.

Shoesmith, D. 2008. The role of dissolved hydrogen on the corrosion/dissoluton of spent nuclear fuel. Nuclear Waste Management Organization Technical Report NWMO TR-2008-19. Toronto, Canada.

Shoesmith, D. and D. Zagidulin. 2010. The Corrosion of Zirconium under Deep Geological Repository Conditions. Nuclear Waste Management Organization Report NWMO TR-2010-19. Toronto, Canada.

SKB (Svensk Kärnbränslehantering AB). 1999. Deep repository for spent fuel. SR 97 – Post-closure safety. SKB Technical Report TR-99-06, Volumes I and II. Stockholm, Sweden.

SKB (Svensk Kärnbränslehantering AB). 2010a. Design, production and initial state of the canister. SKB report TR-10-14. Stockholm, Sweden.

SKB (Svensk Kärnbränslehantering AB). 2010b. Data report for the safety assessment SR-Site. SKB report TR-10-52. Stockholm, Sweden.

SKB (Svensk Kärnbränslehantering AB). 2011. Long-term safety for the final repository for spent fuel at Forsmark. Main report of the SR-Site project. SKB Technical Report SKB TR-11-01. Stockholm, Sweden.

Smith, P., L. Johnson, M. Snellman, B. Pastina, and P. Gribi. 2007. Safety assessment for a KBS-3H spent nuclear fuel repository at Olkiluoto - Evolution report. Posiva Technical Report 2007-08. Olkiluoto, Finland.

SRG (Scientific Review Group). 1995. An evaluation of the environmental impact statement on Atomic Energy of Canada Limited's concept for the disposal of Canada's nuclear fuel waste. Canadian Environmental Assessment Agency Report, Catalog Number En 106-30/1995E. Ottawa, Canada.

Stephenson, M. and J.A.K. Reid. 1996. Technical description of a model of the carbon cycle in Canadian Shield lakes. Atomic Energy of Canada Limited Report, TR-743, COG-961 56. Chalk River, Canada.

Stroes-Gascoyne, S. 1996. Measurements of instant release source terms for Cs-137, Sr-90, I-129, Tc-99 and C-14 in used CANDU fuel. J. Nucl. Mat. 238, 264-277.

Stroes-Gascoyne, S., J.C. Tait, R.J. Porth, J.L. McConnell, T.R. Barnsdale and S. Watson. 1993. Measurements of grain-boundary inventories of ^{137}Cs, ^{90}Sr and ^{99}Tc in used CANDU fuel. Materials Research Society Symposium Proceedings 294, 41-46.

Tait, J.C and J.L, Luht. 1997. Dissolution rates of uranium from unirradiated UO_2 and uranium and radionuclides from used CANDU fuel using the single-pass flow-through apparatus. Ontario Hydro Report 06819-REP-01200-0006-R00. Toronto, Canada.

Tait, J.C., I.C. Gauld and A.H. Kerr. 1995. Validation of the ORIGEN-S code for predicting radionuclide inventories in used CANDU fuel. J. Nucl. Mat. 223, 109-121.

Tait, J.C., H. Roman, and C.A. Morrison. 2000. Characteristics and radionuclide inventories of used fuel from OPG nuclear generating stations; Volume 1 . Main Report. Ontario Power Generation Report 06819-REP-01200-10029-R00. Toronto, Canada.

Therrien, R, R.G. McLaren, E.A. Sudicky, S.M. Panday and V. Guvanasen. 2010. FRAC3DVS_OPG: A three dimensional numerical model describing subsurface flow and solute transport. User's guide. Groundwater Simulations Group, University of Waterloo. Waterloo, Canada.

Therrien, R. and E. Sudicky. 1996. Three-dimensional analysis of variably-saturated flow and solute transport in discretely-fractured porous media. J. of Contaminant Hydrology 23, 1-44.

UNSCEAR (United Nations Scientific Committee on the Effects of Atomic Radiation). 1982. Ionizing radiation: Sources and biological effects, 1982 Report to the General Assembly. United Nations, New York, USA.

Walsh, R. And J. Avis. 2010. Glaciation scenario: Groundwater and radionuclide transport studies. Nuclear Waste Management Organization Technical Report NWMO TR-2010-09. Toronto, Canada.

Werme, L., L.H. Johnson, V.M. Oversby, F. King, K. Spahiu, B.Grambow and D.W. Shoesmith. 2004. Spent fuel performance under repository conditions: a model for use in SR-Can. SKB Technical Report TR-04-19. Stockholm, Sweden.

Wikjord, A.G., P. Baumgartner, L.H. Johnson, F.W. Stanchell, R. Zach, B.W. Goodwin. 1996. The disposal of Canada's nuclear fuel waste: A study of postclosure safety of in-room emplacement of used CANDU fuel in copper containers in permeable plutonic rock. Volume 1: Summary. Atomic Energy of Canada Limited Report, AECL-11494-1. Chalk River, Canada.

Wilson, J.D. 1982a. Turbulent dispersion in the atmospheric surface layer. Boundary Layer Meteorology 22, 399-420.

Wilson, J.D. 1982b. An approximate analytical solution to the diffusion equation for short range dispersion from a continuous ground-level source. Boundary Layer Meteorology 23, 85-103.

Zach, R. and S.C. Sheppard. 1992. The food-chain and dose submodel, CALDOS, for the assessment of Canada's nuclear fuel waste management concept. Atomic Energy of Canada Limited Report AECL-10165. Chalk River, Canada.

Zach, R. and S.C. Sheppard. 1991. The food-chain and dose submodel, CALDOS, for the assessing Canada's nuclear fuel waste management concept. Health Physics 60, 643-656.

APPENDIX A: SUMMARY OF VERIFICATION AND VALIDATION TESTS

Repository Test Summary

Submodel	Basis	Validity Range / Comments	Reference
Radionuclide Inventory; Ingrowth and Decay	Widely used experimentally proven theory	Linear decay chains	Bateman (1910) Any nuclear physics text
	Code Comparison (ORIGEN-S versus SCC402)	Bruce fuel bundle, 280 MWh/kgU burnup, decay to 10^7 years, selected fission products and the 4n actinide decay chain. Maximum absolute difference of 0.23% except for Nb-93m, where discrepancies (up to 22%) arose due to differences in decay scheme used by the two codes. Good agreement was obtained after the decay scheme was made identical.	Goodwin et al. (2002)
Defect failure of container	Copper container fabrication trials	Electron beam and friction stir welding of 50-mm copper shells, approximately 1 m diameter. SKB (2011) concludes that the probability of a defect greater than 20 mm is negligible.	SKB (2011)
	Conservative assumptions	Assume that have early failures of containers in repository with probability of failure from Maak et al. (2001).	NWMO (2012a), Posiva (2012), SKB (1999)
Instant release of nuclides from fuel-cladding gap and fuel cracks when water contacts fuel.	Lab experiments	Short-term tests using CANDU used fuel with various burnups and power ratings. For conservatism, the grain boundary inventory is also assumed to be instantly released.	Stroes-Gascoyne, (1996), Stroes-Gascoyne et al. (1993)
	Widely used model	Similar conservative assumptions used internationally	SKB (2011), Posiva (2012), Johnson et al. (2004)
Congruent release or nuclides from UO_2 grains	Lab experiments.	Short term leach tests on used fuel	Tait and Luht (1997), Johnson et al. (1982), Neal et al. (1988)
	Natural analogs (Cigar Lake)	Relative abundance of fission and activation products in uraninite ore	Cramer and Smellie (1994)

Empirical UO_2 dissolution model	Lab experiments (alpha radiation)	Effect of alpha radiolysis on dissolution of UO_2 fuel measured using samples UO_2 doped with various amounts of alpha-emitters	Poinssot et al. (2005), Shoesmith (2007)
	Lab experiments (gamma radiation)	Effect of beta and gamma radiolysis on dissolution rate of UO_2. Beta and gamma radiolysis are only important for times < 500 years after fuel removed from reactor.	Johnson et al (1996)
	Lab experiments (chemical dissolution)	Chemical dissolution rate of UO_2 under reducing conditions – no radiolysis effects. Compilation of experimental data under appropriate conditions.	Garisto et al. (2012)
	Empirical model agrees with others	Model predicts all fuel in a breached container would dissolve in 13 million years, similar to value predicted by SKB (2011) model	SKB (2011), Werme et al. (2004)
	Natural analog (Cigar Lake and Oklo)	Natural uraninite, which can be considered an analogue for UO_2 fuel, located in reducing environments shows very long-term stability, i.e., up to billions of years. This indicates the empirical fuel dissolution model is likely conservative.	Cramer (1994)
Nuclide releases from Zircaloy	Solubility limited dissolution model	Nuclides are incorporated in ZrO_2 oxide film (which adheres strongly to Zircaloy) and are released as the ZrO_2 dissolves. Dissolution rate of ZrO_2 calculated using solubility limited dissolution model. This model has not been tested.	Johnson et al. (1994)
Solubility in the container	Thermodynamic calculations using PHREEQC	Solubility calculated using internationally accepted thermodynamic data	Duro et al. (2010)
	Widely used approach	Same or similar thermodynamic data used in other international programs (SKB and Nagra)	SKB (2010b), Berner (2002)

Container release (small defects)	Analytical expression	CC4 releases are conservatively calculated since only the smaller of the pinhole or buffer resistances is used in the model.	NWMO (2012b), LeNeveu (1996)
	Code comparison (ANSYS versus SCC402)	Release rates of nuclides (with different buffer K_d values) out of small round defects (< 0.0015 m) compared. On time frames of interest (> 100 years or so), CC4 release rates were higher in all cases because CC4 accounts for only for the smaller of the pinhole or buffer mass transport resistances. However, for times < 20 years, CC4 can underestimate releases (by up to a factor of 3) for cases in which buffer capacity factor is large. The dependence of the release rate of a non-sorbing nuclide on the shape of the defect was also investigated using ANSYS. Releases are mostly dependent on the area of the defect with only a small dependence on the shape.	Goodwin et al. (2002)
	Code comparison (COMSOL versus analytical expressions)	As expected mass transport out of the container influenced by both pinhole and buffer resistances. Analytical expressions are conservative since don't account for depletion of contaminant near entrance to the pinhole.	Beauregard et al. (2010)
	Code comparison (COMSOL versus SCC409.1)	Mass transport out of a container with small defects was compared for various radionuclides and a radionuclide decay chain. As expected, CC4 release rates out of the container were larger than from COMSOL because CC4 accounts for only the smaller of the pinhole of buffer mass transport resistances and, to a smaller extent, the impact of non-uniform concentrations in the container (i.e., nuclide concentrations inside the container near the defect decrease in the COMSOL model as nuclides diffuse out of the defect, reducing the concentration gradient across the defect).	Section 3.6.1 of this report

Container release (large defects)	Code comparison (COMSOL versus SCC409.1)	Mass transport out of a container with large defects was compared for various radionuclides and a radionuclide decay chain. For non-sorbing high-solubility radionuclides, the CC4 and COMSOL models were in good agreement because mass flows out of the container were limited by the radionuclide release rate from the fuel. For sorbing low-solubility radionuclides, the mass flows out of the container were higher in COMSOL than in CC4 but approached the CC4 values at long times. The differences between the two models increase as the defect radius increases.	Section 3.6.2 in this report
Transport in the repository	Code comparison (MOTIF versus PR4)	I-129 cumulative mass flows out of the buffer, backfill and EDZ zones were calculated and compared. These zones were modeled as concentric cylinders (CC4) or concentric cuboids (rectangular prisms). Tests were carried out for two source locations and various groundwater flows. Agreement between the two models was best when groundwater flow was low or perpendicular to cylindrical axis. Differences increased as the horizontal groundwater velocity increased, with the differences depending on the source location in MOTIF. (For CC4, the mass flows are independent of the source location.) CC4 cumulative mass flows were higher than those from MOTIF as long as source was in centre of placement room.	Johnson et al. (1996), LeNeveu and Kolar (1996)
	Code comparison (COMSOL)	The CC4 repository transport model was compared to a COMSOL model in which the geometry of the repository was made identical to the repository geometry used in CC4, i.e., the repository is represented by a set of concentric cylinders. This test compared calculated radionuclide mass flows at the buffer-backfill, backfill-EDZ and EDZ-rock interfaces. The test was carried out for various single radionuclides and a decay chain. The peak mass flows calculated by the two models agreed well at the buffer-backfill and EDZ-rock interfaces. But the peak mass flows from COMSOL were higher at the backfill-EDZ interface. The reason for this difference is not known.	Section 3.7.2 of this report

Transport in the repository (cont'd)		However, the peak mass flows at the EDZ-rock interface determine the calculated impacts of the repository and, for these, the two models differ by no more than 10%.	
	Code comparison (COMSOL)	The CC4 repository transport model was compared to a COMSOL model in which the container is explicitly included to determine the impact of the container on calculated mass flows out of the repository. This test compared calculated radionuclide mass flows at the buffer-backfill, backfill-EDZ and EDZ-rock interfaces. The test was carried out for various single radionuclides and a decay chain. The peak mass flows calculated by CC4 were larger than those from COMSOL at the buffer-backfill and EDZ-rock interfaces, but not at the backfill-EDZ interface (see also previous comparison). Since the peak mass flows at the EDZ-rock interface determine the calculated impacts of the repository, the CC4 model is conservative relative to the COMSOL model with a container.	Section 3.7.2.2 in this report
	Code comparison (FRAC3DVS versus SCC404)	Third Case Study (TCS). CC4 compared to FRAC3DVS near-field model. FRAC3DVS was able to provide a better representation of the actual placement room geometry, although the container is not explicitly included in either model. Comparisons for following nuclides: Cl-36, I-129, Ca-41, U-238 → U-234 chain, and Np-237 → U-233 chain. Agreement was generally good with largest differences for weakly sorbing Ca-41 and strongly sorbing actinides.	Garisto et. al. (2004)
	Code comparison (FRAC3DVS versus SCC405)	Horizontal Borehole Case (HBC) Study. CC4 compared to FRAC3DVS near-field model. FRAC3DVS represented the actual placement room geometry. The container was included in FRAC3DVS model but not CC4 model. Comparisons for following nuclides: Cl-36, I-129, Ca-41, U-238 → U-234 chain, and Np-237 → U-233 chain. Agreement between calculated peak mass flows was generally good.	Garisto et. al. (2005a)

Transport in the repository (cont'd)	Code comparison (FRAC3DVS versus SCC409)	Fourth Case Study (4CS). In 4CS, containers are placed in boreholes drilled into the placement room floor. In the FRAC3DVS model, the repository geometry is represented in detail, including the container. In CC4, only the borehole is represented (along with the surrounding EDZ and rock). Comparisons were made for a variety of radionuclides: I-129, C-14, Cl-36, Ca-41, Cs-135, Sn-126 and the chain U-238 → U-234. However, in both models, there were no releases of either U-238 or U-234 from the repository within the 10^7 year simulation time. For the other nuclides, the calculated peak mass flows from the repository were in good agreement except for Sn-126, for which the two models differed by a factor of about 300 for the reasons outlined in Section 3.7.5.	NWMO (2012a)

Geosphere Test Summary

Submodel	Basis	Validity Range / Comments	Reference
Transport in the geosphere Verification of mathematical algorithms used in GEONET, the CC4 geosphere model	Code comparison Network tests – segmentation and branching of transport path	Initial testing of GEONET was done using cases that included single transport segments and simplified networks. As parameter values (e.g., dispersivity and retardation) were varied, the GEONET code gave expected changes to contaminant breakthrough curve. Segmentation of transport path was shown not to affect breakthrough curves and branching of transport network produced expected results.	Davison et al. (1994)
	Code comparison (INTRACOIN versus SYVAC3-CC3)	Nuclide decay chains with 3 members. Single and multiple layer geosphere. GEONET showed very good agreement with corresponding results published in INTRACOIN (1984).	Davison et al. (1994)
	Code comparison (Numerical methods versus SYVAC3-CC3)	Verification of the analytical response function solutions to the one-dimension advection-dispersion equation for various source terms (impulse flow or constant flow) and parameter values (geosphere layer thickness, diffusion coefficient, K_d, Darcy velocity and nuclide half-life) was carried out by numerically inverting Laplace transform solution. Results generally agreed within expected numerical accuracy.	Chan and Advani (1991)
	Code comparison (SYVAC3-CC3)	GEONET was used to simulate the results reported by Gureghian and Jansen (1985) for transport of a 3-member nuclide chain through a three-layer medium. GEONET simulations were in good agreement with these published results.	Davison et al. (1994)
	Comparison to analytical results (SYVAC3-CC3)	Scientific Review Group (SRG 1995) compared transport of I-129 through fracture zone and into well and compared transport through intact lower rock zone. Agreement was good.	SRG (1995)

Transport in the geosphere (cont'd) Verification of mathematical algorithms used in GEONET, the CC4 geosphere model	Code comparison (FRAC3DVS and COMSOL versus SYVAC3-CC409)	Response function solution from GEONET for a diffusion dominated sedimentary geosphere was compared to numerical results from FRAC3DVS and COMSOL. A mix of response functions was used, depending on the properties of sedimentary formations, to model I-129 transport. Differences between the three models were apparent close to the repository but differences decreased with elevation above the repository. The CC4 mass flows into well are about 2-fold higher, largely because CC4 doesn't model downward diffusion.	Test documented in this report
Transport in the geosphere (cont'd) Check of the GEONET methodology, i.e., how well GEONET represents groundwater flow field.	Code comparison (MOTIF versus SYVAC3-CC3)	Modelled system was 2-D cross-section through Whiteshell Research Area with a hypothetical repository located adjacent to a fracture zone. Comparison of spatial distribution of (non-sorbing) solute flow and total mass flow into fracture showed good agreement, with the agreement being best when GEONET discretization was finest. GEONET network gave conservative results by choosing shortest possible segment lengths.	Chan et al. (1991), Davison et al. (1994)
	Code comparison (PSACOIN)	Test included linear decay chains, advective transport through 2-layer geosphere, well and a drinking water dose pathway. Different modelling codes all calculated mean dose rates that were in excellent agreement.	NEA (1990), Davison et al. (1994)
	Code comparison (FRAC3DVS versus SYVAC3-CC404)	Third Case Study. Repository at 670 m. Canadian Shield sparsely fractured rock. Comparisons for following nuclides: Cl-36, I-129, Ca-41, U-238 → U-234 chain, and Np-237 → U-233 chain. For I-129, Cl-36 and Ca-41, the agreement was good for peak mass flows into biosphere and for time of peak mass flows (i.e., differences < 40%). For actinide nuclides, the FRAC3DVS releases from the geosphere occur earlier and are therefore much larger than the corresponding CC4 releases during the million year simulation period.	Garisto et. al. (2004)

Transport in the geosphere (cont'd) Check of the GEONET methodology, i.e., how well GEONET represents groundwater flow field.	Code comparison (FRAC3DVS versus SYVAC3-CC405)	Horizontal Borehole Case Study. Repository at 670 m. Canadian Shield sparsely fractured rock. Comparisons made for following nuclides: Cl-36, I-129, C-14, Ca-41, Cs-135, and U-238 → U-234 chain. For non-sorbing nuclides (I-129 and Cl-36) the agreement was good for peak mass flows into biosphere (< 60% difference) and for time of peak mass flows (< 10% difference). For weakly sorbing Ca-41, agreement was poorer, with CC4 peak mass flow about 3-fold higher than FRAC3DVS and time of peak about 90% of FRAC3DVS value. For actinides, differences are the same as observed for TCS.	Garisto et. al. (2005a)
	Code comparison (FRAC3DVS versus SCC409)	Fourth Case Study with containers placed in in-floor boreholes. Repository at 500m. Canadian Shield sparsely fractured rock. Comparisons made for following nuclides: Cl-36, I-129, Ca-41, and U-238 → U-234 chain. For this geosphere, the agreement was best for long-lived non-sorbing I-129. For the nuclides C-14, Ca-41, Cl-36, and Cs-135, the time of the peak release was earlier in CC4, with up to a 3-fold difference (for Cs-135). This may partially explain why peak release rates for these nuclides were 2 to 5 times higher in CC4 than FRAC3DVS. For actinides, releases to biosphere were effectively zero in both models.	NWMO (2012a)
	Code comparison (FRAC3DVS versus SYVAC3-CC407)	Glaciation Scenario Case Study. Horizontal borehole placement of containers. Repository 670 m deep. Canadian Shield sparsely fractured rock. Time dependent groundwater flow field modelled in CC4 using 9 "snap-shots" of the flow field. Eight glacial cycles occur over million year simulation period.	Garisto et. al. (2010)

Transport in the geosphere (cont'd) Check of the GEONET methodology, i.e., how well GEONET represents groundwater flow field.		Only I-129 transport modelled. The detailed predictions of the two models are different and the peak I-129 mass flow occurs earlier in FRAC3DVS. However, the comparisons indicate that these very different models predict similar trends for the I-129 mass flow rates into the biosphere. Better agreement would have been obtained if more than 9 snap-shots were used to represent the time dependent flow field.	

Biosphere Test Summary

Submodel	Basis	Validity Range / Comments	Reference
Surface water	Field experiments using P in lakes	P concentrations in lake water within factor of 2 of observed values.	Bird et al.(1992)
	Field experiments using P in wetlands	Calculated P concentrations in water, based on annual inputs into the lake, agreed well for 2 wetlands, but 2 to 5 times lower in 3 wetlands. Underpredictions could be due to internal sources of P. P concentrations in sediments one to two orders of magnitude too low. This could reflect P content of decaying vegetation.	Bird et al. (1992)
	Field experiments using Ca	Ca concentrations in water measured over 3 year period. Calculated concentrations in water close to measured values, but sediment concentrations one third of measured value.	Bird et al. (1992)
	Field experiments using Cd	Atmospheric deposition of Cd. Calculated Cd concentration 3-fold higher than observed value. Sediment concentration 3-fold lower.	Bird et al. (1992)
	Field experiments using Co-60	Model accurately described behaviour of aqueous Co-60 over 11 year period. Sediment concentrations were within factor of 2 of values measured in 1969 and 1989.	Bird et al. (1992)
	Field experiments with Co-60, Cs-134 and H-3	One year study. Calculated H-3 concentrations were in good agreement but Co-60 and Cs-134 concentrations were 4-fold larger than observed values. Total activities of Co-60 and Cs-134 in sediment were in good agreement with measured values.	Bird et al. (1992)
	Field experiments with Cd	Cd added to lake over 4 year period. Calculated Cd concentrations up to 10-fold larger than observed; but observed values fall within range of calculated values. Calculated sediment concentration about 60% of observed value.	Bird et al. (1992)

Surface water (cont'd)	Field experiments with C-14	C-14 spikes added to lakes and field data collected over 16 year period. Short term behaviour of aqueous C-14 adequately predicted. However, medium-term behaviour (2 to 16 years) not well predicted. This is because surface water model developed to simulate long-term net exchange between water and sediment assuming continuous source flux and so it fails to account for internal C-14 fluxes (e.g., from sediment to water) following single pulse addition of C-14.	Stephenson and Reid (1996)
	Code comparison (BIOMOVSII)	Stephenson and Reid (1996) data used to validate models. Study concluded that surface water model provided reasonable predictions of C-14 retention in lake sediments but was too simplistic to provide realistic predictions of water concentrations over the long-term following an acute release of C-14 since internal recycling of C-14 between water body and sediments must be modelled for non-equilibrium conditions.	BIOMOVSII (1996a), Bird et al. (1999)
	Code comparison (BIOMOVS Scenario B3)	Nuclides Ra-226 and Th-230 modelled. Predictions of CC4 did not differ appreciably from those of other six assessment models.	Bergström (1988), Bird et al. (1992)
Upland soil (No tests for shallow soil model)	Code comparison (BIOPROTA)	Soil model compared with two other models for Los Ratones scenario. U-238, U-234, Th-230 and Ra-226 concentrations compared. Calculated soil concentrations for the 3 models varied within about a factor of 3, with exception of Th-230 downstream of mine.	Limer (2012)
Atmosphere	Widely used and accepted model	Atmospheric model is simple and assumes equilibrium conditions. Dispersion relationships based on a widely accepted numerical dispersion theory which agrees well with experimental data (Wilson 1982a,b).	Amiro (1992)
Food chain and dose	Widely used model	Food chain and dose model consistent with CSA N288.1.	CSA (2008)
	Code comparison BIOMOVS I	Predictions of food chain and dose model closely agree with models used in several other countries.	Haegg and Johanson (1988), Zach and Sheppard (1992)

Food chain and dose (cont'd)	Code Comparison (SR97 versus SYVAC3-PR4)	Ten radionuclides included in the test. Radionuclides with largest peak doses were I-129, Cl-36, Se-79, Sn-126, Sb-126 and NI-59 in order of decreasing peak dose. Peat Scenario: Good agreement between the two codes with ratio of PR4 to SR97 doses varying from 0.4 to 1.9. Well Scenario: Agreement was good except for Cl-36, Se-79 and Tc-99. Since soil-plant-man pathway is dominant, the large differences for these nuclides attributed to differences in soil models used in SR97 and PR4.	Garisto et al. (2001)
	Code comparison of H-3 specific activity model (UNSCEAR and NCRP)	Chronic exposure scenarios. UNSCEAR (1982) estimated surface water concentrations and corresponding dose to man from cosmically produced H-3. For same situation, CC4 predicted 30% higher dose rate. NCRP (1979) estimated dose to man from H-3 concentration of 0.037 MBq/L. For same situation, CC4 predicted 20% higher dose rate.	UNSCEAR (1982), NCRP (1979)

System Model Test Summary

Submodel	Basis	Validity Range / Comments	Reference
System model	Mass balance	Mass balance checks were coded into SYVAC3-CC4, Version SCC404. Nuclide masses within the repository and geosphere are conserved within the test criteria. For the biosphere model contaminant mass is overestimated in most cases (with maximum deviation of 70%). This was expected given conservatisms in biosphere model. One case displayed a mass loss of 6% for C-14 due to fact that mass balance test did not account for downwind atmospheric mass loss. This was corrected in later versions of code.	Goodwin et al. (2002)
	Code comparison (PSACOIN Level 0 and Level E)	Tests of the SYVAC3 executive code, Version 03. The following features were tested: input and output, input parameter sampling (constant, uniform, log uniform, normal and lognormal), generation of random numbers, times series calculations, and control and executions of multiple runs. SYVAC3 results agreed well with reference code results.	NEA (1987), NEA (1989)
	Code comparison (PSACOIN Level 1b)	This test focussed on the biosphere. Nuclides included in test were C-14 and U-235→ Pa-231 → Ac-227 chain. AECL developed special system model for use in this test as well as a new SYVAC routine called MULTIC, which was incorporated into SYVAC3, Version 09. AECL results for compartment inventories agreed to much better than 10% with “all codes average” for dominant nuclides and to about 10% for Pa-231 and Ac-227. For probabilistic exercise (1000 runs), the AECL results agreed well with results from other codes.	NEA (1993b)
	Code comparison (UTAP)	SYVAC3 code with special system model was used to check UTAP code. The results showed acceptable agreement lending confidence in SYVAC3.	Goodwin and Andres 1986).